

.bl4019668

U.O.V.S. BIBLIOTEEM

01

ERDIE EKSEMPLAAR MAG ONDER
EEN OMSTANDIGHEDE UIT DIE
BIBLIOTEK VERWYDER WORD NIE

University Free State



34300000971626

Universiteit Vrystaat

**Synthesis and electrochemistry of novel new
ferrocene-containing water-soluble macromolecules
with biomedical applications**

A dissertation submitted in fulfilment of the requirements for the degree

MAGISTER SCIENTIAE

in the
DEPARTMENT OF CHEMISTRY
FACULTY OF SCIENCE

at the
UNIVERSITY OF THE FREE STATE

by

PATRICK THABO NDABA NONJOLA

Supervisor: Prof. J. C. Swarts
January 2002

Universiteit van die
Oranje-Vrystaat
BLOEMFONTEIN

- 9 MAY 2002

UOVS SASOL BIBLIOTEEK

Contents

| | |
|--|-----|
| Abstract | i |
| Opsomming | ii |
| List of abbreviations | iii |
| List of figures | iv |
| List of schemes | vii |
| List of tables | ix |
| Acknowledgements | x |
| | |
| CHAPTER 1 | |
| INTRODUCTION AND AIMS | 2 |
| | |
| CHAPTER 2 | |
| LITERATURE SURVEY | |
| 2.1 Introduction | 6 |
| | |
| 2.2 Polymers as drug carriers | 7 |
| 2.2.1 <i>Introduction</i> | 7 |
| 2.2.2 <i>A possible drug delivery route associated with drug carriers</i> | 8 |
| 2.2.3 <i>Synthetic strategies and properties of polymeric drug carriers</i> | 12 |
| 2.2.4 <i>Selected examples of polymeric drug carriers and polymeric drug carrier/drug conjugates</i> | 15 |
| | |
| 2.3 Ferrocene derivatives | 26 |
| 2.3.1 <i>Introduction</i> | 26 |
| 2.3.2 <i>The chemistry of ferrocene</i> | 27 |
| 2.3.3 <i>Electrochemical studies</i> | 31 |
| 2.3.4 <i>Cytotoxicity and mechanism of action of ferrocene derivatives</i> | 33 |
| | |
| 2.4 General synthetic procedures | 35 |
| 2.4.1 <i>Formation of acid chlorides</i> | 35 |

| | | |
|---------|--------------------------------------|----|
| 2.4.1.1 | Thionyl chloride | 36 |
| 2.4.1.2 | Oxalyl chloride, (COCl) ₂ | 37 |
| 2.4.1.3 | Phosphorus chlorides | 37 |
| 2.4.2 | <i>Amide synthesis</i> | 38 |
| 2.4.3 | <i>Primary amine synthesis</i> | 39 |

CHAPTER 3

RESULTS AND DISCUSSION

| | | |
|---------|---|----|
| 3.1 | Introduction | 41 |
| 3.2 | Syntheses | 41 |
| 3.2.1 | <i>Preparation of ferrocene derivatives</i> | 41 |
| 3.2.1.1 | Carboxylic acids | 41 |
| 3.2.1.2 | Amides | 44 |
| 3.2.1.3 | Amines | 47 |
| 3.2.1.4 | Conclusion | 49 |
| 3.2.2 | <i>Polymer synthesis</i> | 50 |
| 3.2.2.1 | Thermal polymerisation of aspartic acid | 50 |
| 3.2.2.2 | The anchoring of ferrocenylamine derivatives on polysuccinimide | 51 |
| 3.2.2.3 | Conclusion | 54 |
| 3.3 | Electrochemistry | 55 |
| 3.3.1 | <i>Cyclic voltammetry of ferrocenyl derivatives</i> | 55 |
| 3.3.1.1 | Ferrocene amides | 55 |
| 3.3.1.2 | Ferrocene amine hydrochloride electrochemistry in water | 59 |
| 3.3.1.3 | Ferrocene-amine electrochemistry in acetonitrile | 63 |
| 3.3.2 | <i>Cyclic voltammetry of water-soluble polymer-bound ferrocenes</i> | 70 |
| 3.3.3 | <i>Conclusion</i> | 75 |
| 3.4 | Cytotoxicity studies | 76 |
| 3.4.1 | <i>Introduction</i> | 76 |
| 3.4.2 | <i>Small molecule ferrocene-amides and -amines</i> | 77 |

| | | |
|---------------------|---|----|
| 3.4.3 | <i>Polymeric conjugates</i> | 80 |
| CHAPTER 4 | | |
| EXPERIMENTAL | | |
| 4.1 | Materials | 87 |
| 4.2 | Techniques and apparatus | 87 |
| 4.2.1 | <i>Infrared (IR) Spectroscopy</i> | 87 |
| 4.2.2 | <i>Nuclear Magnetic Resonance (NMR) Spectroscopy</i> | 87 |
| 4.2.3 | <i>Determination of the melting points (m.p.)</i> | 87 |
| 4.2.4 | <i>Dialyses and freeze drying of polymers</i> | 87 |
| 4.2.5 | <i>Column chromatography</i> | 88 |
| 4.2.6 | <i>Cyclic voltammetry</i> | 88 |
| 4.2.7 | <i>Cytotoxicity tests</i> | 89 |
| 4.3 | Synthesis and functionalisation of the ferrocene | 90 |
| 4.3.1 | <i>2-Chlorobenzoylferrocene (60) [Scheme 3.1, page 42]</i> | 90 |
| 4.3.2 | <i>Ferrocenoic acid (47a) [Scheme 3.1, page 42]</i> | 90 |
| 4.3.3 | <i>N,N-dimethylaminomethylferrocene methiodide (61) [Scheme 3.1, page 42]</i> | 91 |
| 4.3.4 | <i>Ferrocenylacetonitrile (62) [Scheme 3.1, page 42]</i> | 91 |
| 4.3.5 | <i>Ferrocenylacetic acid (47b) [Scheme 3.1, page 42]</i> | 92 |
| 4.3.6 | <i>Ferrocenecarboxaldehyde (46) [Scheme 3.1, page 42]</i> | 92 |
| 4.3.7 | <i>3-Ferrocenylacrylic acid (63) [Scheme 3.1, page 42]</i> | 93 |
| 4.3.8 | <i>3-Ferrocenylpropanoic acid (47c) [Scheme 3.1, page 42]</i> | 94 |
| 4.3.9 | <i>3-Ferrocenoylpropanoic acid (64) [Scheme 3.1, page 42]</i> | 94 |
| 4.3.10 | <i>4-Ferrocenylbutanoic acid (47d) [Scheme 3.1, page 42]</i> | 95 |
| 4.3.11 | <i>Ferrocenecarboxaldoxime (68) [Scheme 3.3, page 48]</i> | 95 |
| 4.3.12 | <i>Ferrocenylcarboxamide (66a) [Scheme 3.2, page 45]</i> | 96 |
| 4.3.12.1 | Oxalyl chloride method | 96 |
| 4.3.12.2 | Thionyl chloride method | 97 |
| 4.3.12.3 | Phosphorus trichloride method | 97 |
| 4.3.13 | <i>Ferrocenylacetamide (66b) [Scheme 3.2, page 45]</i> | 98 |
| 4.3.13.1 | Oxalyl chloride method | 98 |
| 4.3.13.2 | Phosphorus trichloride method | 98 |
| 4.3.14 | <i>3-Ferrocenylpropionamide (66c) [Scheme 3.2, page 45]</i> | 99 |

| | | |
|----------|---|-----|
| 4.3.15 | <i>4-Ferrocenylbutanamide (66d) [Scheme 3.2, page 45]</i> | 99 |
| 4.3.16 | <i>Ferrocenylmethanamine (67a)</i> | 100 |
| 4.3.16.1 | Reduction of amide method [Scheme 3.2, page 45] | 100 |
| 4.3.16.2 | Ferrocenecarbaldehyde oxime method [Scheme 3.3, page 48] | 100 |
| 4.3.17 | <i>2-Ferrocenylethylamine (48)</i> | 101 |
| 4.3.17.1 | By the reduction of ferrocenylacetonitrile (62) [Scheme 3.4, page 49] | 101 |
| 4.3.17.2 | By the reduction of 2-ferrocenylacetamide (66b) [Scheme 3.2, page 45] | 101 |
| 4.3.18 | <i>3-Ferrocenylpropylamine (67b) [Scheme 3.2, page 45]</i> | 102 |
| 4.3.19 | <i>4-Ferrocenylbutylamine (67c) [Scheme 3.2, page 45]</i> | 102 |
| 4.4 | Synthesis of the polymeric carriers and the anchoring of the ferrocene | 103 |
| 4.4.1 | <i>Poly-DL-succinimide (2) (Scheme 3.5, page 50)</i> | 103 |
| 4.4.2 | <i>Polymer (69) [Scheme 3.6, page 52]</i> | 104 |

CHAPTER 5

| | |
|---|-----|
| SUMMARY, CONCLUSIONS AND FUTURE PERSPECTIVES | 107 |
|---|-----|

| | |
|-------------------|-----|
| REFERENCES | 111 |
|-------------------|-----|

| | |
|---|-----|
| NUCLEAR MAGNETIC RESONANCE SPECTRA | 119 |
|---|-----|

ABSTRACT

The side effects associated with chemotherapy have caused an intensive research effort to find new ways of delivering a chemotherapeutic drug to a cancerous growth. One of these includes use of polymeric drug carriers. In this thesis is reported the syntheses, characterisation and electrochemistry of a series of antineoplastic ferrocene-containing amides and amines which was obtained from the corresponding ferrocene-containing carboxylic acids precursors. It is also described how the amines may be covalently anchored onto a water-soluble polymeric drug carrier to give the water-soluble ferrocene-containing polymers with biomedical applications. The influence of side chain length (i.e. the number of CH₂ spacers) and type of the functional group (X = CONH₂, NH₂, NH₃⁺ and NHCO) on the ferrocenyl (Fc) formal reduction potential in compounds of the type Fc-(CH₂)_nX with n = 1- 4 is also highlighted.

Cytotoxicity tests on all the amines, amides and polymers were investigated utilising HeLa, a human cervix epitheloid cancer cell line and CoLo DM320, an intrinsically multidrug resistant human colorectal cell line. Results showed that there exists a definite relationship between the length of the carbon chains linking the ferrocenyl antineoplastic moiety with either the polymer main chain of NH₂ and CONH₂ functional group and effective cell death. Comparison of the cytotoxic results of the polymeric devices and monomeric antineoplastic ferrocene-containing amides and amines suggested that the benefits of a polymeric drug carrier is only observed in practice when the length of the side chain connecting drug and polymer main chain exceeds 5 atoms.

Keywords: Ferrocene, polymeric drug carriers, electrochemistry, and cytotoxicity

OPSOMMING

Die nuwe-effekte wat met chemoterapie geassosieer word het 'n intensiewe navorsingspoging tot gevolg gehad om nuwe maniere te vind om 'n chemoterapeutiese middel aan 'n kankertumor toe te dien. Een manier behels die gebruik van polimeriese geneesmiddeldraers. In hierdie tesis word verslag gedoen oor die sintese, karakterisering en elektrochemie van 'n reeks antineoplastiese ferroseenbevattende amiede en amiene wat verkry is vanaf die ooreenstemmende ferroseenbevattende karboksiesuur voorlopers. Daar is ook beskryf hoe die amiene kovalent aan 'n water-oplosbare polimeriese geneesmiddeldraer geanker kan word om die water-oplosbare ferroseenbevattende polimere met biomediese toepassings te lewer. Die invloed van sykettinglengte (*d.w.s.* die aantal CH_2 skakels) en tipe funksionele groep ($\text{X} = \text{CONH}_2$, NH_2 , NH_3^+ , en NHCO) op die ferroseniel (Fc) formele reduksiepotensiaal in dierbindings van die tipe $\text{Fc}-(\text{CH}_2)_n\text{X}$ met $n = 1 - 4$ word ook uitgelig.

Toetse vir sitotoksiteit op al die amiene, amiede en polimere is uitgevoer deur van HeLa, die menslike serviksepiteloïede kankersellyn en CoLo DM320, 'n intrinsieke multigeneesmiddel weerstandige menslike kolorektale sellyn gebruik te maak. Resultate het getoon dat daar 'n besliste verband tussen die lengte van die koolstofketting wat die ferroseniel antineoplastiese groep met die polimeer-hoofketting, of die NH_2 of CONH_2 funksionele groepe verbind, en effektiewe seldood bestaan. 'n Vergelyking van sitotoksiese resultate van die polimeriese molekule met dié van die monomeriese antineoplastiese ferroseenbevattende amiede en amiene het getoon dat die voordele wat met 'n polimeriese geneesmiddeldraer geassosieer word, eers prakties waarneembaar is as die lengte van die ketting wat geneesmiddel met polimeer-hoofketting verbind vyf atome oorslag.

Sleutelwoorde: Ferroseenverbindinge, polimeriese geneesmiddeldraers, elektrochemie, sitotoksiteit.

List of abbreviations

| | |
|------------------|--|
| Å | angstrom units (10^{-10} m) |
| DMSO | dimethyl sulfoxide |
| DMF | N,N-dimethyl formamide |
| FCS | fatal calf serum |
| Fc | ferrocenyl |
| $E^{o/}$ | formal reduction potential |
| E_{pa} | anodic peak potential |
| E_{pc} | cathodic peak potential |
| i_{pa} | anodic peak current |
| i_{pc} | cathodic peak current |
| IR | infrared |
| m.p. | melting point |
| MMT | 3-(4,5-dimethylthiazol-2-yl)-diphenyltetrasodium bromide |
| $^1\text{H NMR}$ | proton nuclear magnetic resonance |
| ppm | parts per million |
| THF | tetrahydrofuran |
| cm^{-1} | wave number |

List of figures

- Figure 2. 1** Cellular pinocytotic uptake of polymers (Figure from Ref 5).....11
- Figure 2. 2** General guidelines for the synthesis of a polymeric drug carrier/drug conjugates.14
- Figure 2. 3** Ester, amide, urethane and O-acylated hydroxamic acid bonds were utilized to anchor the cytotoxic agent bis(2-chloroethyl)amine onto a methacrylate based polymeric carrier. The main chain of this polymeric system is not biodegradable.18
- Figure 2. 4** Dimethyl sulfoxide and phenolic residues incorporated on polymers 12 and 13 respectively.19
- Figure 2. 5** Grafting of poly(ethylene oxide) onto polyaspartamide.20
- Figure 2. 6** Attempts to anchor 1-ferrocenylethylamine directly on polysuccinimide derivatives (compound 24) or *via* an acrylated intermediate on polymer 15 to obtain 25 were inefficient reactions.....21
- Figure 2. 7** Addition of 1-ferrocenylethylamine onto an acrylated derivative of 15 to give 26 was only 40% effective. Ferrocenecarboxaldehyde does not interact with 14 to give Schiff base compounds. Rather, the cyclic imine derivative 27 is formed.....22
- Figure 2. 8** Anchoring of carboxylic acid-containing ferrocene derivatives on the biodegradable drug carrier 15 liberates polymers 28 and 29.23
- Figure 2. 9** Platinum co-ordination with amine-functionalised polymeric drug carriers.....24
- Figure 2. 10** Relationship of E^0 (V) *vs.* n, where n = number of CH₂ groups separating a functional groups from the ferrocenyl moiety for the acids series 47 and the polymers 28.33
- Figure 3. 1** Infrared spectra (47b and 66 in KBr. 65 in petroleum ether solution and 48 between using NaCl discs as they are oils) with assignments and structures of ferrocene derivatives.46
- Figure 3. 2** ¹H NMR and ¹³C NMR signals of polysuccinimide in DMSO-d₆.51
- Figure 3. 3** The proton assignment in the ¹H NMR spectrum of polymer 69: 1.48 (6H, s, β-CH₂), 2.15 (6H, s, δ-CH₂), 2.31 (12H, s, γ-CH₂), 2.58 (10H, s, 4 asp-CH₂ + α'-CH₂), 2.99 (6H, s, α-CH₂), 3.50 (12H, s, ε-CH₂), 3.91-4.05 (9H, s, C₁₀H₆), 4.28-4.44 (4H, s, asp-CH).53

- Figure 3. 4** Cyclic voltammograms of **66a - 66d**, scan rates (ν) are 50 (smallest i_p value), 100, 150, 200 and 250 mV/s.56
- Figure 3. 5** Cyclic voltammograms of *ca.* 1 mmol dm⁻³ solutions of the hydrochloride salts of **48**, **67a**, **67b** and **67c** in water containing 1 mol dm⁻³ KCl and 10 mmol dm⁻³ HCl at 25°C at a scan rate 150 mV/s utilising a glassy carbon working electrode.59
- Figure 3. 6** Relation between $E^{o'}$ and n . "n" is the number of CH₂ groups that separate the ferrocenyl group from either the NH₃⁺ group in compounds of type Fc-(CH₂)_nNH₃⁺ (**48**, **67a - c** in water, ▲, $E^{o'}$ vs. Ag/AgCl) or from the type CONH₂ group in compounds of the type Fc-(CH₂)_nCONH₂ (in acetonitrile, **66a** = ●, a conjugated system and **66b - d** = ■, non conjugated systems, $E^{o'}$ vs. Ag/Ag⁻), Fc = ferrocenyl. The slope dy/dx becomes steeper with shorter chain length indicating that with shorter chain lengths the Fc/Fc⁺ couple is under the influence of stronger electron withdrawing functional groups, here NH₃⁺ or CONH₂. Since dy/dx is larger for NH₃⁺ than for the corresponding CONH₂ compounds, it follows that NH₃⁺ is a stronger electron-withdrawing group than the CONH₂ group.....62
- Figure 3. 7** Cyclic voltammograms of *ca.* 1 mmol dm⁻³ solutions of the ferrocene-containing amine series (Fc-(CH₂)_n-NH₂) in CH₃CN containing 0.1 mol dm⁻³ tetrabutylammonium hexafluorophosphate at 25°C at a scan rate of 250 mV/s on a Pt working electrode. Insert bottom right: Enlargement of the 200 mV/s scan of **67a** highlighting the two observed electrochemical couples for this compound.64
- Figure 3. 8** Relation between $E^{o'}$ and n . 'n' is the number of CH₂ groups that separates the ferrocenyl group from the NH₂ group of the type Fc(CH₂)_nNH₂ = (●) (**48**, **67a - c** in acetonitrile, $E^{o'}$ (V) vs. Ag/Ag⁺) and NH₃⁺Cl⁻ of the type Fc(CH₂)_nNH₃⁺Cl⁻ = (◆), in water, $E^{o'}$ (V) vs. Ag/AgCl. Fc = ferrocenyl. For **67a**, couple I was used in this plot.66
- Figure 3. 9** Cyclic voltammogram and structure of diferrocenylmethane **53e** (left) and ferrocenylmethanamine **67a** (right).68
- Figure 3. 10** Cyclic voltammograms of 1 mmol dm⁻³ solution of polymers **69 - 72** in water containing 1 mol dm⁻³ at 25°C at a scan rate of 100 mV/s on a glassy carbon working electrode.71
- Figure 3. 11** Chemically induced intramolecular electron transfer for the oxidised form of polymer **69** is more possible than for the oxidised form of polymer **72**.73
- Figure 3. 12** Comparison of $E^{o'}$ vs. n (number of CH₂ groups separating the indicated functional group from the ferrocenyl moiety) for the ferrocene-containing amides **66a - d** (■), amines **48**, **67a - c** (◆), amine hydrochlorides **48.HCl**, **67(a - c).HCl** (▲) and polymers **69 - 72** (●). $n = 0, 1, 2, 3$ or 474
- Figure 3. 13** Percentage cell survival for HeLa and DM320 cancer cell lines, relative to the control vs. concentration (μ g/ml) of amides **66a - 66d** and amines **48**, **67a** and **67c** after 7 days incubation. Sited potentials are versus a Ag/Ag⁺ reference in acetonitrile.77

- Figure 3. 14** Relation between E^0 (V) and IC_{50} ($\mu\text{g/ml}$) (left), and between "n" (in $(\text{CH}_2)_n$) and IC_{50} ($\mu\text{g/ml}$) (right) for the amides **66** and amines **48**, **67a** and **67c**.80
- Figure 3. 15** Effects of polymers **69**, **70**, **71** and **72** on HeLa and CoLo DM320 cancer cell lines after 24 hours and 7 days of incubation. Cited potentials are versus an Ag/AgCl reference electrode in water. Percentage cell survival are expressed as a percentage of living cells in relation to a control that was not exposed to the drug.81
- Figure 3. 16** Relation between E^0 and IC_{50} (left) and between "n" (in $(\text{CH}_2)_n$) and IC_{50} (right) on HeLa and CoLo DM320 cell lines for polymers **66** – **72**.83
- Figure 3. 17** Relation between HeLa cell IC_{50} values against side chain length for the amides **66a** - **d**, the amines **48**, **67a**, **67c** and the polymers **69** – **72**. Actual drug content IC_{50} values for the polymers and not the total polymer drug values were used in this graph. The inert graph is a blow up of the main graph for better reading.....84
- Figure 3. 18** Examples of polymers.85

List of Schemes

- Scheme 2. 1** The effect of different experimental conditions on the polymerization of aspartic acid and α,β -Poly(N-2-hydroxyethyl)-DL-aspartamide synthesis, a proposed blood plasma expander. It should be realised that **4** actually consists of a mixture of α and β isomer **5**, but for simplicity, in this study only the α -isomer will constantly be shown.....17
- Scheme 2. 2** The synthesis of a co-polymer of lysine and aspartic acid to which a phthalocyanine group has been anchored. M = Co or Zn. (See footnote).18
- Scheme 2. 3** Potential polymeric drug carriers.20
- Scheme 2. 4** Oxidation of ferrocene **37a** to give the ferricenium cation **38** which can undergo reductive coupling with radicals, R \cdot , to give substituted ferrocenes **37b**.26
- Scheme 2. 5** Precursors to various substituted ferrocenes.28
- Scheme 2. 6** Chemistry of ferrocene. X $^-$ = [CCl $_3$ COO] $^-$.2CCl $_3$ COOH in **54**.29
- Scheme 2. 7** Reagents for acid chloride synthesis36
- Scheme 2. 8** Synthesis of 1,1'-ferrocenyldicarboxylic acid chloride **56**.37
- Scheme 3. 1** Syntheses of ferrocene-containing carboxylic acids (**47a** - **47d**), TMMDA = tetramethylmethylenediamine, (CH $_3$) $_2$ NCH $_2$ N(CH $_3$) $_2$ and N-MeFA = N-methylformanilide, C $_8$ H $_9$ NO.42
- Scheme 3. 2** General synthetic route towards ferrocene-containing amides **66** and amines (**48** and **67**) respectively. Of the three methods investigated for acid chloride synthesis, only the PCl $_3$ route proved to be a general procedure. Derivatives **67b** and **67c** tend to oxidise and decompose when treated with HCl to produce quaternary ammonium salts.45
- Scheme 3. 3** Synthesis of ferrocenylmethylamine, **67a**, from **46**.48
- Scheme 3. 4** Synthesis of 2-ferrocenylethylamine, **48**, from **37a**. TMMDA = tetramethylmethylenediamine, C $_8$ H $_9$ NO.49
- Scheme 3. 5** Thermal polymerisation of DL-aspartic acid **1**.50

- Scheme 3. 6** The synthesis of polymeric drug carriers with the ferrocenyl moiety covalently anchored onto it.....52
- Scheme 3. 7** Intramolecular electron transfer from the free electron pair on the NH_2 group or the O-atom or even from the π -electron cloud in the carbonyl group may reduce the Fe^{III} ferricenium nucleus to a Fe^{II} ferrocene species thereby lowering the concentration of the ferricenium species that are available for reduction during the cathodic sweep.....58
- Scheme 3. 8** Canonical forms explain the conjugation between the electron donating ferrocenyl group and adjacent carbonyl group. For clarity, only one ferrocenyl isomer is shown for the two structures on the left but in reality there exist the normal mixtures of isomers corresponding, for example, to the zwitter ionic structure on the right. A CH_2 spacer between the ferrocenyl and amide groups will break this conjugation and it will result in much less positive reduction potentials for the ferrocene/ferricenium cation couple.59
- Scheme 3. 9** Interaction of the free electron pair of H_2O with the electrochemically generated ferricenium species may result in a variety of reduced Fe^{II} ferrocene species including the shown hydroxylated compound. See Chapter 2, page 26.61
- Scheme 3. 10** The possible explanation of the broadening of the peaks of ferrocenylmethylamine, **67a**, during oxidation-reduction processes.....67

List of Tables

| | | |
|-------------------|---|----|
| Table 2. 1 | Maximum tolerated dose levels ^a for polymer-platinum conjugates 30 - 36 | 25 |
| Table 2. 2 | Formal reduction potentials ^a , $E^{o'} = (E_{pc} + E_{pa})/2$ versus SCE and peak currents ratios ^a i_{pc}/i_{pa} for the indicated compounds at 25°C. | 32 |
| Table 3. 1 | Characterisation data of ferrocene-containing acids 47 amides 66 and amines 48 and 67 | 47 |
| Table 3. 2 | Electrochemical data for ferrocene-containing amides 66a - 66d in acetonitrile vs. Ag/Ag ⁻ at scan rates between 50 and 250 mV/s. E_{pa} = anodic peak potentials, $\Delta E_p = E_{pa} - E_{pc}$ (E_{pc} = cathodic peak potentials), formal reduction potentials, $E^{o'} = (E_{pa} + E_{pc})/2$, i_{pa} = anodic peak currents and i_{pc}/i_{pa} = peak current ratios with i_{pc} = cathodic peak currents. | 57 |
| Table 3. 3 | Peak anodic potentials, E_{pa} , difference in peak anodic and peak cathodic potentials, $\Delta E_p = (E_{pa} - E_{pc})$, formal reduction potentials, $E^{o'} = (E_{pa} + E_{pc})/2$, peak anodic currents, i_{pa} and peak cathodic/anodic current ratios, i_{pc}/i_{pa} for the indicated ferrocene-containing amines as the hydrochlorides in water containing 10 mmol dm ⁻³ HCl and 1 mol m ⁻³ KCl as supporting electrolyte at 25°C. Working electrolyte = glassy carbon, [ferrocene-amine hydrochloride] = 1 mmol dm ⁻³ | 60 |
| Table 3. 4 | Electrochemical data for the ferrocene-containing amines 48 , 67b and 67c in CH ₃ CN containing 0.1 mol dm ⁻³ tetrabutylammonium hexafluorophosphate as a supporting electrolyte at 25°C. | 65 |
| Table 3. 5 | Peak anodic potentials, E_{pa} , difference in peak anodic and peak cathodic potentials, $\Delta E_p = (E_{pa} - E_{pc})$, formal reduction potentials, $E^{o'} = (E_{pa} + E_{pc})/2$, peak anodic currents, i_{pa} and peak cathodic/anodic current ratios, i_{pc}/i_{pa} , (i_{pc} = peak cathodic currents) for the polymeric conjugates 69 - 72 . [Polymeric conjugates] = 1 mmol dm ⁻³ , with 1 mol dm ⁻³ KCl) as supporting electrolyte. | 72 |
| Table 3. 6 | Formal reduction potentials, $E^{o'}$, (vs. Ag/Ag ⁺ in acetonitrile) and IC ₅₀ values of the amides 66 and amines 48 and 67 in <i>in vitro</i> cancer cells after 7 days of incubation utilising CoLo DM320 and HeLa cell lines. | 79 |
| Table 3. 7 | HeLa and CoLo DM320 cell lines cell death after 24 hours and 7 days incubation with polymer-ferrocene drugs. | 82 |

Acknowledgements

I hereby wish to express my sincere gratitude towards the following people who all contributed directly or indirectly to the preparation of this thesis.

Prof. J. C. Swarts, my promoter, for his leadership during this study and for introducing me to the very exciting application of water-soluble polymeric drug carriers for biomedical applications. I especially appreciated the many hours he spent with me in his office and lab that very often kept him away from his family.

Collectively, all my post-graduate colleagues for their interest in my studies as well as their helpful advice in experimental techniques.

I particularly want to thank Ina du Plessis for her great help with the cyclic voltammetry, Dr. Jeanet Conradie and Hardi Koortzen for the many NMR spectra they drew for me, even on very short notice as well as Mrs Elke Kreft from the Department of Immunology, Institute for Pathology at the University of Pretoria for performing biological tests.

Lastly to my family for constant support and understanding during difficult times and for showing a keen interest in my progress.

For financial assistance during the course of my study I would like to thank NRF as well as CANSA.

Patrick Nonjola

2002

CHAPTER 1

INTRODUCTION AND AIMS

The side effects associated with chemotherapy have caused an intensive research effort to find new ways of fighting cancer. The discovery that platinum-containing compounds show marked chemotherapeutic activity spurred a vast effort to perfect the clinical use of the platinum-family of drugs. As a result, platinum based drugs are the most widely used metal-containing chemotherapeutic drug in clinical use today; of these, cisplatin [cis-diamminedichloroplatinum(II)] and newer analogues such as melano- and carboplatin are the most important examples.¹ However, potentially good chemotherapeutic drugs often find limited clinical use, owing to the many negative medical and physical side effects they show. For cisplatin, these negative side-effects or undesired chemical and physical properties include *inter alia* lack of aqueous solubility, high toxicity especially to the kidneys and bone marrow, it induces a loss of appetite (anorexia) in many patients and it is excreted at a very high rate from the body.² In addition, the development of drug resistance after a continued drug dosage limits the long-term use of this drug. The reason for all the detrimental side-effects of any chemotherapeutic drug, including cisplatin, is centered around the drug's inability to distinguish between healthy and cancerous cells. To overcome these negative aspects associated with chemotherapy, new antineoplastic materials are continuously being synthesized and evaluated. New methods of delivering an active drug to a cancerous growth are being developed,³ combination therapy has been investigated in the hope of finding synergistic effects⁴ and even completely new methods of fighting cancer such as photodynamic therapy have been developed.⁵

In recent years a new dimension in drug research has developed as a result of studies on the potential pharmacological benefits obtained by anchoring pharmaceutical agents to suitable polymeric carriers possessing solubility in water.⁶ Polymers as drug carriers may

significantly enhance the therapeutic effectiveness of the polymer-bound drugs as compared to the free agents in terms of:

- a) accelerated and unencumbered distribution in the aqueous central circulation system of the body;
- b) reducing the risk of premature excretion and even degradation;
- c) cell entry *via* endocytosis, a cell penetration mechanism generally unavailable to small molecules but highly desirable in therapy;
- d) restricting the drug concentration to the gap between toxic and minimum effective levels and;
- e) achieving an enhanced depot effect through delayed drug release from the polymer-bound conjugates.

The properties of a suitable polymeric drug carrier include⁷ bio-compatibility, water solubility, it must have a large number of drug attachment sites, binding of the drug to these drug anchoring sites must proceed easily without side reactions to generate a biodegradable bond between drug and polymer, it must have a sufficiently large molecular mass to prevent quick excretion from the body yet it must itself be biodegradable to allow ultimate elimination of the spent polymer carrier from the body after its payload of drug has been delivered to the target site and it must be non-toxic, non-antigenic or non-provocative in any other respect.

In terms of new antineoplastic material (i.e. compounds that have cytotoxic properties but are not in clinical use), it was shown in this laboratory that ferrocene-containing β -diketones and alcohols containing a ferrocenyl group have very promising ID_{50} values.⁸ The chemotherapeutic effectiveness of ferrocene-containing carboxylic acids and the alcohol derivatives was shown to be directly related to the formal reduction potential of the ferrocenyl

group. In particular, for the carboxylic acid derivatives, activity was only observed if the formal reduction potential of the ferrocenyl group was less positive than 0.217 V vs. a saturated calomel electrode (SCE).⁹ For both the alcohols and the carboxylic derivatives, activity increased as the formal reduction potential becomes less positive. Furthermore, by comparing the activity of 3-ferrocenylbutanoic acid with that of the same drug, this time anchored onto a water-soluble poly-aspartate carrier,⁹ it was found that the polymer bound drug was almost one order of magnitude (8 times) more effective than the free drug. However, to date, no attempt was successfully made to anchor amines bearing a ferrocenyl group onto a water-soluble drug carrier.

With this background, the following goals were set for this study:

1. Synthesis of a water-soluble, linear, biocompatible polymeric drug carrier capable of undergoing coupling reactions to bind amine-functionalised ferrocene derivatives.
2. Development of a general technique to synthesize a series of ferrocene-containing amines of the type $\text{Fc}-(\text{CH}_2)_n-\text{NH}_2$, with Fc = ferrocenyl, and $1 \leq n \leq 4$.
3. Development of techniques to anchor the amines of goal 2 on the polymeric drug carrier of goal 1.
4. To investigate the electrochemical properties of the ferrocene-containing amines, their precursors as well as the electrochemical properties of the polymer-bound ferrocenyl derivatives.
5. To perform as many cytotoxic test on the new metal-containing compounds that was synthesised in this study as was possible within the timescale and framework of a suitably bordered MSc study.

CHAPTER 2

LITERATURE SURVEY

2.1 Introduction

Apart from radical surgery, two major techniques used for the treatment of cancer are radiotherapy and chemotherapy. Both methods can induce disabling and life-threatening side effects mainly because they destroy indiscriminately normal and healthy tissues.¹⁰ Because chemotherapeutic agents are actually poisons, the defence mechanism of the body (reticuloendothelial system) recognise them as such and try to remove them as fast as possible. A high rate of excretion from the body, however, often proves to be very detrimental in chemotherapy. This often causes the concentration of the chemotherapeutic agent in the body to oscillate between successive administering times (which may even be daily) from values notably larger than IC_{50} concentrations to values so small that the drug has no effect on the disease (IC_{50} = 50% inhibiting dosage, i.e. drug concentration that induces 50% cell killing). Cisplatin,^{11,12} one of the most successful chemotherapeutic drugs of the past decades, is an example of a chemotherapeutic agent which suffers from this phenomenon. The excretion profile described above explains many of the negative side effects associated with chemotherapy. Many chemotherapeutic agents are also moderately carcinogenic and can induce, for example, lung cancer in a patient¹³ over a period of 15 years. The most important limiting factor in the clinical use of most, if not all, chemotherapeutic drugs is therefore associated with the inability of the drug to distinguish between the normal and cancerous cells.⁶ To combat these negative aspects associated with many chemotherapeutic drugs, new antineoplastic materials are continuously being synthesized and evaluated,¹⁴ combination therapy has been investigated in the hope of finding synergistic effects,⁴ completely new ways of fighting cancer, such as photodynamic cancer therapy,⁵ is being investigated, and new methods of delivering an active drug to a cancerous growth are being developed.³

2.2 Polymers as drug carriers

2.2.1 Introduction

Numerous chemotherapeutic drugs are dose limited due to poor solubility in aqueous media or due to the severe side effects they exhibit at high concentration. The therapeutic effectiveness of these agents is often diminished by their inability to gain access to the infected site at an appropriate dosage. In addition, the metastatic nature of the tumour cells requires that total tumour cell destruction be achieved early in treatment, before resistance to the drug is developed, or a mutation in the cancer cell line will render the drug totally ineffective. The multitude of problems associated with chemotherapy implies that vehicles capable of carrying the cytotoxic agent in a highly concentrated form exclusively to the tumour target, thus allowing for efficient cell kill while largely sparing surrounding healthy tissues, are required. Synthetic water-soluble polymeric drug carriers may be tailored to fulfil this role. Therefore, part of the main theme of this study is to synthesise water-soluble macromolecules or polymers that may be used as drug carriers.

Regarding drug delivery devices that will improve cancer cell specificity of a drug during chemotherapy, what is needed, is a transporting device which actually behaves as a shield or a protective envelope into which the drug may be placed. While attached to, or absorbed by this transporting device, the drug should be totally inert in a biological environment. The administered transport device, with the drug attached to it, should then be capable of utilising the bodies central circulation department to be distributed through the body in order to reach or gain access to a cancerous growth without being recognised as undesirable by the bodies own defence mechanism, the reticuloendethelial system.¹⁵ The carrier device should be capable of distinguishing between healthy and cancerous cells, that is, it should be absorbed by the cancer cells only, not by the healthy cells. Once absorbed by a cancer cell, the

polymeric carrier should be degraded to release its payload of drug inside a cancer cell. Once released, the drug should again be active and thus be capable of killing the cancer cell.

2.2.2 A possible drug delivery route associated with drug carriers

The goal of any controlled drug delivery system is to assure the transit of drug molecules from the site of administration to a specific location on or within a particular population of cells within a particular organ or body tissue. For the purpose of this thesis, drug carriers are understood to be soluble synthetic polymers or macromolecules. However, they may also be natural occurring compounds such as antibiotics or other biological macromolecules, liposomes and polymeric microspheres or microbeads. Several different routes of administration are available for drug delivery systems: oral, intravenous intraperitoneal, subcutaneous, intrathecal and even direct injection into the diseased or infected tissue. For the majority of cancers, though, one might expect that it is best to utilise the body's own distribution network, namely the vascular system, to deliver a drug to the target tissue or organ in question.

The lumen of the vasculature is circumscribed by a layer of endothelial cells, which serve to demarcate the vascular and extravascular compartments and to regulate the flow of solute molecules (especially macromolecules with relative molecular mass in excess of 5 000-10 000 between these compartments^{16,17} *via* a route called transcytosis. In most of the capillary endothelial cells, which allows access into specific cells, a layer of dense fibrillar material, which is termed the basal lamina or the basement membrane, subtends the capillary endothelium.¹⁷ The ability of macromolecular drug-carrier complexes to transit the basal lamina of the capillary endothelia depends not only on the size and charge of the carrier complex, but also on specific macromolecular binding characteristics.¹⁸

In order for a drug-carrier complex to successfully reach target cells within a certain tissue, it must not only be able to exit from the circulation and pass through the endothelial and basal lamina barriers, but it must also be able to escape *en route* the grasp of the reticuloendothelial system, the body's disposal mechanism for foreign particles and macromolecules. The reticuloendothelial system is comprised of a set of mononuclear phagocytic cells. These cells originate from precursors in the bone marrow, enter the circulation as monocytes, then pass into macrophages¹⁹ and perform a variety of functions.^{20,21} The macrophages are crucial components of the body's defence system: they are involved in antibody responses *via* the processing and presentation of antigens, they are responsible for secreting factors which regulate the function of lymphoid cells²² and finally they are themselves effector cells which can acquire the capacity to attack and destroy pathogens and tumour cells.²³

One of the simplest functions of macrophages (sometimes called professional phagocytes) is the uptake of foreign particles and macromolecules. The efficiency of these phagocytic processes is extraordinary. For example, a mouse peritoneal macrophage can "eat" its own weight in liposomes (that may contain the drug carrier and drug) in 1 hour.¹⁵ Macrophages take up not only particles, but also certain proteins when these are capable of interacting with receptors on the macrophage surface. Therefore, if a suitable polymeric drug carrier resembles proteins, they, together with their payload of drug, may be removed from the body. Another aspect is that many of the proposed protein-type drug carriers are likely to be rather immunogenic themselves, leading to the formation (upon repeated use) of anticarrier antibodies and subsequent clearance of the carrier-antibody complexes by the reticuloendothelial system.

The removal of particulate or macromolecular drug carriers by the reticuloendothelial system has two unfortunate consequences. First it reduces the amount of drug available for interaction with target sites. Second and perhaps the more important, it poses the danger of selectively destroying macrophages, thus generating grave consequences for the body's defence system (it may actually inactivate or destroy it). After passing the endothelial and basement membrane barriers and escaping the reticuloendothelial system, drug-carrier complexes must then reach their ultimate site of action within a specific cell population. The problem of drug "targeting", or of obtaining interaction of the drug-carrier complex with a particular set of cells, has received a good deal of thought and attention.^{24,25,26} The movement of proteins and other macromolecules between various compartments within a cell, the so-called "sorting problem", has emerged as one of the central themes of cell biology. A large number of reviews and research articles have been devoted to the processes of intracellular and intercellular movements of proteins.^{24,25,26} Cells possess at least three distinct processes for the uptake or internalisation (i.e. endocytosis) of particulate and dissolved macromolecules.

The first is phagocytosis where the cell internalizes a large particle (1000 Å or greater) by engulfing it into a membrane-bound vesicle. The latter is then internalised and ultimately fused with lysosomes. Phagocytosis is largely an adaptation of specialised host defense cells such as macrophages and granulocytes.²⁷ Secondly, cells can also internalise material by "non-specific" or "fluid phase" pinocytosis. Here cells pinch off and internalise small fluid-filled plasma membrane vesicles of about 250 Å in diameter. These vesicles, like phagocytic vacuoles, ultimately fuse with and deliver their contents to lysosomes. The third process may be labelled receptor-mediated or adsorptive pinocytosis. Here, the cellular receptors for a variety of polypeptide hormones, growth factors, and serum proteins undergo a process of

continuous recycling from the plasma membrane to the cell interior and back again. If the polymeric drug carrier has sequences that can be recognized by these cellular receptors, they may bind to cell surfaces and thus be internalized by adsorptive pinocytosis. Any potential drug carrier must be compatible with any one of these three possible processes, which are demonstrated in Figure 2.1.

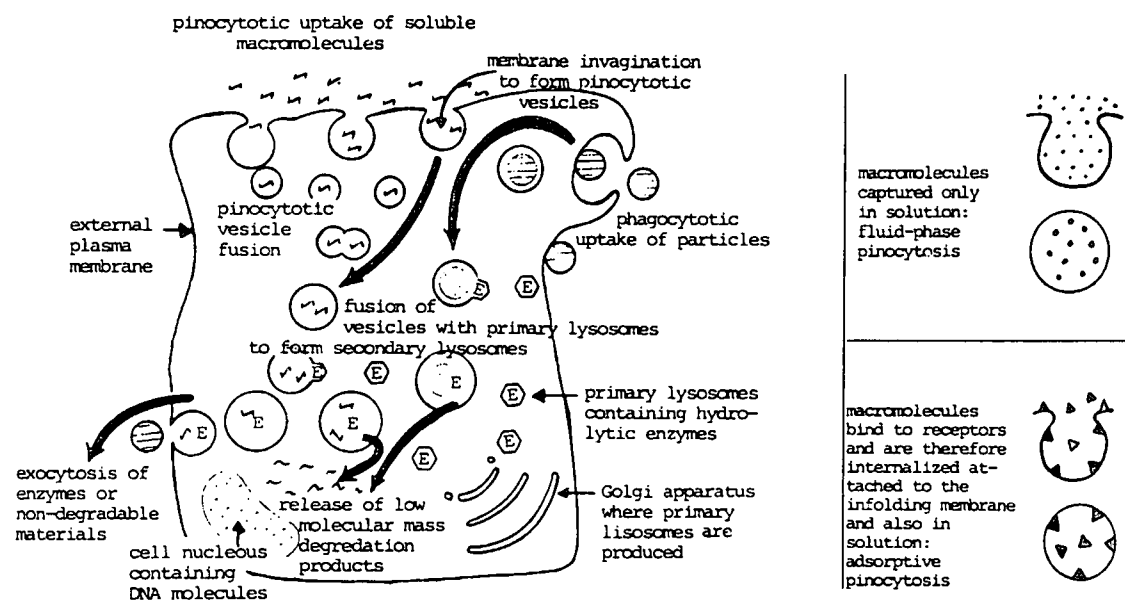


Figure 2. 1 Cellular pinocytotic uptake of polymers (Figure from Ref 6).

Release of the drug from the dissolved (adsorbed) polymeric drug carriers inside the cell should occur by enzymatic hydrolysis of biodegradable bonds (e.g. amide bonds constructed from L-amino acids) after fusion of primary lysosomes containing more than 50 hydrolytic enzymes that are generated in the Golgi apparatus with the pinocytotic vesicles containing the dissolved macromolecules.²⁸ After polymer degradation, the low molecular mass products are released and pass through the secondary lysosome membrane into the cytoplasm, either for re-utilisation or for removal from the cell.²⁹ The release of low molecular mass products, which must now include the released drug itself, allows targeted access of the drug to the cell nucleus containing DNA. If a polymeric drug carrier can be targeted to a cancer cell it follows that the released drug will exclusively destroy a cancer and not any normal healthy

cells. Non-biodegradable macromolecules accumulate within secondary lysosomes and are slowly released by exocytosis. The distribution and elimination patterns of a macromolecular system depend mainly on its physico-chemical properties, such as molecular size, charge, hydrophilic or lipophilic properties, shape, flexibility and deformability and the anatomical characteristics of endothelial capillaries.^{30,31,32} For example, cationic macromolecules are widely distributed in the liver due to the presence of discontinuous endothelium capillaries, which presents a wide contact surface area with hepatic parenchymal cells, and to ionic interactions with the negatively charged cell surface.³²

2.2.3 Synthetic strategies and properties of polymeric drug carriers

The polymeric drug carriers should meet the following structural prerequisites:³³

1. They should be biodegradable by virtue of biofissionable bonds (peptide, nucleotide or sugar bonds) that bind monomers in the polymeric main chain together.
2. Reactive functional groups must be provided as binding sites for drug attachment. The binding site should preferably be separated from the polymer main chain by spacer segments so as to make them more accessible during drug anchoring reactions.
3. In order to meet the pharmacological requirement of *in vivo* drug release from the carrier, the spacer segment must comprise one or more biofissionable groups, such as amide or urethane, sugar or nucleotide groups. At least one of these links must be sufficiently remote from the main chain to permit the approach of proteolytic enzymes engaged in the bond-breaking process.
4. A sufficient number of hydrosolubilising groups should be contained in the polymeric structure in order to provide complete water-solubility of the polymer-drug conjugate.

Ideally, macromolecules designed to function as drug carriers should be easily synthesised at low cost, highly water-soluble, non-toxic, non-immunogenic and well characterised from the physico-chemical point of view.³⁴ Synthetic polymers with a C-C backbone are generally not biodegradable. For a synthetic polymer to be enzymatically degradable, the active site of an enzyme must undergo a number of interactions with the substrate leading to the formation of an enzyme-substrate complex. This process will be possible if relatively short synthetic polymer chains or monomers are linked to each other by bonds susceptible to enzymatic attack.^{35,36,37}

The general strategy to synthesise water-soluble polymeric drug carriers and to anchor potential drugs covalently to them is schematically demonstrated in Figure 2.2. To generate a polymeric backbone, step reaction polymerization reactions between monomers of the AB or AA and BB type (A and B represent functional groups that are suitable to generate biodegradable -ab- bonds between monomeric units) are particularly useful. The advantage of a polymeric drug carrier with a biodegradable main chain is that the rate of scission of the bonds can be controlled by small structural changes and by changing the amount, and the type of biodegradable-ab-bonds, and by changing the size of monomer subunits.

Solubility in aqueous media is required for drugs to be administered by intravenous or intracavitary techniques, for example, in the treatment of cancer by chemotherapy. For this purpose aqueous solubilising agents should be anchored to the polymeric backbone. Following this, the synthetic polymer must be tailored to have a number of functional groups available for drug binding. This is labelled as site C in Figure 2.2. In order to covalently bind a drug to the drug carrier at site C, the drug itself must be modified in such a way that it can react with this site. Therefore, the drug itself needs to be functionalised in such a way that it

contains an active site D capable of interacting with site C. It stands to reason that the chemical methods of drug binding to polymers must be designed so as to accommodate the particular solubility behaviour of the polymeric carrier

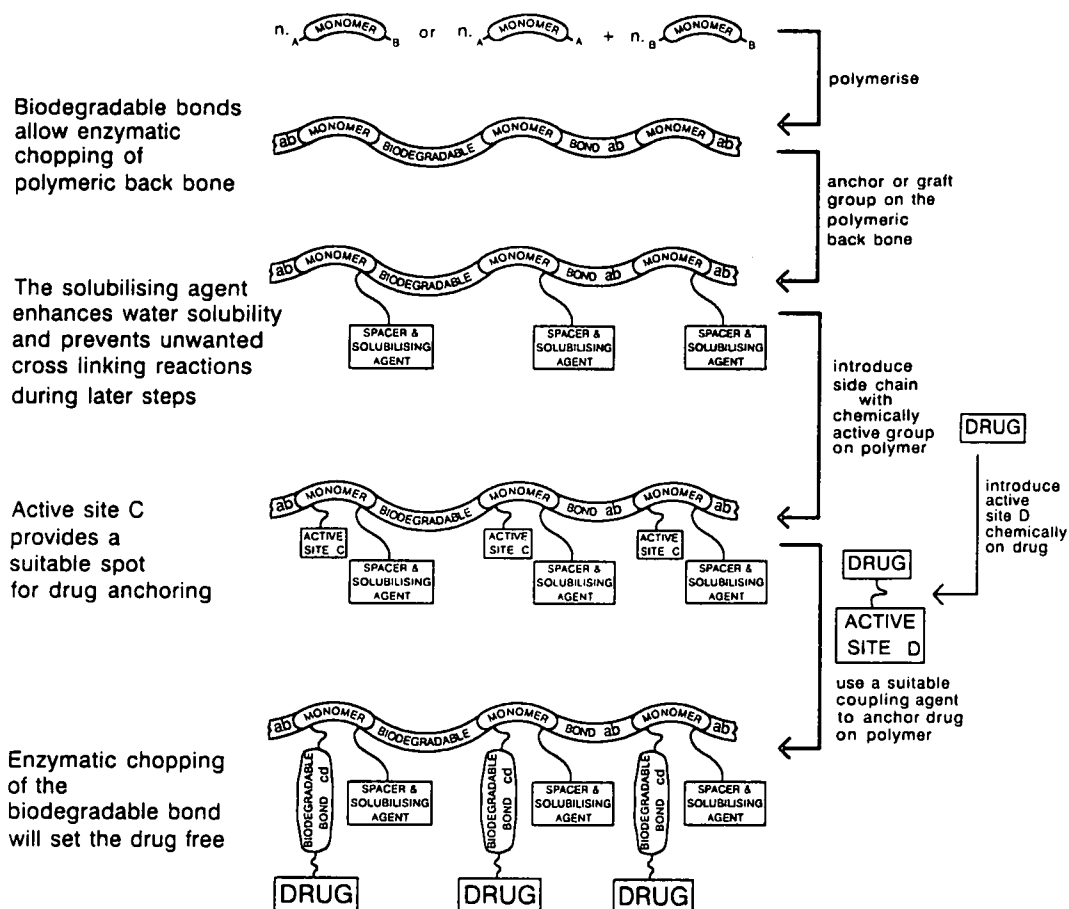


Figure 2.2 General guidelines for the synthesis of a polymeric drug carrier/drug conjugates.

Hence, experimental conditions must be developed that will *inter alia* permit drug coupling reactions in aqueous or mixed aqueous-organic media as the drug itself is designed to be exclusively water-soluble.

Attachment of drugs to macromolecular carriers alters their rate of excretion from the body (it may even prevent it) and provides the possibility for sustained release over a prolonged period. Because it limits the uptake of drugs by cells to the process of endocytosis, it provides the opportunity to direct the drug to the particular cell type where its activity is

required. Owing to the extensive chemistry associated with the process schematically demonstrated in Figure 2.2, it follows that synthetic polymers can more easily be modified to meet a certain desired need, here drug carriers, than natural polymers because the former are more susceptible to chemical modifications. This implies, for example, that synthetic polymers can be tailored to carry a high payload of drug but natural polymers not.

In conclusion then, the preparation of the ideal polymeric carrier requires optimisation and control of a number of properties of the polymer that is biologically important. These include *inter alia*, biodegradability of the backbone by the choice of monomer linking bonds, control of the number of the drug attachment sites, synthetic methods for drug anchoring and the regulation of non-specific binding by charge association (charge-hydrophobicity effect). Another important parameter in the determination of the biological activity of a polymer is the molecular mass. For example, the rate of elimination of the polymer from the blood stream, the deposition in organs³⁸ as well as the rate of uptake of the polymer into the cells by pinocytosis,³⁹ are influenced by both molecular mass and molecular mass distribution.

Now that some general aspects surrounding polymeric drug carrier devices have been discussed, it is appropriate to look at a small set of actual compounds that was made to fulfil the requirements that was elaborated on in the sections above.

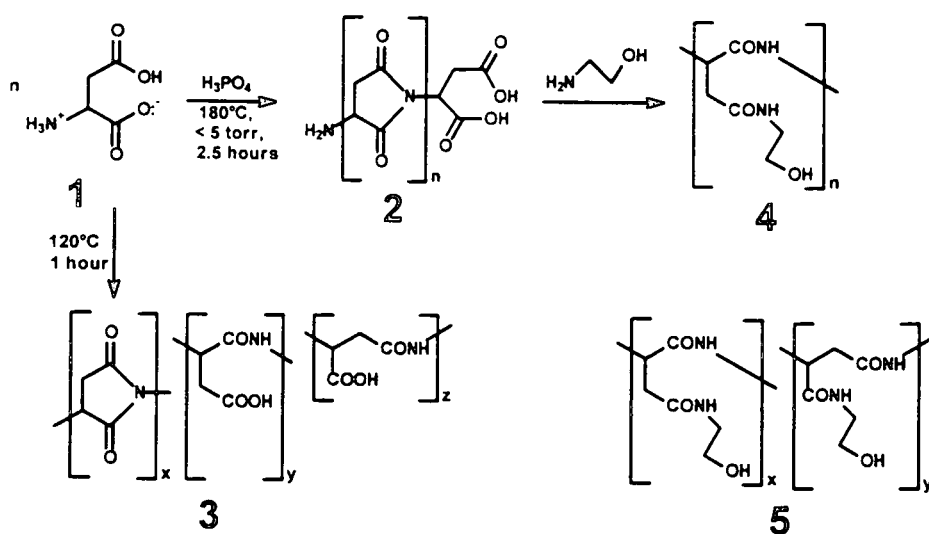
2.2.4 Selected examples of polymeric drug carriers and polymeric drug carrier/drug conjugates

Water-soluble poly(L- α -amino acids) often show immunogenic properties. Nevertheless, they are attractive choices of carriers since they are easily biodegradable. Also, copolymerisation of amino acids with especially ethylene glycols, has successfully eliminated

immunogenic properties of poly(α -amino acids).⁴⁰ Several attempts have been made to synthesise non-immunogenic poly(L- α -amino acids) for biological use.⁴¹ Of these, derivatives of poly(aspartic acid) are central to this study. Neri and Antoni⁴² polymerised aspartic acid, 1, thermally to polysuccinimide, 2, of molecular mass 57 000 within 2,5 h at 180°C according to Scheme 2. 1. It was also demonstrated in this laboratory that less harsh polymerisation conditions to convert aspartic acid to polysuccinimide, 2, (120°C, 1 h) lead to a polymer in which not all the aspartic acid molecules that are polymerized underwent cyclization. Part of the monomer remained in the uncyclized state, structure 3. The five-membered succinimide ring in 2 can afterwards be opened by nucleophilic attack with, for example, amines.

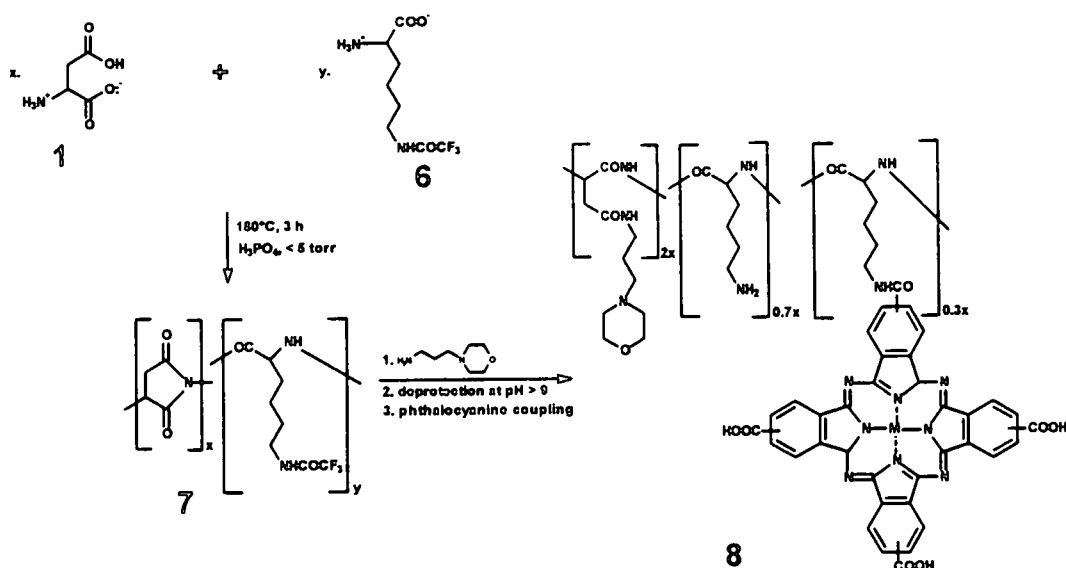
In this way, the water-soluble biocompatible polymer, 4, α,β -poly(N-2-hydroxyethyl)-DL-aspartamide^{43,44} of relative molecular mass 70 000 Mr was obtained by a simple reaction of ethanolamine with a polysuccinimide, 2. The polymer, 4, is so biocompatible that it has been proposed as a blood plasma expander.⁴⁵ In a potential drug anchoring step, the OH functional group of 4 can be reacted with a drug that is functionalised to have either a carboxylic acid or isocyanate group (reactions not shown). Some anti-inflammatory and antiviral drugs have been covalently linked to 4.⁴⁵

Peptidyl carbamate molecules, which are human leukocyte elastase (HLE) inhibitors, have also been linked to 4 and the resulting synthetic macromolecular system maintained the *in vitro* HLE inhibitory capacity of free low molecular weight drugs.⁴⁵



Scheme 2. 1 The effect of different experimental conditions on the polymerization of aspartic acid and α,β -Poly(N-2-hydroxyethyl)-DL-aspartamide synthesis, a proposed blood plasma expander. It should be realised that 4 actually consists of a mixture of α and β isomers but for simplicity, in this study only the α -isomer will constantly be shown.

Swarts and Maree⁴⁶ co-polymerised aspartic acid, 1, with N^{E} -trifluoroacetyl-L-lysine, 6,⁴⁷ the target co-polymeric drug being, 7, (Scheme 2.2) with an x:y ratio of 2:1. However, in practice, an x:y of 7:1 was found on 7 and ring opening reactions of the succinimide fraction of 7, removal of the trifluoroacetyl protecting group has lead to a polymer which was water-soluble and has side chain, containing an amine functional group as drug anchoring site. Maree utilized 7 to synthesise the water-soluble conjugate 8, which contains the phthalocyanine moiety. The phthalocyanine moiety is active in photodynamic cancer therapy provided $\text{M} = \text{Zn}$ or Al . It was established^{48,49} that drug anchoring becomes progressively easier with more methylene spacers separating the polymer from the functional group that will be utilised for anchoring purposes. Polymer 8 has 4 CH_2 spacer groups between polymer main chain and drug anchoring site.



Scheme 2.2 The synthesis of a co-polymer of lysine and aspartic acid* to which a phthalocyanine group has been anchored. M = Co or Zn. (See footnote).

Molz *et al.*⁵⁰ synthesised compounds containing the cytostatic bis(2-chloroethyl)amino group linked *via* urethane or O-acylated hydroxamic acid bonds to polymerisable methacrylic acid derivatives. Co-polymerisation with hydrophilic monomers such as 2-(methyl-sulfinyl)ethyl methacrylate yielded biologically active compounds of the structure, 9, 10 and 11 in Figure 2.3.

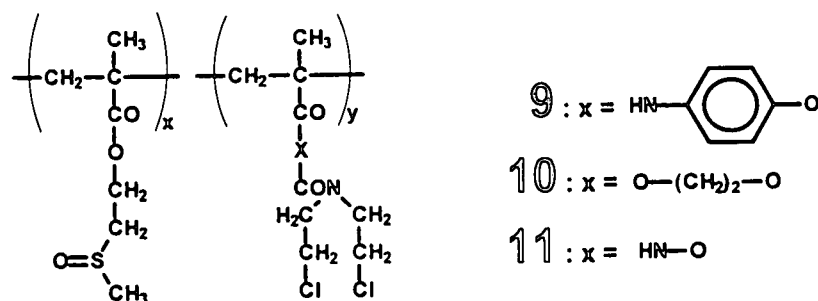


Figure 2.3 Ester, amide, urethane and O-acylated hydroxamic acid bonds were utilised to anchor the cytotoxic agent bis(2-chloroethyl)amine onto a methacrylate based polymeric carrier. The main chain of this polymeric system is not biodegradable.

* Although not indicated in any scheme in this study, it should be emphasised that all co-polymers, which were prepared, consisted of backbones in which the repeat units are expected to follow a random distribution.

Since it is known that dimethyl sulfoxide (DMSO) enhances the penetration of pharmaceutical agents through the skin, Hofmann *et al.*⁵¹ synthesised the polymer poly[2-(methylsulfinyl)ethyl acrylate], **12**, utilising an ester bond in the side chain for anchoring purposes to see if polymeric carriers containing a DMSO moiety could also be transported through the skin. They could not. However, the incorporation of phenolic or tyrosil residues into macromolecules such as **13** greatly increased the rate of pinocytotic capture of poly aspartate derivatives by cells.⁵² (For advantages of pinocytotic capture of polymers, see page 10 – 12. This will also be the process by which the polymers of this study will be internalised in cells).

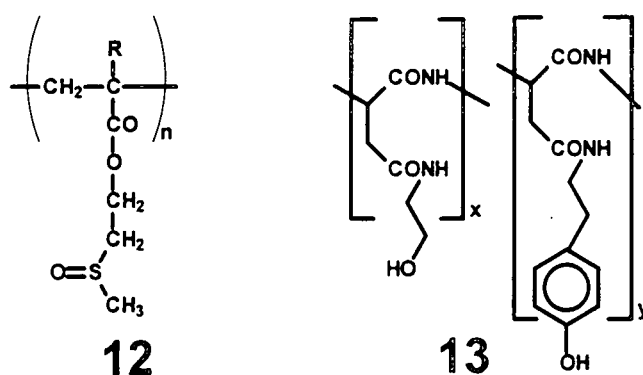
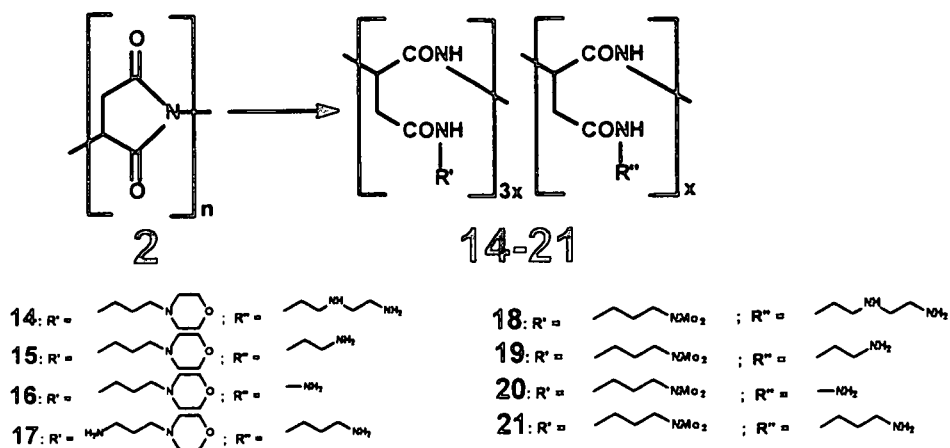


Figure 2.4 Dimethyl sulfoxide and phenolic residues incorporated on polymers **12** and **13** respectively.

Neuse and Perlwitz⁵³ synthesised several derivatives of aspartic acid *via* polysuccinimide, **2**, to obtain a series of drug carriers (Scheme 2.). Each of the substituents was chosen in such a manner that certain desirable properties were built into the polymeric drug carriers.



Scheme 2.3 Potential polymeric drug carriers.

The function of the R' substituent is mainly to enhance the water solubility of the carrier polymer. R'' side group is chosen with the particular aim of providing the all-important active site onto which a desired drug could ultimately be anchored. Neuse *et al*⁵⁴ also reported the anchoring of poly(ethylene oxide) (PEO) chains onto drug carrier-type polyaspartamide to give polyampholyte 22 and 23 (Figure 2.5).

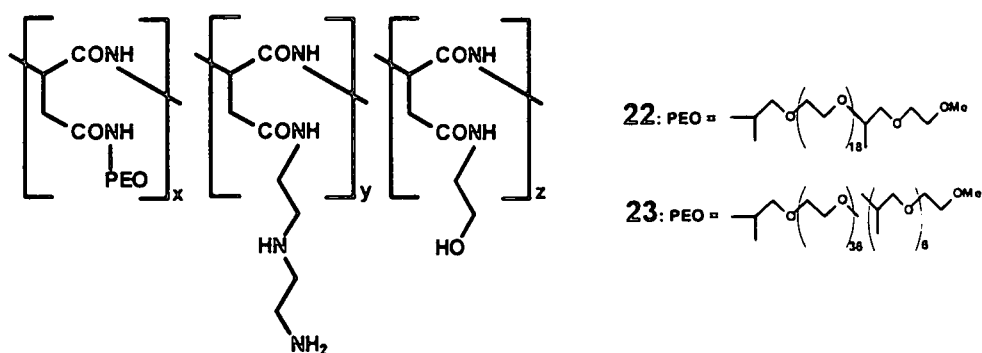


Figure 2.5 Grafting of poly(ethylene oxide) onto polyaspartamide.

The purpose of this was to increase the carrier hydrophilicity, reduce immunogenicity and enhance resistance to both protein binding and capture by the reticuloendothelial system with concomitant prolonging of residence time in serum circulation.

As this study is concerned with the anchoring of the ferrocenyl group as antineoplastic agent on a polymeric drug carrier, it is appropriate to discuss a few literature cases of polymer-bound ferrocene complexes. The high success rate and well-behaved manner in which polysuccinimide **2** was converted to various polyaspartamide (described in the preceding paragraph) made nucleophilic attack of an aminated ferrocene such as 1-ferrocenylethylamine^{55,56} (for structure, see Scheme 2. 6, page 29, compound **50**) on **2** to give polymer, **24**, (Figure 2.6), an obvious choice. This would imply that a drug moiety like ferrocene could be anchored directly on a carrier polymer. However, the reaction was found to be extremely sluggish. The ferrocenyl content of **24** was less than 5% as determined by ¹H-NMR spectroscopy even after prolonged reaction times (48 h).⁵⁷

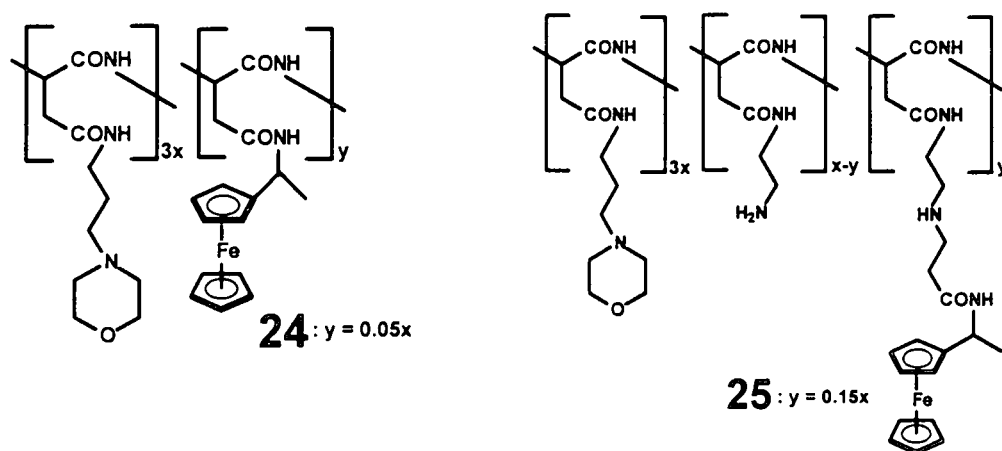


Figure 2. 6 Attempts to anchor 1-ferrocenylethylamine directly on polysuccinimide derivatives (compound **24**) or *via* an acrylated intermediate on polymer **15** to obtain **25** were inefficient reactions.

N-(1-ferrocenylethyl)acrylamide,⁵⁷ could be anchored only 15% successfully on **15** to give polymer, **25**, Figure 2. 6. When polymer **15** was acrylated and then reacted with 1-ferrocenylethylamine, polymer **26** was obtained with 0.4x equivalents of the ferrocene-containing drug successfully anchored (Figure 2.7).

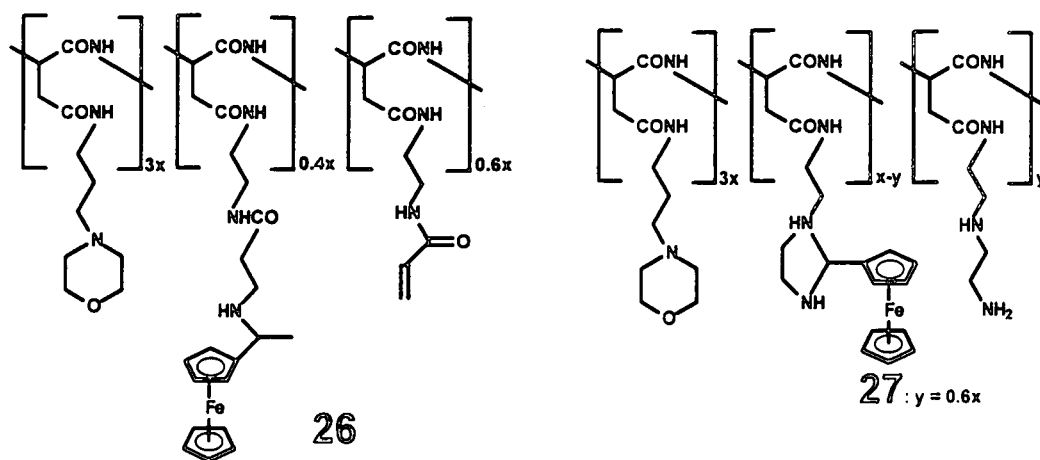


Figure 2. 7 Addition of 1-ferrocenylethylamine onto an acrylated derivative of 15 to give 26 was only 40% effective. Ferrocenecarboxaldehyde does not interact with 14 to give Schiff base compounds. Rather, the cyclic imine derivative 27 is formed.

The lack of nucleophile strength of 1-ferrocenylamine was judged as the cause for the poor success rate of anchoring this particular amine-containing ferrocenyl derivative onto the carrier polymer, although steric factors may also play a contributing role. The described observations surrounding the difficulty to anchor 1-ferrocenylethylamine onto polymeric drug carriers such as 15 was the reason why in this study several ferrocene-containing amines were synthesised and why methods of anchoring them onto a polymeric drug carrier were investigated. When ferrocenecarboxaldehyde⁵⁸ was allowed to react with 14 to give polymer 27 (Figure 2. 7). Only 0.6 equivalents ferrocenyl groups were incorporated in the product 27.⁵⁷ The isolation of 27 rather than the Schiff base product is the consequence of the close proximity of the two amine functional group in the side chain of the present polymeric drug carrier 14.

Another way of anchoring ferrocene on a polymeric drug carrier would, for example, be to anchor carboxylic acid-containing ferrocenes onto an amine-functionalised polymer such as 15 under the influence of a coupling agent. This approach led to the anchoring of a variety of

carboxylic¹⁸ acids on **15**, to give polymers **28** and **29** (Figure 2. 8). The authors found that O-benzotriazolyl-N,N,N'N'-tetramethyluronium hexafluorophosphate is a vastly superior coupling reagent for amide bond formation than N-hydroxysuccinimide or N-hydroxybenzotriazole.

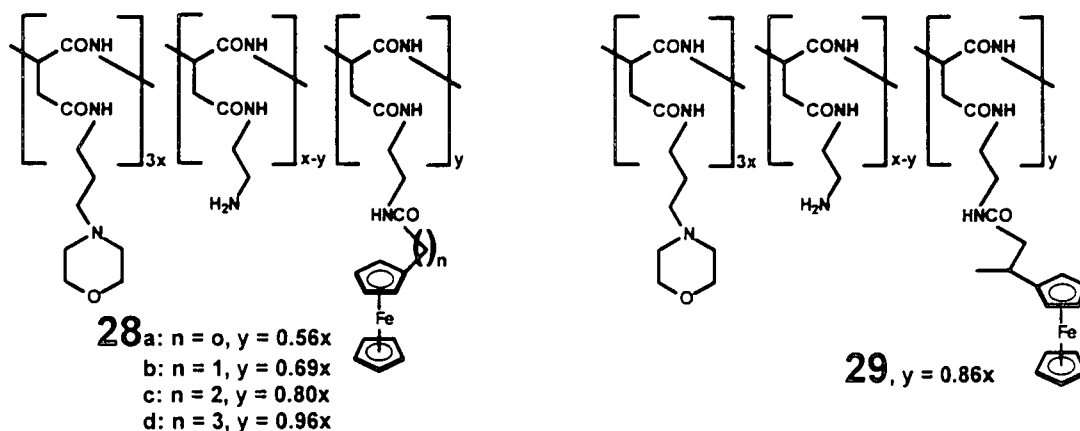


Figure 2. 8 Anchoring of carboxylic acid-containing ferrocene derivatives on the biodegradable drug carrier **15** liberates polymers **28** and **29**.

The synthesis of water-soluble and biodegradable polymer-platinum conjugates were described in which monoamine- and *cis*-diamine-platinum complexes related to the anticancer drug cisplatin were co-ordinately bound to linear macromolecular drug carrier molecules.^{59,60,61,62,63,64} In this regard, the polymer-drug conjugates, **30** - **36**, Figure 2.9, page 24, were synthesised to serve as potential prodrugs in cancer chemotherapy. The rationale behind these syntheses was that improved pharmacokinetic efficacy should lead to selective accumulation of the platinum based drug in cancer tissue by means of endocytotic cell entry. Hydrolytic action on the conjugate in the lysosomal compartment caused the release of the platinum moiety from the carrier for ultimate interaction with the DNA of the affected target cells. Reduced platinum toxicity and increased bioavailability and concomitantly enhanced therapeutic effectiveness are expected for these new polymeric devices.

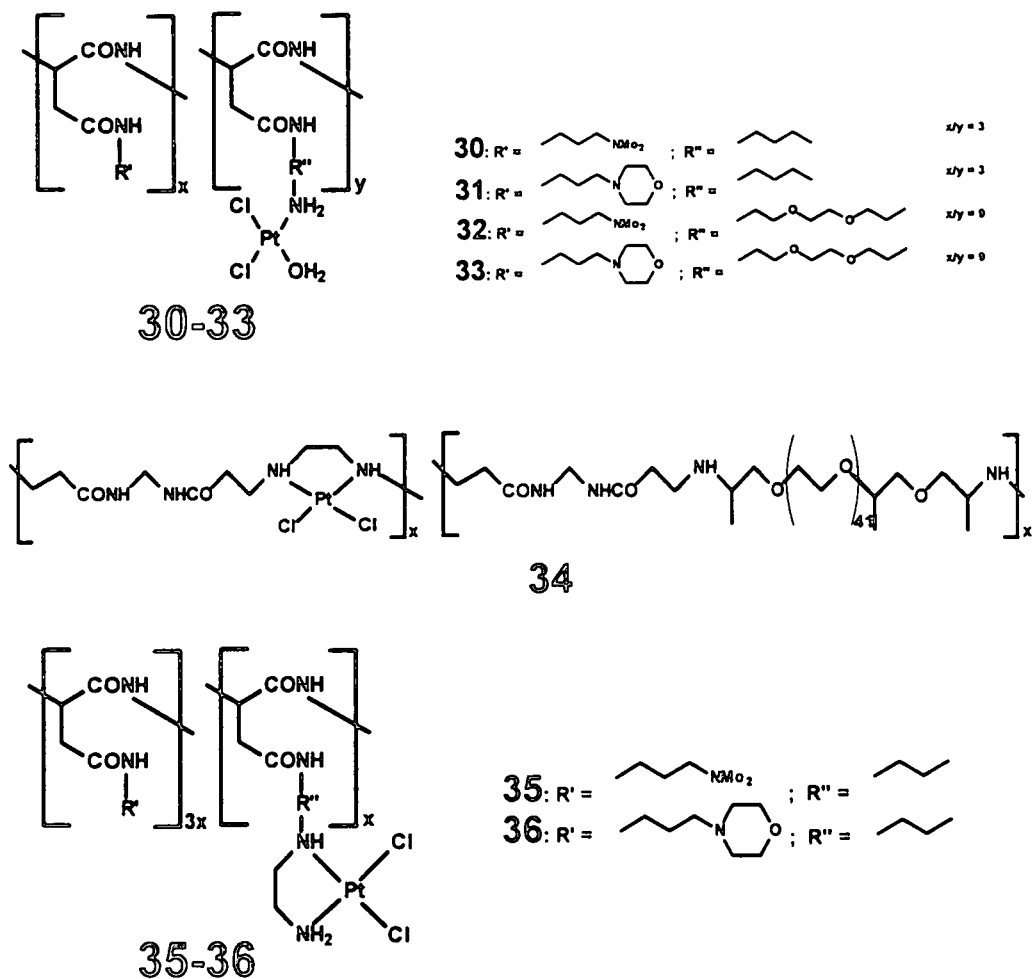


Figure 2.9 Platinum co-ordination with amine-functionalised polymeric drug carriers.

These platinum conjugates were recently tested *in vitro* for antiproliferative activity against human cervical carcinoma (HeLa)^{3,65} and other cell lines with encouraging results (Table 2.1).⁶⁶

Table 2.1 Maximum tolerated dose levels⁶⁶ for polymer-platinum conjugates 30-36.

| Conjugate | Number of mice per test | Nominal Pt content (%) ^b | Max. tolerated dose ^a | |
|-----------|-------------------------|-------------------------------------|--|---|
| | | | Expressed as mg polymer kg ⁻¹ test animal | Expressed as mg Pt kg ⁻¹ test animal |
| 30 | 8 | 18.5 | 2800 | 518 |
| 31 | 5 | 16.5 | 900 | 145 |
| 32 | 8 | 8.4 | 500 | 42 |
| 33 | 9 | 7.2 | 375 | 27 |
| 34 | 8 | 7.4 | 200 | 160 |
| 35 | 5 | 18.3 | <150 | <27 |
| 36 | 4 | 16.4 | <150 | <25 |
| Cisplatin | 2 | 65.0 | 4.6 ^c | 3-4 |

^a For experimental procedure.⁶⁶

^b Mass percentage of platinum in unprotonated polymers.

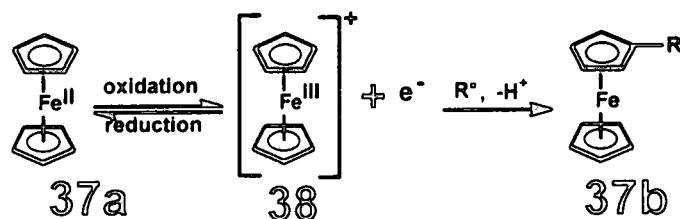
^c Given as mg cisplatin kg⁻¹.⁶⁶ In other investigations,^{67,68} 7.5 mg cisplatin kg⁻¹ was found to be toxic, 4 mg cisplatin kg⁻¹ to be non-toxic,⁶⁹ and 5 mg cisplatin kg⁻¹ to be borderline, causing 40% death⁶⁷ but no death.⁶⁸

For polymer-platinum conjugate, **30**, compared to cisplatin, the conjugate proved less toxic by a factor greater than 100 and for the analogue **31**, the tolerated dose was low although nearly 50 times higher than cisplatin. Results summarized in Table 2.1 indicate that the aminopropylmorpholine-containing complexes, **31** and **36** are more toxic than the dimethylaminopropyl-containing polymers, **30** and **35** respectively. The poly(ethylene oxide)-modified conjugate **34** allows a large tolerated dose while both **35** and **36** were found to be lethally toxic even at the lowest dose level tested.⁶² This led to speculation that the toxicities may have resulted from factors unconnected with the platinum complex structure, such as coagulation or clotting in central circulation department of the tested animal.⁶²

2.3 Ferrocene derivatives

2.3.1 Introduction

With respect to this research program, ferrocene and its derivatives stand at the centre as active drug components that have to be anchored onto a suitable polymeric drug carrier. For this reason it was deemed appropriate to highlight the cytotoxic behaviour of ferrocene and some of its derivatives as well as the chemistry and physical properties of these compounds. For the purpose of this study, electrochemical properties were regarded as an important physical parameter to pursue. Ferrocene **37a** has a remarkable geometry in that it possesses a sandwiched structure in which two cyclopentadienyl rings lie parallel to one another with an iron (II) cation buried in the π -electron cloud between them. The Fe (II) centre is very reluctant to participate in further co-ordination bonds.



Scheme 2.4 Oxidation of ferrocene* **37a** to give the ferricenium cation **38** which can undergo reductive coupling with radicals, R^{\bullet} , to give substituted ferrocenes **37b**.

Ferrocene, **37a**, is readily oxidised to the ferricenium cation, **38**, by hydrogen peroxide⁷⁰ or other oxidising agents. The reverse reaction, reduction of the ferricenium cation to neutral ferrocene, is mediated by NADH,⁷¹ metalloproteins⁷² and other strong reducing agents. The ferricenium cation, **38**, itself an ion-radical species of appreciable stability, interacts readily

* The structure of ferrocene shown in all figures is in the staggered D_{5d} conformation. It can also exist in the eclipsed D_{5h} conformation.

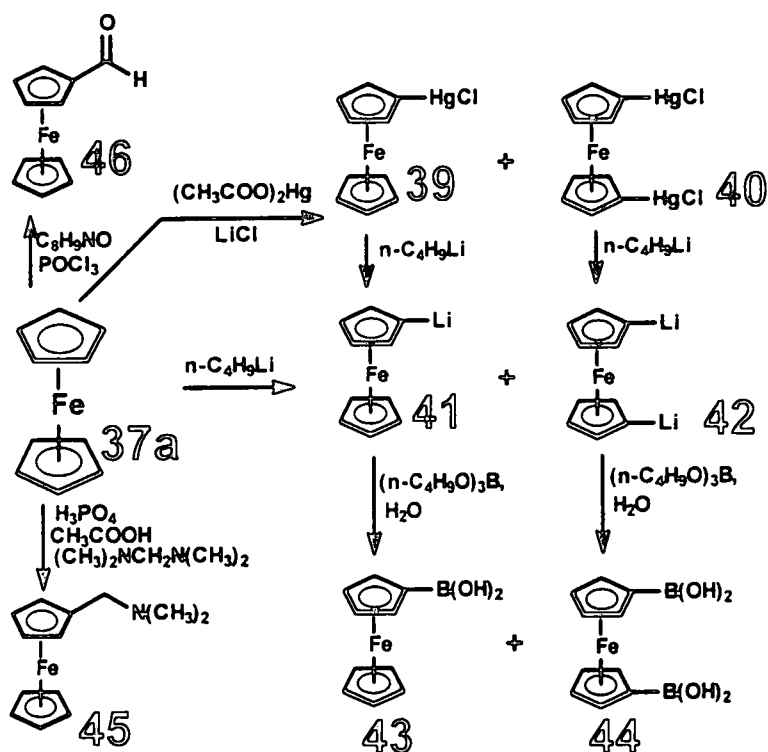
with free radical precursors and a variety of biologically important electron donor compounds as well as with other nucleophiles.⁷³ The low formal reduction potential of ferrocene **37a** in water ($E^{0'} = 0.127$ V vs. saturated SCE at 25°C⁷⁴) renders this metallocene prone to biologically controlled oxidation-reduction processes. Ferricenium cation **38** undergoes recombination reaction with free radicals, which, after proton elimination, leads to substituted, uncharged ferrocene compounds.⁷⁵

2.3.2 The chemistry of ferrocene

The chemistry of ferrocene and its derivatives has been well documented.^{75,76,77,78,79,80} Only selected features related to this study will be discussed below. Most ferrocene-containing compounds may be prepared from only a few different starting materials (Scheme 2. 5). In general these are acylated, dimethylaminomethylated or metalated ferrocene derivatives. All are easily prepared from ferrocene and are sufficiently versatile to be converted to many derivatives.

Both mono- and dilithioferrocene **41** and **42** can be prepared by allowing ferrocene to react with n-butyllithium. However, it is not possible to obtain either one of these two compounds in a pure state⁷⁹ in this way as **41** and **42** cannot easily be separated from each other. However, if chloromercuriferrocene **39** and 1,1'-bis(chloromercuri)ferrocene **40** are first prepared⁸⁰ and then lithiated, it is possible to obtain **41** and **42** as pure compounds^{81,82} because **39** and **40** can conveniently be separated. Reaction of **41** with CO₂ will, for example give ferrocenoic acid. Ferroceneboronic acid **43** and 1,1'-ferrocenediboronic acid **44** are prepared by allowing the correct lithiated ferrocene to react with tri-n-butyl borate⁸³ and are exceptionally versatile precursors in many syntheses.

Aminomethylation of ferrocene to obtain *N,N*-dimethylaminomethylferrocene **45** is possible by means of reacting ferrocene with *N,N,N',N'*-tetramethyldiaminomethane^{84,85} in the presence of acetic and phosphoric acid. The most useful reaction of dimethylaminomethylferrocene **45** is that with methyl iodide to give (ferrocenylmethyl)trimethyl ammonium iodide,⁸⁶ which undergoes S_N^2 displacement of trimethylamine by many nucleophiles. Ferrocenylcarboxaldehyde **46** can be obtained by treatment of ferrocene with phosphorus oxychloride and *N*-methylformanilide in yields as high as 76%.⁸⁷ The aldehyde **46** is reactive to amines to form Schiff base complexes (but this is in contrast to polymer **27**, Figure 2. 7, page 21) or can easily be reduced either by $LiAlH_4$ or $NaBH_4$ to ferrocenyl methanol.

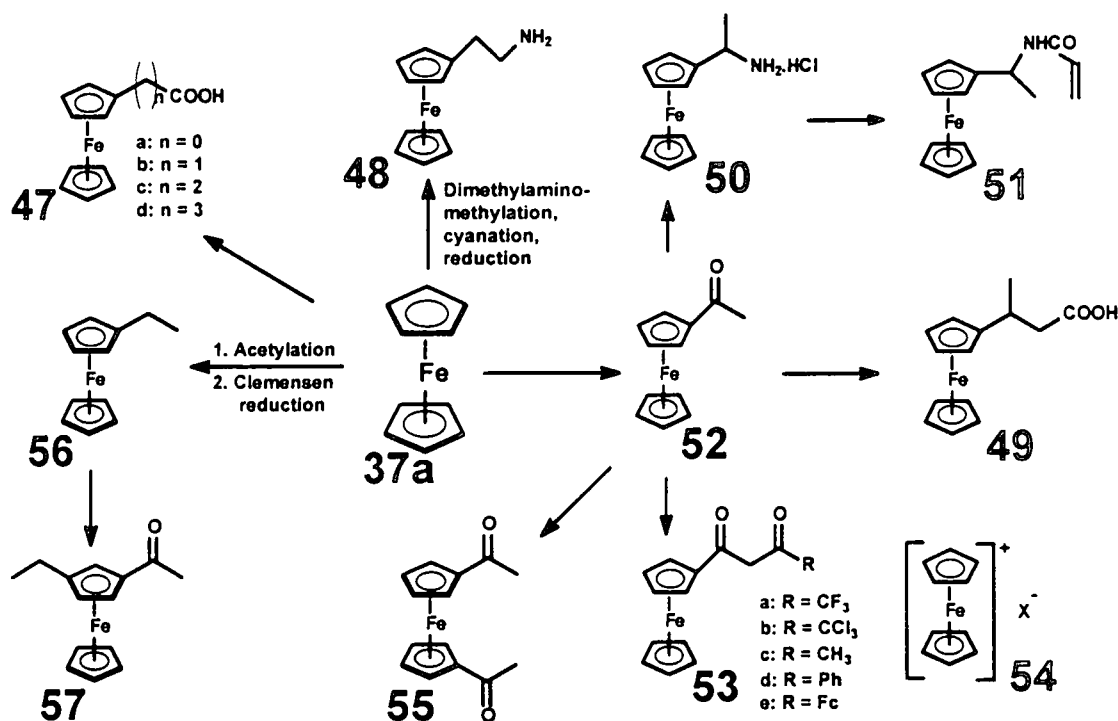


Scheme 2. 5 Precursors to various substituted ferrocenes.

Considering one of the goals of this study, which is the anchoring of the ferrocenyl moiety onto a water-soluble polymeric drug carrier, one of the objectives was to synthesise a series of substituted ferrocenes containing reactive side groups capable of undergoing coupling

reactions with the polymer. The literature provides a fair amount of information on these types of compounds, some of which are shown in Scheme 2. 6.

The enhanced aromatic reactivity of ferrocene makes possible a wide range of electrophilic substitution reactions, which can often be effected under mild conditions.^{75,77} Ferrocene is much more reactive towards Friedel-Crafts acylation^{51,88,89,90} in for example the preparation of acetylferrocene, **52**, than either benzene or anisole.



Scheme 2. 6 Chemistry of ferrocene. $\text{X}^- = [\text{CCl}_3\text{COO}] \cdot 2\text{CCl}_3\text{COOH}$ in 54.

Hydrogen substitution of mono-substituted ferrocenes may or may not proceed with ease, depending on whether the existing substituent is an electron donating, such as alkyl, or an electron-withdrawing substituent, such as acetyl. The former activate the ferrocene complex, and substitution takes place preferably on the same cyclopentadienyl ring that contains the activating substituent as shown in the acetylation of ethylferrocene, **56** to give **57**. The latter de-activates the complex, leading almost exclusively to the heteroannular 1,1'-substituted

products.⁹¹ This is demonstrated by the acylation of acetylferrocene, **52** to give 1,1'-diacetylferrocene **55**. Acyl ferrocenes are useful synthetic intermediates *en route* to other ferrocenes,⁹² as they are capable of undergoing a large variety of reactions such as Clemmensen reduction, lithium aluminium hydride reduction to alcohols and a whole variety of common ketone condensation reactions. Foremost of these may be cited the Claisen condensation of acetylferrocene with an appropriate ester to give the β -diketones **53**.⁹³

Ferrocenoic acid, **47a**, has been prepared in many ways,⁷⁷ the most important being carbonation of lithioferrocene^{94,95} **41**, or by oxidation of acetylferrocene^{77,96} **52** and by the 2-chlorobenzoyl-chloride method.⁹⁷ Ferrocenylacetic acid, **47b**, may be prepared from N,N-dimethylaminomethylferrocene methiodide^{85,86,98} after cyanation followed by hydrolysis of the resulting ferrocenylacetonitrile. 3-Ferrocenylpropanoic acid, **47c**, may be prepared from ferrocenecarboxaldehyde, **46**, and malonic acid⁹⁹ (Doebner condensation), followed by hydrogenation of the intermediate. 4-Ferrocenylbutanoic acid, **47d**, can be prepared by Clemmensen reduction¹⁰⁰ of 3-ferrocenylpropanoic acid.¹⁰¹ 3-Ferrocenylbutanoic acid, **49**, was obtained by the Reformatsky reaction between acetylferrocene and malonic acid followed by catalytic hydrogenation of the obtained intermediate 3-ferrocenyl-3-methylacrylic acid.¹⁰²

Reductive amination of acetylferrocene, **52**, with cyanoborohydride, in the presence of ammonium acetate followed by treatment with HCl, gave 1-ferrocenylethylamine hydrochloride, **50**.^{51,103} Conversion of **50** to N-(1-ferrocenylethyl)acrylamide, **51**, was achieved by allowing neutralised **50** to react with acryloyl chloride in the presence of triethylamine.⁵³ The preparation of amine functionality slightly removed from the ferrocenyl moiety by methylene spacer is demonstrated by the synthesis ferrocenylethylamine, **48**, which is accomplished by the reduction of ferrocenylacetonitrile with LiAlH_4 ,⁸⁶ obtained from

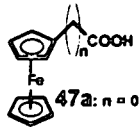
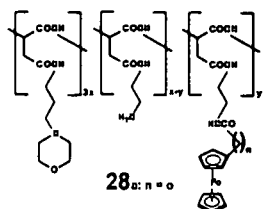
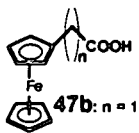
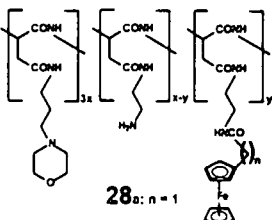
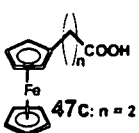
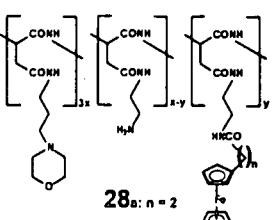
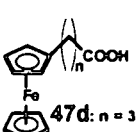
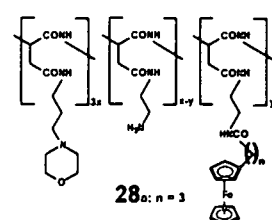
ferrocenylmethyl(trimethylammonium)iodide.^{84,82,98} Finally, Neuse and others¹⁰⁴ have pursued studies in which ferricenium salts, **54**, were prepared and isolated *inter alia* for biological test.

2.3.3 Electrochemical studies

The reversible electron transfer process involving the ferrocenyl moiety (paragraph 2.3.2) has led to many well documented electrochemical studies both in organic media and in aqueous media. The reversibility and high rate of electron transfer of the ferrocenyl moiety invariably leads to $\Delta E_p = E_{pa} - E_{pc}$ close to 59 mV (E_{pa} = anodic peak potentials and E_{pc} = cathodic peak potentials) and i_{pc}/i_{pa} ratios close to 1 (i_{pc} = cathodic peak currents and i_{pa} = anodic peak currents) during cyclic voltammetry studies.¹⁰⁵ Related to this study, Blom *et al*¹⁰⁰ documented the formal reduction potential of the acid series **47a-47d** in acetonitrile and Swarts *et al*⁴⁸ determined the formal reduction potential of the polymer/ferrocene conjugates **28a-28d**. Results are summarized in Table 2.2.

It is important to observe that the closer the carbonyl group on **47a-47d** and **28a-28d** is to the ferrocenyl moiety the more positive the formal reduction potential of the ferrocenyl moiety becomes. It appears that the electron withdrawing properties of the carbonyl group is masked very well when the spacer chain length becomes $-(CH_2)_3-$ in both the acid series **47** and the polymer series **28** (see Figure 2.10).

Table 2.2 Formal reduction potentials^a, $E^{o'} = (E_{pc} + E_{pa})/2$ versus SCE and peak currents ratios^a i_{pc}/i_{pa} for the indicated compounds at 25°C.

| Compound ^b | $E^{o'}$ (V) | i_{pc}/i_{pa} | Compound ^c | $E^{o'}$ (V) | i_{pc}/i_{pa} |
|---|--------------|-----------------|---|--------------|-----------------|
|  47a: n = 0 | 0.57 | 0.916 |  28a: n = 0 | 0.430 | 0.37 |
|  47b: n = 1 | 0.34 | 0.979 |  28b: n = 1 | 0.244 | 0.46 |
|  47c: n = 2 | 0.31 | 0.988 |  28c: n = 2 | 0.204 | 0.72 |
|  47d: n = 3 | 0.29 | 0.966 |  28d: n = 3 | 0.181 | 0.80 |

^a E_{pa} = anodic peak potentials, E_{pc} = cathodic peak potentials, i_{pa} = anodic peak currents and i_{pc} = cathodic peak currents.

^b Conditions for series 47: In CH_3CN containing 0.1 mol dm^{-3} LiClO_4 , substrate concentration = 1 mmol dm^{-3} , see Ref. 100.

^c Conditions for series 28: In H_2O containing 1 mol dm^{-3} KCl , substrate concentration = 1 mmol dm^{-3} , see Ref. 48.

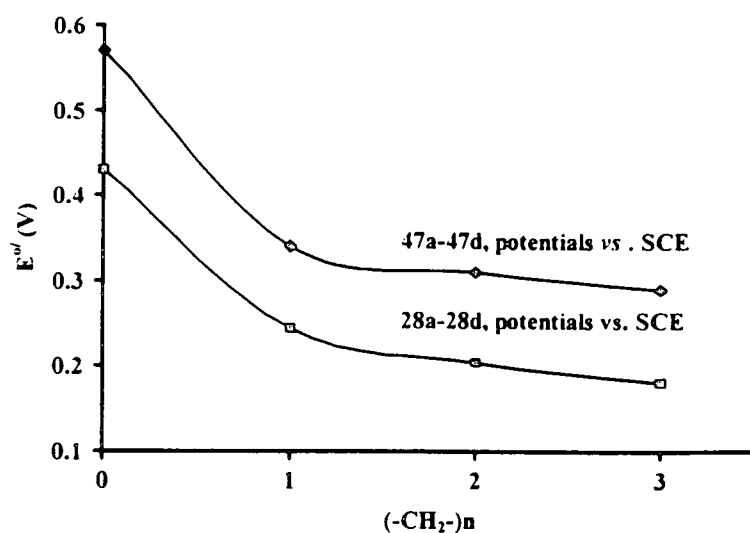


Figure 2.10 Relationship of $E^{o/}$ (V) vs. n , where n = number of CH_2 groups separating a functional groups from the ferrocenyl moiety for the acids series 47 and the polymers 28.

In addition, electrochemical studies on the β -diketones, 53a-53e, were used to determine group electronegativities of the $-\text{CF}_3$, $-\text{CCl}_3$, $-\text{CH}_3$, $-\text{Ph}$ and $-\text{Fc}$ groups⁹³ and Ogata *et al*¹⁰⁶ determined that for ferrocenophanes, the formal reduction potential, $E^{o/}$, of the ferrocenyl group varies linearly according to the equation:

$$E^{o/} = -0.02221N + 0.3654$$

where N is the number of methylene units in each ferrocenophane.

With respect to this study, a series of new ferrocene-containing amines, amides and polymer bound ferrocenes were subjected to cyclic voltammetric studies in aqueous and/or organic media.

2.3.4 Cytotoxicity and mechanism of action of ferrocene derivatives

In 1984 Köpf-Maier *et al*¹⁰⁴ was the first to show that the ferricenium species in compounds such as 54 (Scheme 2. 6, page 29) has appreciative activity against cancer. In particular it

was found that **54** ($X = [\text{CCl}_3\text{COO}] \cdot 2\text{CCl}_3\text{COOH}$) has a ID_{100} (ID = inhibiting dosage) value of 480 mg/kg test animal (mice) weight and that it has a TI value of 2.0 (TI = therapeutic index). Cisplatin also has a TI value of 2.0. The optimum dosage of cisplatin (7 mg/kg mass of test animals) is, however, much less than that of **54**, which act optimally at dosages of 220-300 mg/kg mass of test animal. In contrast, it was found that ferrocene itself it is totally inactive, presumably due to its total lack of aqueous solubility.

In follow up studies, it was shown by Neuse and co-workers¹⁰⁷ that ferrocenylacetic acid, **47b**, induced good to excellent cure rates against human adenocarcinoma, squamous cell carcinoma and large-cell carcinoma of the lung in *in vitro* human tumour clonogenic assays. The latest research on the cytotoxic capabilities of ferrocene compounds has been performed in this laboratory. It was reported in 2001,⁹ for example, that the acid **49** (Scheme 2. 6, page 29) is one order of magnitude more active against Murine EMT-6 cancer cells when anchored on the water-soluble polymer **29** (Figure 2.8, page 23) compared to its cytotoxicity when it is a free monomeric drug. The LD_{90} value for **49** was found to be 500 $\mu\text{g}/\text{ml}$ while for the polymer **29** it is only 60 $\mu\text{g}/\text{ml}$ of active drug species. In addition, from this laboratory was filed a patent (December 2000) which described the cytotoxic properties of the β -diketones **53** and their rhodium and iridium complexes. In particular it was found that the IC_{50} -values of the CF_3 complex **53a** was much more favourable than that of cisplatin, even against platinum resistant cell lines such as COR L23, a sensitive human lung large cell carcinoma cell line. Also, the therapeutic index (TI) of these compounds exceeds 8 compared to the 2 for cisplatin. The most impressive result to date, though was obtained for the rhodium-cyclooctadiene complex of **53a** which showed an LD_{90} value of 0.39 $\mu\text{M}/\text{kg}$ mass of test animal when irradiated with a radiation dose of 5 Gy.⁸ The corresponding value for cisplatin is 4.5 $\mu\text{M}/\text{kg}$ mass test animal.

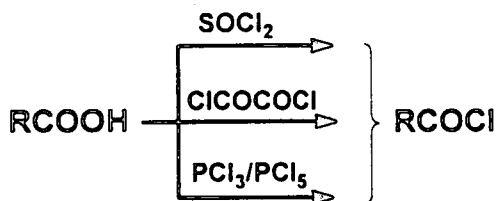
To conclude this section, Osella and co-workers¹⁰⁸ have recently determined the mechanism of action of the ferrocenyl moiety in chemotherapy. It is based on electron transfer processes. The Fe^{II}-containing ferrocenyl group needs first to be activated by oxidation to a Fe^{III}-containing ferricenium species by redox-active enzymes in a particular body compartment. The ferricenium species then interact with water and oxygen to generate a hydroxyl radical (OH[•]). The hydroxyl radical then cleaves the DNA strands which results in cell death. Electrochemical and biological studies^{8,9} indicated that only ferrocenyl derivatives with formal reduction potential less than ca. 0.216 V vs. a saturated calomel electrode (SCE) are inactive in cytotoxicity experiments. Ferrocenyl oxidation by redox enzymes in the cell becomes thermodynamically impossible in compounds with much more positive formal reduction potentials and the ferrocenyl derivatives become for all practical purposes inactive.

2.4 General synthetic procedures

2.4.1 Formation of acid chlorides

To obtain amides, it is necessary to condense an amine with a carboxylic acid. However, this condensation reaction is sluggish and normally requires high temperatures and long reaction times. These severe conditions may lead to undesired side reactions and degradation of liable moieties in the reacting molecules. To allow amide formation under less drastic conditions, the carboxylic acid may be converted to a more reactive compound such as an activated ester, an anhydride or an acid chloride. A carboxylic acid is more often converted into the acid chloride than into any other of its derivatives. From the highly reactive acid chloride there can be obtained many other types of compounds, including esters and amides. Acid chlorides are prepared by substitution of the carboxylic acids hydroxyl groups (OH) for chlorine (Cl).

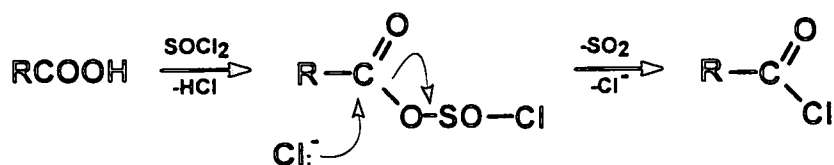
Scheme 2. 7, illustrates three of the many reactions and reagents that may be used to effect the transformation.



Scheme 2. 7 Reagents for acid chloride synthesis

2.4.1.1 Thionyl chloride

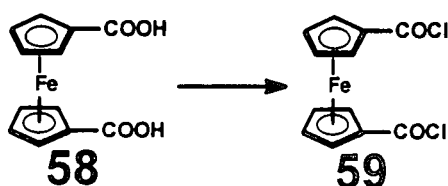
With respect to the methods used in this thesis, use was firstly made of thionyl chloride, SOCl_2 , as chlorinating reagent. Thionyl chloride is usually used in excess over the desired compound, or even as the solvent during chlorination. The side products formed, besides the desired acid chloride, are gases^{109,110,111} (CO_2 and HCl), which are easily separated from the formed acid chloride. Any excess of the low boiling thionyl chloride (b.p. 79°C) is easily removed by distillation. Many reactions require the use of a catalyst such as pyridine,^{112,113} triethylamine,^{114,115} or dimethylformamide¹¹⁶ in addition to thionyl chloride. The mechanism of the reaction probably proceeds *via* the formation of an intermediate chlorosulphite.¹¹⁷



2.4.1.2 Oxalyl chloride, (COCl)₂



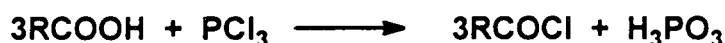
Oxalyl chloride is quite useful for converting carboxylic acids to their acid chlorides because the residual monochloro oxalic acid decomposes to hydrochloric acid (HCl) carbon monoxide (CO) and carbon dioxide (CO₂) gas, thus driving the equilibrium to the side of the acyl halide. Oxalyl chloride, with pyridine as a catalyst, is used for heat or strong acid/base sensitive compounds, such as 1,1'-ferrocenedicarboxylic acid, **58**, (Scheme 2.8). The acid, **58**, upon reaction with oxalyl chloride in the presence of pyridine produces the acid chloride, **59**, in 90% yield.¹¹⁸ Other catalysts may also be used include DMF¹¹⁹ for base sensitive compounds.¹²⁰



Scheme 2.8 Synthesis of 1,1'-ferrocenyldicarboxylic acid chloride **59**.

2.4.1.3 Phosphorus chlorides

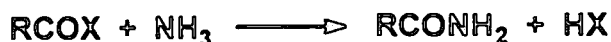
Instead of SOCl₂ the phosphorus chlorides PCl₃ and PCl₅ may be used to prepared acyl chlorides from carboxylic acids.^{121,122} The carboxylic acid reacts with a 25-100% excess of PCl₃ based on the reaction.



In some cases PCl₃ is the preferred agent over SOCl₂ or (COCl)₂. The reaction of PCl₃ with 2-ethylmercaptopropionic acid¹²³ yields the colourless acid chloride in 64% yield, whereas thionyl chloride gives a less pure, slightly coloured product. Phosphorus pentachloride has also been used extensively for the preparation of acid chlorides. High molecular-mass acyl

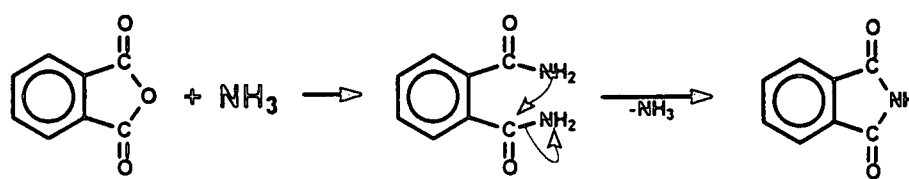
chlorides may be prepared¹²⁴ by the reaction of PCl_5 on the acid dissolved in an inert solvent such as benzene, carbon tetrachloride or methylene chloride.

2.4.2 Amide synthesis



The treatment of acyl halides with ammonia or amines is a very general reaction for the preparation of amides.¹²⁵ The reaction is highly exothermic and must be carefully controlled, usually by cooling or dilution. Ammonia gives unsubstituted amides, primary amines give N-substituted amides, and secondary amines give N,N-disubstituted amides. Arylamines can be similarly acylated. In some cases aqueous alkali is added to the reaction mixture to neutralise with the liberated HCl. This procedure is called the *Schotten Baumann procedure*.¹²⁶

However, ammonia and primary amines may also give imides, in which two acyl groups are attached to the nitrogen. This is especially easy with cyclic anhydrides, which produce cyclic imides.¹²⁷



The second step in this case, which is much slower than the first, is the attack of the amide nitrogen on the carbonyl group with simultaneous release of NH_3 .



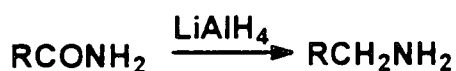
When carboxylic acids are treated with ammonia or amines, salts are obtained. The salts of ammonia or primary or secondary amines can be pyrolyzed to give amides,¹²⁸ but the method

is less convenient than the conversion of acyl halides, anhydrides and esters¹²⁹ and is seldom of preparative value.



The conversion of esters to amides is a useful reaction, and unsubstituted, N-substituted, and N,N-disubstituted amides can also be prepared from the appropriate amine.¹³⁰ Both R and R' may be alkyl or aryl. The reaction is particularly useful because many esters are readily available or easy to prepare, even in cases where the corresponding acyl halide or anhydride is not.

2.4.3 Primary amine synthesis



Amides can be reduced^{131,132,133} to amines with lithium aluminium hydride (LiAlH_4) or by catalytic hydrogenation, though high temperatures and pressures are usually required for the latter. Even with LiAlH_4 the reaction is more difficult than the reduction of most other functional groups, and other groups can be often be reduced without disturbing an amide function. Sodium boron hydride (NaBH_4) by itself does not reduce amides, though it does in the presence of certain other reagents¹³⁴ such as Pd/C. Another method for the reduction of mono- and disubstituted amides in high yields consists of treatment with triethyloxonium fluoroborate ($\text{Et}_3\text{O}^+\text{BF}_3^-$) to give the imino ether fluoroborate [$\text{RC}(\text{COEt})=\text{NR}_2^+\text{BF}_3^-$], followed by reduction of this with NaBH_4 in ethanol.

CHAPTER 3

RESULTS AND DISCUSSION

3.1 Introduction

In this research program results are ordered firstly to discuss the synthesis of a series of antineoplastic ferrocene-containing amines from the corresponding amides *via* suitable carboxylic acid precursors (Scheme 3.2, page 42). This discussion is followed by describing the technique how the above mentioned antineoplastic ferrocene amines are covalently anchored onto a water-soluble polymeric carrier to give water-soluble ferrocene-containing polymers with biomedical applications. This is followed by a detailed discussion of the electrochemistry of all the ferrocene-containing complexes. The influence of coupling side chain length (i.e. the number of CH₂ groups separating functional groups from the ferrocenyl moiety) on the ferrocenyl formal reduction potential will *inter alia* be highlighted. Finally, a discussion of a cytotoxicity study on the synthesised ferrocene derivatives will highlight relationships between cytotoxicity, structure and ferrocenyl reduction potential.

3.2 Syntheses

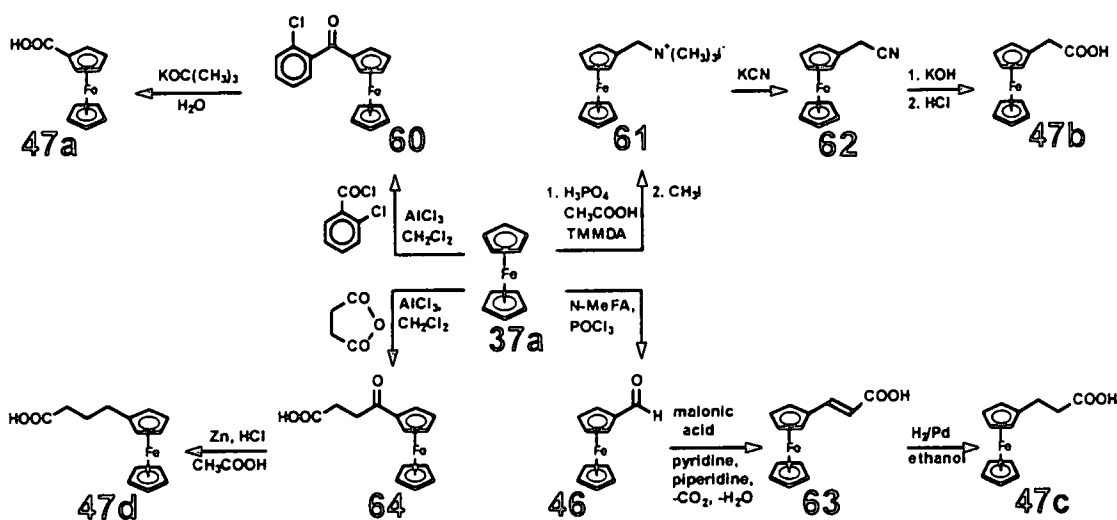
3.2.1 Preparation of ferrocene derivatives

3.2.1.1 Carboxylic acids

In order to attach the antineoplastic drug, ferrocene, to the water-soluble polymers, it is necessary to functionalise ferrocene. For the purpose of this study, polymer anchoring is achieved by means of an amide bond. To make this possible amine-containing side chains were introduced onto the ferrocenyl molecule in multi step reactions starting with the formation of carboxylic acid-functionalised ferrocenes.

The first ferrocene compound to be synthesised was ferrocenoic acid, **47a**, in a two step reaction from ferrocene, **37a**, by the method of Reeves⁹⁷ according to Scheme 3. 1. The first

step was a Friedel crafts reaction to produce 2-chlorobenzoylferrocene **60** as a dark red solid in 67% yield. This compound was characterized by ^1H NMR spectroscopy (spectrum 1: see appendix at the end of this thesis). Treatment of **60** with potassium *tert*-butoxide gave ferrocenoic acid **47a** as an air stable yellow powder in 86% yield. The appearance of a carbonyl ($\text{C}=\text{O}$) peak in the infrared spectrum of **47a** at 1617 cm^{-1} was clearly identified. The peaks observed at 1107 and 998 cm^{-1} (corresponding with 9 and $10\text{ }\mu\text{m}$ respectively), are associated with the unsubstituted⁸ cyclopentadienyl ring of **47a**.



Scheme 3. 1 Syntheses of ferrocene-containing carboxylic acids (**47a-47d**), TMMDA = tetramethylmethylenediamine, $(\text{CH}_3)_2\text{NCH}_2\text{N}(\text{CH}_3)_2$ and N-MeFA = N-methylformanilide, $\text{C}_8\text{H}_9\text{NO}$.

The preparation of 2-ferrocenylacetic acid, **47b**, involved the displacement of trimethylamine^{85,98} **45** from *N,N*-dimethylaminomethylferrocene methiodide⁸⁶, **61**, by a cyanide anion and hydrolysis of the resulting ferrocenylacetonitrile, **62**, to give yellow solid, **47b**, in 80% yield according to Scheme 3. 1. 2-Ferrocenylacetic acid, **47b**, was characterised by both IR (Figure 3. 1, page 46) and ^1H NMR (spectrum 4) where a peak at $\delta 3.71$ indicated

*These two peaks, although not mentioned throughout this thesis, were also observed for all the other monosubstituted ferrocene derivatives. These two peaks are in accordance with the so-called "9-10" rule for ferrocene derivatives having at least one unsubstituted cyclopentadienyl ring.

the 2 protons of the methylene group in the side chain of **47b**. The intermediate **61** was obtained by dimethylaminomethylation of ferrocene, **37a**, followed by reaction of the product with methyl iodide.⁸⁶ This is NOT shown in Scheme 3.1, but an interested reader will find the reaction involved in Chapter 2, Scheme 2.5, page 28.

Ferrocenylcarboxaldehyde, **46**, was used as a precursor in the synthesis of 3-ferrocenylpropanoic acid, **47c**. Ferrocenylcarboxaldehyde, **46**, was prepared by treatment of ferrocene with phosphorus oxychloride and N-methylformanilide. The aldehyde **46** was obtained in yields as high as 76%. The Michael addition of malonic acid to ferrocenylcarboxaldehyde **46** in pyridine, treated with a few drops of piperidine as catalyst, produced a brick red solid, 3-ferrocenylacrylic acid, **63**, in 73% yield.⁹⁹ Catalytic hydrogenation⁹⁹ of the substituted acrylic acid **63** was performed with hydrogen gas in absolute ethanol catalysed by palladium on activated charcoal (Scheme 3. 1). The reaction was performed over 7 hours to obtain 3-ferrocenylpropanoic acid **47c** in 81% yield. The side chain of the acid, **47c**, showed two peaks, each representing the 2 protons, of a CH₂ group in its ¹H NMR spectrum at δ 2.61 and δ 2.71 respectively (spectrum 5). Infrared transmission peaks at 3088 cm⁻¹ and at 1710 cm⁻¹ confirmed the presence of the -OH and of C=O respectively.

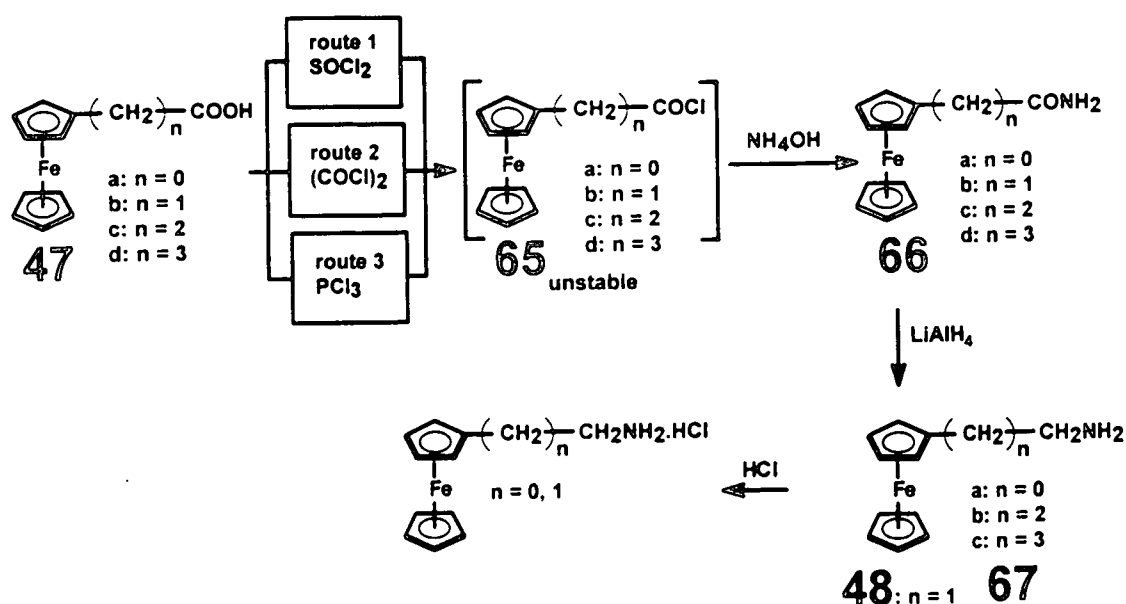
4-Ferrocenylbutanoic acid, **47d**, was obtained in fair yields, according to Scheme 3.1, utilising published procedures.^{100,101} The reaction of ferrocene, **37a**, with succinic anhydride afforded 4-ferrocenylpropionic acid, **64**, in 32% yield. This reaction was much less efficient than expected. The formation of an oily side-product really impeded isolation and purification of intermediate **64**. Clemmensen reduction of **64** gave yellow, solid, 4-ferrocenylbutanoic acid, **47d**, in 67% yield after 42 hours. The side chain of acid **47d** showed

signals for each of the free CH₂ groups in its ¹H NMR spectrum corresponding to 2 protons at δ1.81 and 4 protons at δ2.41 (spectrum 6). The infrared transmission peaks at 3418 cm⁻¹ and at 1710 cm⁻¹ indicated -OH and C=O respectively.

3.2.1.2 Amides

The ferrocene-containing amides shown in Scheme 3.2, have all been prepared by reacting aqueous ammonia with an acid chloride under interfacial (*Schotten Baumen*) conditions.¹²⁶ The acid chloride precursors were prepared by chlorination of the corresponding carboxylic acids.

Various methods were investigated to synthesise the acid chlorides **65a** – **65d** (Scheme 3.2). Traditional chlorination by refluxing with thionyl chloride (SOCl₂),^{110,111} route 1, worked only for the synthesis of **65a**. When SOCl₂ was used for the conversion of **47b**, **47c** and **47d** to the corresponding acid chlorides, excessive oxidation of the ferrocenyl moiety to the corresponding ferricenium derivatives, followed by compound decomposition was observed. The reason why the acid chloride **65a** could be obtained but the acid chlorides, **65b**, **65c** and **65d** not *via* the SOCl₂ route, may be found in the reduction potentials of the precursor carboxylic acids, **47a**, **47b**, **47c** and **47d**. From the results of Blom *et al*¹⁰⁰ (Table 2.3, page 32), the formal reduction potential, E^{o'}, of ferrocenoic acid, **47a**, in acetonitrile as solvent, is 0.57 V vs. SCE. All the other derivatives have E^{o'} values of 0.34 V or less. This indicates that ferrocenoic acid, **47a**, is much more resistant towards oxidation than the acids, **47b**, **47c** and **47d**. We concluded that the electrochemical driving force for the known acid-catalysed oxygen-induced oxidation of a ferrocenyl group, is large enough to oxidise **47b**, **47c** and **47d** during SOCl₂ mediated chlorination, but not large enough to oxidise **47a**.



Scheme 3.2 General synthetic route towards ferrocene-containing amides (66 and amines (48 and 67) respectively. Of the three methods investigated for acid chloride synthesis, only the PCl_3 route proved to be a general procedure. Derivatives 67b and 67c tend to oxidise and decompose when treated with HCl to produce quaternary ammonium salts.

This explains why 65a was the only acid chloride that could be successfully synthesised by route 1. Oxalyl chloride, $(\text{COCl})_2$, route 2, in Scheme 3.2 is a milder chlorinating reagent than SOCl_2 but also generates acid chlorides in good yield at room temperature.¹¹⁸ When the acids, 47a-47d were treated with $(\text{COCl})_2$, only the acid chlorides, 65a and 65b could be isolated. Acid chlorides 65c and 65d were still unobtainable *via* this method, *inter alia* because the liberated HCl again catalysed ferrocenyl oxidation of the two easily oxidisable acids 65c and 65d.

The chlorinating reagent of choice for this class of ferrocene-containing carboxylic acids, however, was found to be phosphorus trichloride (PCl_3), route 3. Following standard laboratory techniques utilising the reagent PCl_3 , all the carboxylic acid chlorides, 65a, 65b, 65c and 65d could be obtained.¹²¹ The instability of the acid chlorides 65a - 65d caused us not to isolate and store them, but rather to proceed with amidation utilising the crude *in situ*-

obtained acid chlorides dissolved in dichloromethane. Saturated aqueous ammonia was used as amidating reagent to liberate the amides **66a**, **66b**, **66c** and **66d** in fair yields (41, 24, 62 and 73% respectively). However, for characterisation purposes, the IR spectra of the acid chlorides were recorded in petroleum ether and they showed the $\nu_{\text{C=O}}$ stretching frequency at $\sim 1800 \text{ cm}^{-1}$ (Figure 3.1). The ferrocenyl amide derivatives were characterised by both infrared and $^1\text{H-NMR}$ spectroscopy. In Figure 3.1 the IR spectra of the amides **66** is shown together with inserts and assignments of the carboxylic acids **47** and acid chlorides **65**

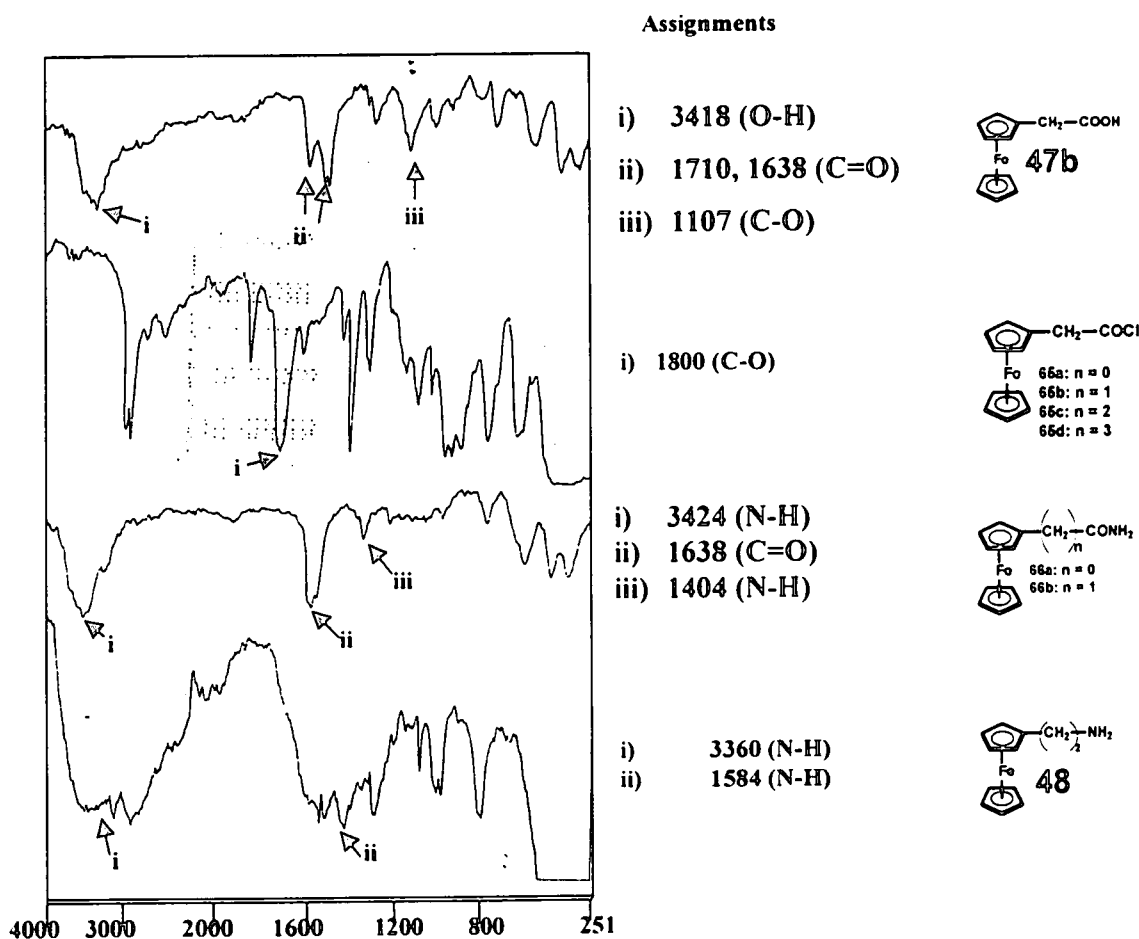


Figure 3.1 Infrared spectra (**47b** and **66** in KBr, **65** in petroleum ether solution and **48** between using NaCl discs as they are oils) with dominant assignments and structures of ferrocene derivatives.

3.2.1.3 Amines

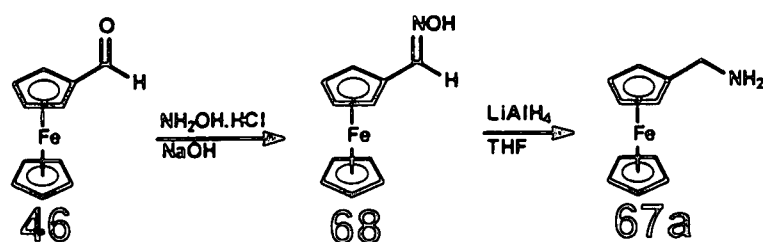
Since it is the aim of this study to anchor ferrocene derivatives onto a polymeric drug carrier *via* biodegradable amide bonds (goal 2 and 3 in chapter 1), the syntheses of ferrocene-containing amines were selected as the chief goal in synthesis of ferrocene derivatives. The ferrocene-containing amines **48** and **67** shown in Scheme 3.2 have all been prepared by a general procedure by reduction with LiAlH_4^{133} in anhydrous tetrahydrofuran (THF) at room temperature from the corresponding amide precursors that have already been described. Infrared transmission peaks at 3360 cm^{-1} and 1584 cm^{-1} confirmed the presence of a NH_2 -group (Figure 3. 1, page 46), while ^1H NMR again clearly showed the signals associated with each of the side chains of **48** and **67**. Characterisation data of all the ferrocene-containing acids **47**, amides **66** and amines **48** and **67** are given in Table 3. 1.

Table 3. 1 Characterisation data of ferrocene-containing acids **47** amides **66** and amines **48** and **67**.

| Compound | Formula | Yield % | M.p/ °C | % Found (requires) | | | IR $\nu_{\text{C=O}}$ cm^{-1} |
|------------|---|---------|------------|---------------------------|------------|------------|---|
| | | | | C | H | N | |
| 47a | $\text{C}_{11}\text{H}_{10}\text{O}_2\text{Fe}$ | 86 | 198-210 | 57.40(57.40) ^a | 4.51(4.35) | - | 1710 |
| 47b | $\text{C}_{12}\text{H}_{12}\text{O}_2\text{Fe}$ | 80 | 150-155 | 59.40(59.05) ^a | 4.96(5.34) | - | 1710 |
| 47c | $\text{C}_{13}\text{H}_{14}\text{O}_2\text{Fe}$ | 81 | 115 | 60.44(60.49) ^a | 5.62(5.47) | - | 1710 |
| 47d | $\text{C}_{14}\text{H}_{16}\text{O}_2\text{Fe}$ | 67 | 107 | 61.79(61.79) ^a | 5.73(5.93) | - | 1710 |
| 66a | $\text{C}_{11}\text{H}_{11}\text{NOFe}$ | 41 | 165 | 57.49(57.68) | 4.78(4.84) | 5.73(6.12) | 1638 |
| 66b | $\text{C}_{12}\text{H}_{13}\text{NOFe}$ | 24 | 163 | 58.83(59.29) | 5.54(5.39) | 5.70(5.76) | 1638 |
| 66c | $\text{C}_{13}\text{H}_{15}\text{NOFe}$ | 62 | 96 | 60.56(60.73) | 5.99(5.88) | 5.18(5.45) | 1638 |
| 66d | $\text{C}_{14}\text{H}_{17}\text{NOFe}$ | 73 | 82 | 60.14(62.02) | 6.56(6.32) | 4.78(5.17) | 1638 |
| 67a | $\text{C}_{11}\text{H}_{13}\text{NFe}$ | 56 | oil | 61.18(61.43) ^b | 5.76(6.09) | 6.45(6.51) | 1584 ^d |
| 48 | $\text{C}_{12}\text{H}_{15}\text{NFe}$ | 67 | oil | 62.79(62.91) ^c | 6.88(6.60) | 6.04(6.11) | 1584 ^d |
| 67c | $\text{C}_{13}\text{H}_{17}\text{NFe}$ | 82 | oil | 63.85(64.22) | 6.68(7.05) | 5.40(5.76) | 1584 ^d |
| 67d | $\text{C}_{14}\text{H}_{19}\text{NFe}$ | 76 | oil | 65.13(65.39) | 7.52(7.45) | 5.61(5.47) | 1584 ^d |

^a From Ref. 101. ^b From Ref. 133. ^c From Ref. 86. ^d $\nu_{\text{N-H}}$.

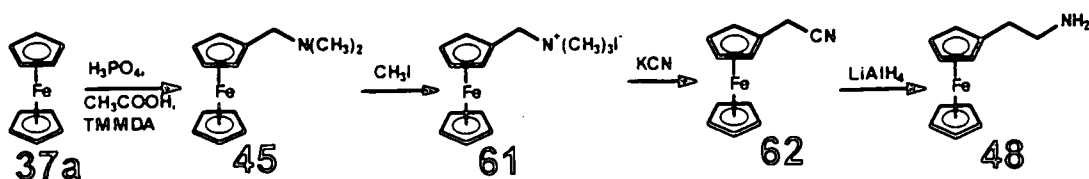
Various other methods were also utilised to synthesise some of the amines relevant to this study. To this effect ferrocenecarboxaldehyde, **46**, was used as a starting material for the synthesis of ferrocenylmethylamine, **67a** (Scheme 3. 1). Ferrocenecarboxaldehyde, **46**, was initially converted into ferrocenecarboxaldoxime¹³² **68** by condensation with hydroxylamine in the presence of sodium hydroxide.



Scheme 3. 3 Synthesis of ferrocenylmethylamine, **67a**, from **46**.

Reduction of **68** to the amine was achieved by stirring with lithium aluminium hydride in THF at room temperature.¹³³ After aqueous work-up, pure ferrocenylmethylamine, **67a**, was isolated as a yellow solid in 56% yield. Amine **67a** produced by the procedure shown in Scheme 3.3 were spectroscopically identical for **67a** produced by the procedure shown in Scheme 3.2 (page 45).

In an alternative four-step procedure to synthesise 2-ferrocenylethylamine, **48**, the first step involves the synthesis of N,N-dimethylaminomethylferrocene, **45**, according to Scheme 3.4, followed by the treatment of the latter⁸⁵ with methyl iodide to give **61** in 79% yield. Ferrocenylacetonitrile⁸⁶ **62** was prepared by refluxing the quaternary ammonium salt **61** with potassium cyanide for 2.5 hours to give the substituted acetonitrile **62** in 76% yield. Isolation of **62** from the reaction mixture proved to be difficult and tended to lower yields dramatically if care is not taken. The last reaction in the synthesis of **48** according to this route involves the reduction of the ferrocenylacetonitrile,⁸⁶ **62**, by LiAlH₄ in dry ether.



Scheme 3.4 Synthesis of 2-ferrocenylethylamine, **48**, from **37a**. TMMDA = tetramethylmethylenediamine, $C_8H_{19}NO$.

The reduction of the nitrile **62** proceeded for 1 hour while refluxing at $34^{\circ}C$ and after workup, a dark brown oil residue was obtained. The residual oil was distilled at 0.5 mmHg, $126^{\circ}C$ to give 2-ferrocenylethylamine **48** as a red oil in 81% yield. It should be noted that amine **48** produced by the procedure shown in Scheme 3.4 was spectroscopically identical to **48** produced by the procedure shown in Scheme 3.2 (page 45). Compound **48**, as well as all the other aminated ferrocenes **67a** – **67c** are not stable but decomposed with time. Normally ferrocene-containing amines would be stored as the more stable hydrochloride salt, but care has to be taken when converting the amines to the hydrochloride salt with HCl. Especially **67b** and **67c** (Scheme 3.2, page 45) are very unstable in the media required to produce the hydrochloride salts due to acid catalysed Fe^{II} oxidation to a ferricenium derivative followed by decomposition. Therefore, after synthesis, amines were stored in the refrigerator at $-50^{\circ}C$. At this temperature they were stable for periods up to 3 months.

3.2.1.4 Conclusion

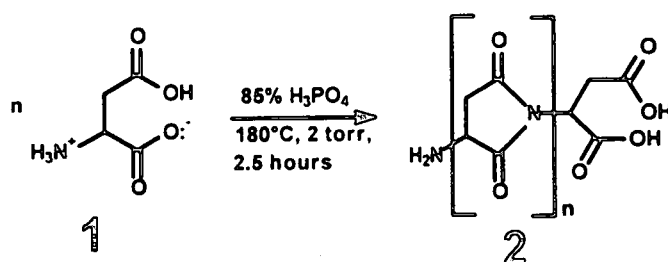
In the forgoing paragraphs, methods were described how to synthesise 26 derivatives of ferrocene. Of these seven compounds, notably acid chlorides **65c** and **65d** (Scheme 3.2), the amides **66b**, **66c** and **66d**, and the amines **67b** and **67c** are new compounds that were hitherto unknown.

3.2.2 Polymer synthesis

3.2.2.1 Thermal polymerisation of aspartic acid

Having synthesised the ferrocene-containing amine derivatives described above, attention was focused on the synthesis of polymers that can be used as polymeric drug carriers. Once the desired properties of polymeric drug carriers (see Chapter 2, paragraph 2.2.3, page 12) had been taken into account, it was decided to concentrate on modifications of polysuccinimide 2.

The known⁴² thermal polymerisation of aspartic acid, 1, at 185°C and under reduced pressure for 2.5 hours led to polysuccinimide, 2, as a white solid in 95% yield (Scheme 3.5).



Scheme 3.5 Thermal polymerisation of DL-aspartic acid 1.

Polysuccinimide 2 is insoluble in water, methanol and most organic solvents except DMF or DMSO. It was reported elsewhere^{43,44} that 2, prepared in this way, has a molecular mass of 57 000 g/mol. Its ¹H NMR spectrum showed signals at 5.28 ppm (1H, CH), 3.13 ppm (1H, CH₂) and 2.70 ppm (1H, CH₂) in DMSO-d₆ (Figure 3.2). The absence of a ¹H NMR signal at ~4.80 ppm indicated that there were no observable uncyclized aspartic acid units in the backbone of 2, (see Chapter 2, Scheme 2.1, page 16 for an example of a polymer where cyclisation of aspartic acid is incomplete). The ¹³C spectrum of 2 shows two signals between 170 and 175 ppm, which corresponds to the carbonyl carbon atoms of 2, while the signal of the other two C-atoms, can be found at 33 and 43 ppm respectively.

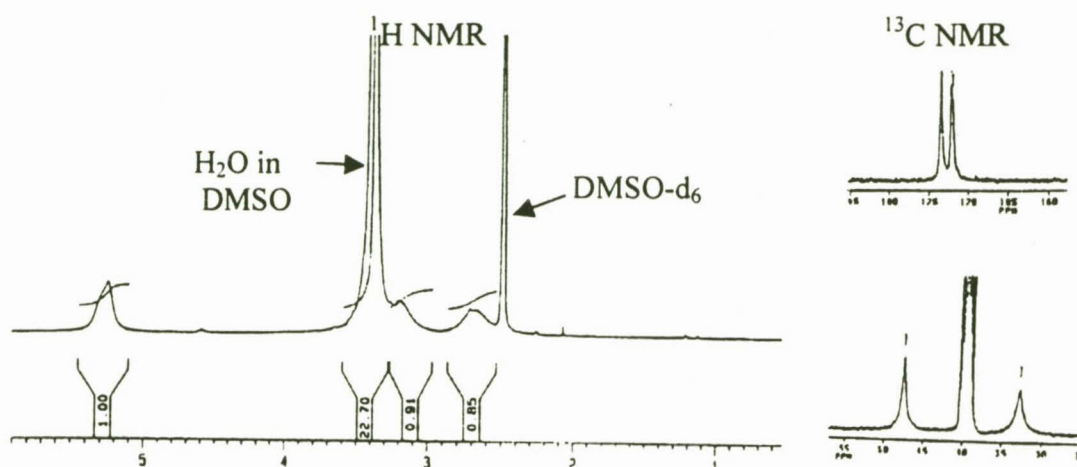


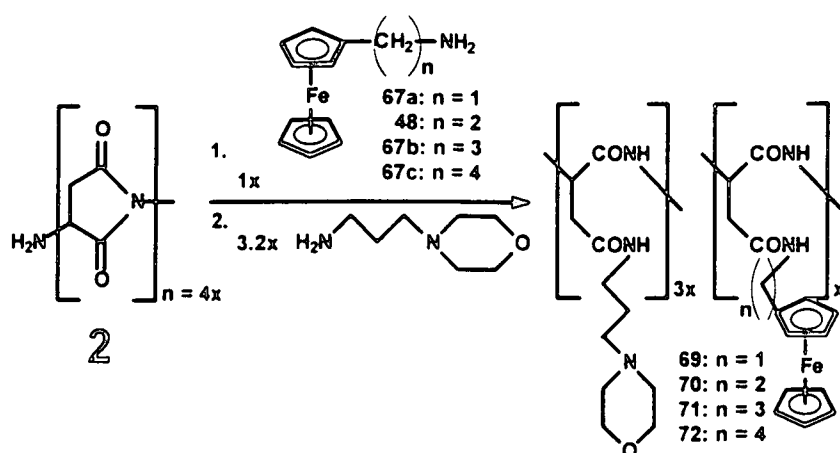
Figure 3.2 ^1H NMR and ^{13}C NMR signals of polysuccinimide in DMSO-d_6 .

3.2.2.2 The anchoring of ferrocenylamine derivatives on polysuccinimide

From goal 3 (page 3) of this study, the ferrocenylamine derivatives **48** and **67a - 67c** are to be anchored onto a polymer with suitable solubility properties. The reactions involved to achieve this are shown in Scheme 3.6. To establish the reaction conditions of this ferrocene-anchoring step on **2**, attention was first focussed on the synthesis of polymer **69**. Polymer **69** had as target one ferrocenyl group anchored to it for every three morpholine-containing side chains. The purpose of the morpholino group is to enhance the aqueous solubility of polymer **69**, while the ferrocenyl group represents the drug portion of the polymeric drug carrier/drug conjugate **69**.

i15714445

U.O.V.S. BIBLIOTEK



Scheme 3.6 The synthesis of polymeric drug carriers with the ferrocenyl moiety covalently anchored onto it.

As shown in Scheme 3.6, 4 equivalents of repeating units of polysuccinimide, **2**, were first reacted with one equivalent of ferrocenylmethylamine, **67a**, for 5 hours at 0°C in DMF and then at room temperature for a further 16 hours. The resulting intermediate was then treated with 3.2 equivalents of N-(3-aminopropyl)morpholine. The resulting product was dialysed and freeze-dried to give polymer **69** as a yellow solid. The target side chain ratio was one ferrocenyl group for every three morpholine-containing side chains. The ratio of side chains actually obtained was determined by ^1H NMR according to the following guidelines: The ϵ -protons of the morpholine side chain are found at 3.50 ppm (see Figure 3.3). If there are three morpholine-containing side chains on **69**, it follows that this ^1H NMR signal must account for 12 protons. The integral of this signal was therefore locked on 12 integral units (i.e. one proton corresponds to an integral value of 1 integral units). The ^1H NMR signal for the nine ferrocenyl protons are found at 3.80 – 4.10 ppm. The combined integral count for this signal is $5.23 + 3.21 = 8.44$ rather than the expected 9. The practically obtained success ratio of ferrocenyl-anchoring is therefore $8.44/9 = 0.94$, and corresponds to a side chain ratio of morpholino groups:ferrocenyl groups = 3:0.94 compared to the target ratio of 3:1. This is regarded as a very good result.

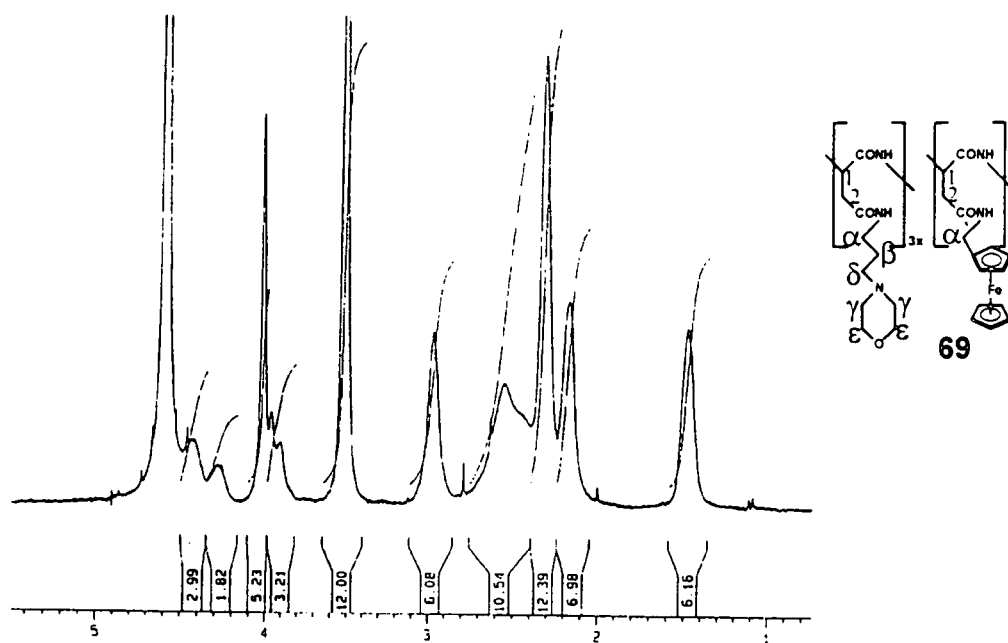


Figure 3.3 The proton assignment in the ^1H NMR spectrum of polymer 69: 1.48 (6H, s, β - CH_2), 2.15 (6H, s, δ - CH_2), 2.31 (12H, s, γ - CH_2), 2.58 (10H, s, 4 asp- CH_2 + α' - CH_2), 2.99 (6H, s, α - CH_2), 3.50 (12H, s, ϵ - CH_2), 3.91-4.05 (9H, s, C_{10}H_9), 4.28-4.44 (4H, s, asp-CH).

Having established a simple, quick and highly effective procedure for the anchoring of amines and N-(3-aminopropyl)morpholine onto polysuccinimide **2**, a series of experiments were conducted to anchor the ferrocenylamines **48**, **67b** and **67c** (Scheme 3.2, page 45) to obtain polymers **70**, **71** and **72** according to Scheme 3. 6.

Polymer **70** was obtained after dialysis in 12 000 molecular mass cut off dialysis tubing in 18% yield with one equivalent of 2-ferrocenylethylamine **48** for every three equivalents of 3-aminopropyl morpholine units successfully anchored onto **2**. Polymer **71** was obtained in 18% yield with side chain ratio of 3:0.95 (3-aminopropyl morpholine:3-ferrocenylpropylamine **67b**). Polymer **72** was obtained in 17% yield with 1.75 equivalents of **67c** anchored onto **2** for every three equivalents of 3-aminopropyl morpholine side chains.

The anchoring observed in polymer 72 stands in contrast to the results obtained in polymers 69, 70 and 71 and is most probably due to a weighing error that occurred during the experiment. Determination of the side chain ratio of each polymer was performed by ^1H NMR analysis following the general guidelines given for polymer 69.

Polymers 69 – 72 (Scheme 3.6) satisfy the criteria for drug carriers described in Chapter 2 in the following way: The degradation of the polymers in a biological environment is possible by means of enzymatic induced amide bond hydrolysis both in the main polymer chain and the side chains. Although polyaspartamides have no specific recognition sites for cancer cells in their structure, they are constructed from the amino acid, aspartic acid. Taking into consideration the greater need for nutrients and metabolic precursors, such as amino acids and peptides, by tumour cell as compared to healthy cells, it may be expected that cancer cells would take up or internalize polymers 69 – 72 faster than healthy cells. The 3-aminopropyl morpholine side chains in polymers 69 – 72 makes these stable polymers exceptionally water-soluble, even though the free drugs 48 and 67a – 67c are not soluble in basic aqueous solvents and decompose in acidic aqueous solvents.

3.2.2.3 Conclusion

In the polymer section of this research program, five polymers were synthesised and characterised, four of which (69 – 72) were completely new compounds. The rationale behind the increasing chain length of the aliphatic chain connecting the ferrocenyl moiety with the polymer main chain in polymers 69 - 72 is to obtain polymers possessing the ferrocenyl group with a continuous decrease in formal reduction potential for the ferrocenyl/ferricenium couple. This is important, as has been described elsewhere⁹ that

3.3 Electrochemistry

The fourth aim of this study (Chapter 1) was to investigate some of the electrochemical properties of ferrocene-containing amines, their precursors as well as the electrochemical properties of the polymer-bound ferrocenyl derivatives.

3.3.1 Cyclic voltammetry of ferrocenyl derivatives

3.3.1.1 Ferrocene amides

The amides **66a** - **66d** were dissolved in concentrations of *ca.* 1.5 mmol dm⁻³ and the solutions contained 0.1 mol dm⁻³ tetrabutylammoniumhexafluorophosphate supporting electrolyte in acetonitrile. The three-electrode system used consisted of a platinum wire auxiliary electrode with a platinum working electrode and a Ag/Ag⁺ non-aqueous reference electrode. The peak anodic (E_{pa}) and peak cathodic (E_{pc}) potentials (referenced against (Ag/Ag⁺) as well as their differences (ΔE_p) = $E_{pa} - E_{pc}$, ratio of peak cathodic and peak anodic currents (i_{pc}/i_{pa}) were determined by reading off the appropriate values on the cyclic voltammogram as shown in Figure 3.5. Formal reduction potentials ($E^{o'}$) = $(E_{pa} + E_{pc})/2$ of each of the ferrocenylamide derivatives were also calculated. Results are summarised in Table 3. 2. The differences in peak anodic, E_{pa} , and peak cathodic, E_{pc} , potentials, ΔE_p , for all amides except ferrocenylcarboxamide, **66a**, were below 75 mV and indicate reasonable electrochemical reversibility.

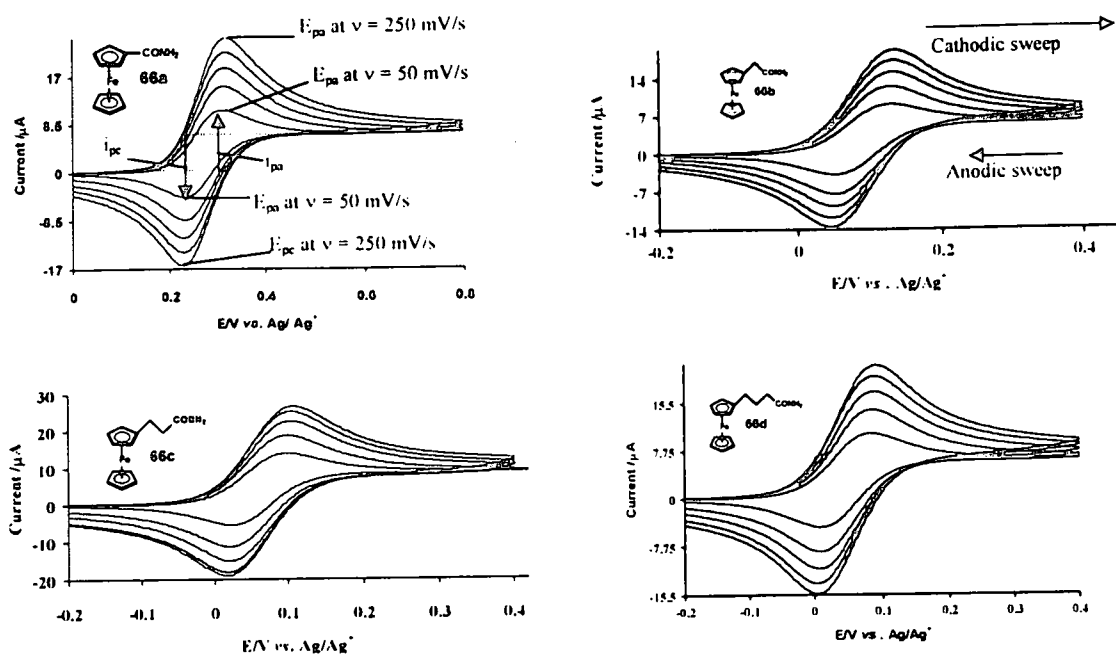
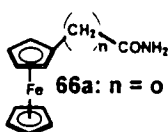
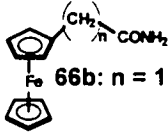
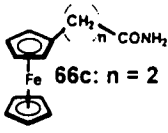
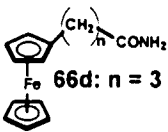


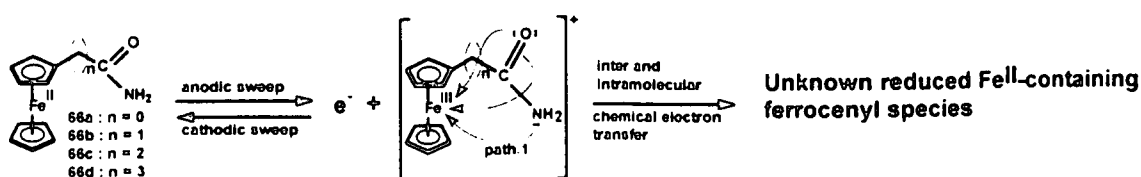
Figure 3.4 Cyclic voltammograms of 66a - 66d, scan rates (ν) are 50 (smallest i_p value), 100, 150, 200 and 250 mV/s.

Electrochemical reversibility¹⁰⁵ of a one electron process at 25 °C is characterised theoretically by $\Delta E_p = 59$ mV and is independent of scan rate. All $E^{o'}$ values for the amides 66a - 66d are independent of scan rates within the range 50 – 250 mV/s. As shown in Table 3. 2, peak current ratios i_{pc}/i_{pa} are all well below 1. If these ratios were equal to 1, it would imply that the oxidised ferricenium species, which is generated in the anodic sweep, are chemically stable in acetonitrile and are reduced electrochemically quantitatively in the ensuing cathodic sweep. However, our results indicate that i_{pc} is much smaller than i_{pa} . This implies that, in acetonitrile, the oxidised ferricenium amides that are generated electrochemically during the anodic sweep destroy itself partially before the cathodic sweep can reduce them again. The fact that the ratio i_{pc}/i_{pa} becomes larger with increase in scan rate, supports this conclusion because it is consistent with the fact that at faster scan rates the electrochemically generated ferricenium amides have less time to self-destruct before cathodic reduction takes place during the cathodic sweep.

Table 3.2 Electrochemical data for ferrocene-containing amides 66a - 66d in acetonitrile vs. Ag/Ag⁺ at scan rates between 50 and 250 mV/s. E_{pa} = anodic peak potentials. ΔE_p = E_{pa} - E_{pc} (E_{pc} = cathodic peak potentials), formal reduction potentials, E^{o/} = (E_{pa} + E_{pc})/2, i_{pa} = anodic peak currents and i_{pc}/i_{pa} = peak current ratios with i_{pc} = cathodic peak currents.

| Compound | v | E _{pa} / | ΔE _p / | E ^{o/} / | i _{pa} / | i _{pc} /i _{pa} |
|---|------|-------------------|-------------------|-------------------|-------------------|----------------------------------|
| | mV/s | V | mV | V | μA | |
|  66a: n = 0 | 50 | 0.313 | 83 | 0.272 | 11.2 | 0.39 |
| | 100 | 0.313 | 83 | 0.272 | 15.4 | 0.54 |
| | 150 | 0.313 | 83 | 0.272 | 18.7 | 0.61 |
| | 200 | 0.312 | 80 | 0.272 | 21.5 | 0.65 |
| | 250 | 0.312 | 82 | 0.271 | 24.0 | 0.68 |
| E ^{o/} _{av} = 0.272 V | | | | | | |
|  66b: n = 1 | 50 | 0.125 | 74 | 0.088 | 9.38 | 0.39 |
| | 100 | 0.125 | 74 | 0.088 | 12.7 | 0.57 |
| | 150 | 0.125 | 75 | 0.088 | 15.4 | 0.62 |
| | 200 | 0.126 | 76 | 0.088 | 17.6 | 0.67 |
| | 250 | 0.125 | 75 | 0.088 | 19.6 | 0.69 |
| E ^{o/} _{av} = 0.088 V | | | | | | |
|  66c: n = 2 | 50 | 0.101 | 71 | 0.066 | 13.9 | 0.39 |
| | 100 | 0.102 | 72 | 0.066 | 18.7 | 0.60 |
| | 150 | 0.102 | 72 | 0.066 | 22.6 | 0.67 |
| | 200 | 0.104 | 74 | 0.067 | 25.2 | 0.72 |
| | 250 | 0.102 | 72 | 0.066 | 26.6 | 0.71 |
| E ^{o/} _{av} = 0.066 V | | | | | | |
|  66d: n = 3 | 50 | 0.085 | 76 | 0.047 | 10.5 | 0.44 |
| | 100 | 0.084 | 75 | 0.047 | 14.4 | 0.60 |
| | 150 | 0.084 | 73 | 0.047 | 17.7 | 0.65 |
| | 200 | 0.084 | 73 | 0.048 | 19.9 | 0.67 |
| | 250 | 0.084 | 75 | 0.047 | 21.7 | 0.71 |
| E ^{o/} _{av} = 0.047 V | | | | | | |

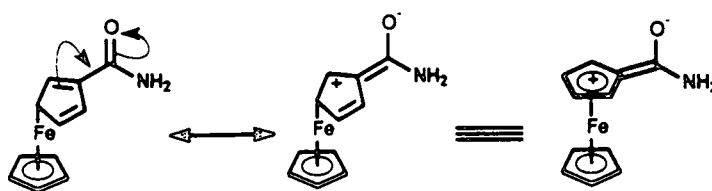
Exactly how the electrochemically generated ferricenium amides self-destruct is uncertain at this stage, but it is conceivable that intermolecular or intramolecular electron transfer between the free or π electrons of the amide functional group and the ferric ion nucleus of the oxidised species may occur as shown in Scheme 3.7.



Scheme 3.7 Intramolecular electron transfer from the free electron pair on the NH₂ group or the O-atom or even from the π -electron cloud in the carbonyl group may reduce the Fe^{III} ferricenium nucleus to a Fe^{II} ferrocene species thereby lowering the concentration of the ferricenium species that are available for reduction during the cathodic sweep.

Previous studies¹⁰⁰ on the carboxylic acid precursors of the amides **66a-d**, i.e. the acids **47a-d** (Scheme 3.1, page 42) showed i_{pc}/i_{pa} ratios much closer to one at slow scan rates than the amides **66**. Current ratios for the acids were equal to one at high scan rates. Since both the acids and the amides functional group have a carbonyl group, we concluded that the -NH₂ portion of amides **66a-d** are more involved in destroying the electrochemically generated ferricenium cation than the carbonyl group. This is indicated by path 1 in Scheme 3.7 above.

Finally, it is noted that $E^{o'}$ becomes larger (more positive) with a decrease in (CH₂)_n-chain length. This is to be expected as larger (CH₂)_n chain lengths more successfully isolate (shield) the electron-withdrawing properties of the amide carbonyl group from the ferrocenyl moiety. The shortest chain length, i.e. **66a** with n = 0, had a much larger $E^{o'}$ value (0.272 V) than all the other amides which did have a CH₂ isolating spacer separating the amide and ferrocenyl group. This is to be expected as only **66a** can conjugate with the ferrocenyl group as shown in Scheme 3.8. Compounds **66b**, **66c** and **66d** cannot conjugate in this way because the isolating CH₂ groups separates the ferrocenyl and amide groups.



Scheme 3.8 Canonical forms explain the conjugation between the electron donating ferrocenyl group and adjacent carbonyl group. For clarity, only one ferrocenyl isomer is shown for the two structures on the left but in reality they exist the normal mixtures of isomers corresponding, for example, to the zwitter ionic structure on the right. A CH_2 spacer between the ferrocenyl and amide groups will break this conjugation and it will result in much less positive reduction potentials for the ferrocene/ferricenium cation couple.

3.3.1.2 Ferrocene amine hydrochloride electrochemistry in water

The electrochemistry of the ferrocene-containing amines **48** and **67a** – **67c** were investigated in water as these compounds are soluble as hydrochloride salts in 10 mmol dm^{-3} aqueous HCl.

The electrode system used for aqueous cyclic voltammetry measurements consisted of a Pt wire auxiliary electrode, glassy carbon working electrode and an Ag/AgCl reference electrode. The supporting electrolyte was 1 mol dm^{-3} KCl and the concentrations of each amine were *ca.* 1 mmol dm^{-3} .

The cyclic voltammetry behaviour of ferrocene-containing amine hydrochloride derivatives are shown in Figure 3.5 at a scan rate of 150 mV/s .

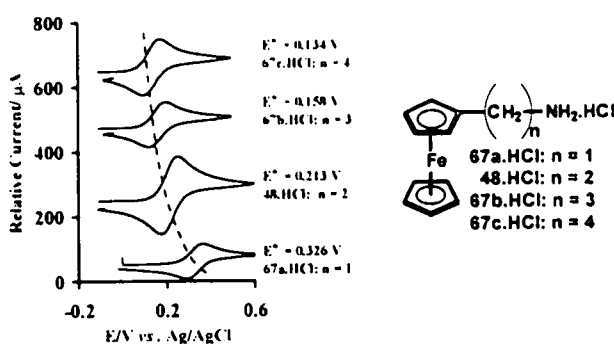
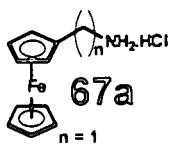
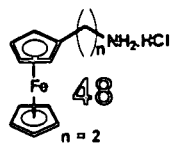
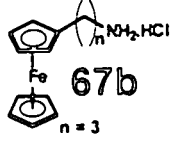
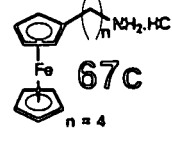


Figure 3.5 Cyclic voltammograms of *ca.* 1 mmol dm^{-3} solutions of the hydrochloride salts of **48**, **67a**, **67b** and **67c** in water containing 1 mol dm^{-3} KCl and 10 mmol dm^{-3} HCl at 25°C at a scan rate 150 mV/s utilising a glassy carbon working electrode.

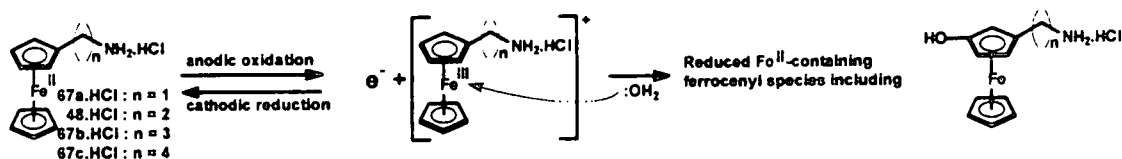
The electrochemical data relevant to each amine hydrochloride is summarised in Table 3. 3. The first conclusion, that can be drawn from the data repeated in Table 3. 3 is that all the hydrochloride salts of compounds 48, 67a, 67b and 67c underwent one-electron diffusion-controlled electrochemically reversible processes because ΔE_p .

Table 3. 3 Peak anodic potentials, E_{pa} , difference in peak anodic and peak cathodic potentials, $\Delta E_p = (E_{pa} - E_{pc})$, formal reduction potentials, $E^{o'} = (E_{pa} + E_{pc})/2$, peak anodic currents, i_{pa} and peak cathodic/anodic current ratios, i_{pc}/i_{pa} for the indicated ferrocene-containing amines as the hydrochlorides in water containing 10 mmol dm⁻³ HCl and 1 mol m⁻³ KCl as supporting electrolyte at 25°C. Working electrolyte = glassy carbon, [ferrocene-amine hydrochloride] = 1 mmol dm⁻³.

| Compound | Scan rate mV/s | E_{pa} V | ΔE_p mV | $E^{o'}$ V | i_{pa} μA | i_{pc}/i_{pa} |
|---|-------------------|---------------|--------------------|---------------|---------------------|-----------------|
|  67a n = 1 | 50 | 0.356 | 69 | 0.321 | 35.77 | 0.84 |
| | 100 | 0.352 | 63 | 0.321 | 49.45 | 0.82 |
| | 150 | 0.365 | 78 | 0.326 | 61.15 | 0.83 |
| | 200 | 0.361 | 81 | 0.321 | 71.08 | 0.80 |
| | 250 | 0.361 | 79 | 0.321 | 78.23 | 0.83 |
| Average | | | | 0.322 | | 0.82 |
|  48 n = 2 | 50 | 0.243 | 65 | 0.210 | 83.07 | 0.87 |
| | 100 | 0.247 | 71 | 0.212 | 114.83 | 0.87 |
| | 150 | 0.253 | 80 | 0.213 | 138.28 | 0.86 |
| | 200 | 0.249 | 80 | 0.209 | 164.67 | 0.85 |
| | 250 | 0.254 | 84 | 0.212 | 175.91 | 0.89 |
| Average | | | | 0.212 | | 0.87 |
|  67b n = 3 | 50 | 0.186 | 65 | 0.153 | 47.56 | 0.80 |
| | 100 | 0.189 | 67 | 0.156 | 64.77 | 0.79 |
| | 150 | 0.198 | 79 | 0.158 | 78.18 | 0.80 |
| | 200 | 0.198 | 83 | 0.157 | 89.86 | 0.78 |
| | 250 | 0.193 | 77 | 0.154 | 100.66 | 0.81 |
| Average | | | | 0.156 | | 0.80 |
|  67c n = 4 | 50 | 0.166 | 69 | 0.132 | 59.08 | 0.81 |
| | 100 | 0.167 | 73 | 0.131 | 79.38 | 0.84 |
| | 150 | 0.173 | 80 | 0.134 | 96.00 | 0.83 |
| | 200 | 0.175 | 85 | 0.133 | 110.77 | 0.82 |
| | 250 | 0.173 | 84 | 0.131 | 123.69 | 0.82 |
| Average | | | | 0.132 | | 0.82 |

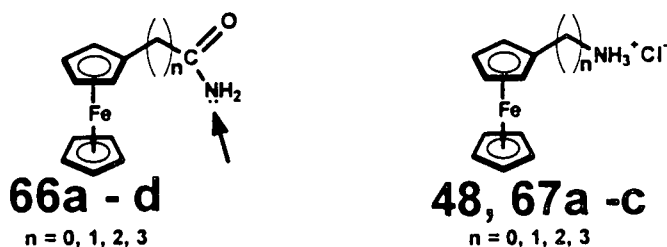
especially at slow scan rates, are very close to the theoretical value of 59 mV. The i_{pc}/i_{pa} ratio is not one, but lies between 0.80 and 0.87. This is much closer to one than was observed for the amides of the previous section and is quite normal for aqueous electrochemistry of ferrocene derivatives.⁹³

The deviation from 1 is attributed to the interaction of the free electron pair of H_2O with the electrochemically generated ferricenium species as shown in Scheme 3.9 below.



Scheme 3.9 Interaction of the free electron pair of H_2O with the electrochemically generated ferricenium species may result in a variety of reduced Fe^{II} ferrocene species including the shown hydroxylated compound. See Chapter 2, page 26.

It is notable that for the hydrochloride salts of compounds 48 and 67a – c, there are no free electron pairs on the functional group, while the amides have a free electron pair on the NH_2 portion of the molecule 66a – d as shown below.



This observation, together with the observation that the i_{pc}/i_{pa} ratios of the amides as described in the previous section are deviating much more from one than the amine hydrochlorides of this section, gives further proof that it really is the free electron pair on the NH_2 group of the amides that causes the deviation from unity for the i_{pc}/i_{pa} ratio of the amide compounds.

When one considers the average formal reduction potentials, $E^{o'}$ (vs. Ag/AgCl), tabulated in Table 3.3, it becomes apparent that the formal reduction potentials of each compound are manipulated by the increase in aliphatic chain length separating the amine hydrochloride functional group from ferrocenyl moiety. The relationship between $E^{o'}$ and spacer chain length separating the ferrocenyl and NH_3^+ as well as the ferrocenyl and CONH_2 groups is shown in Figure 3.6.

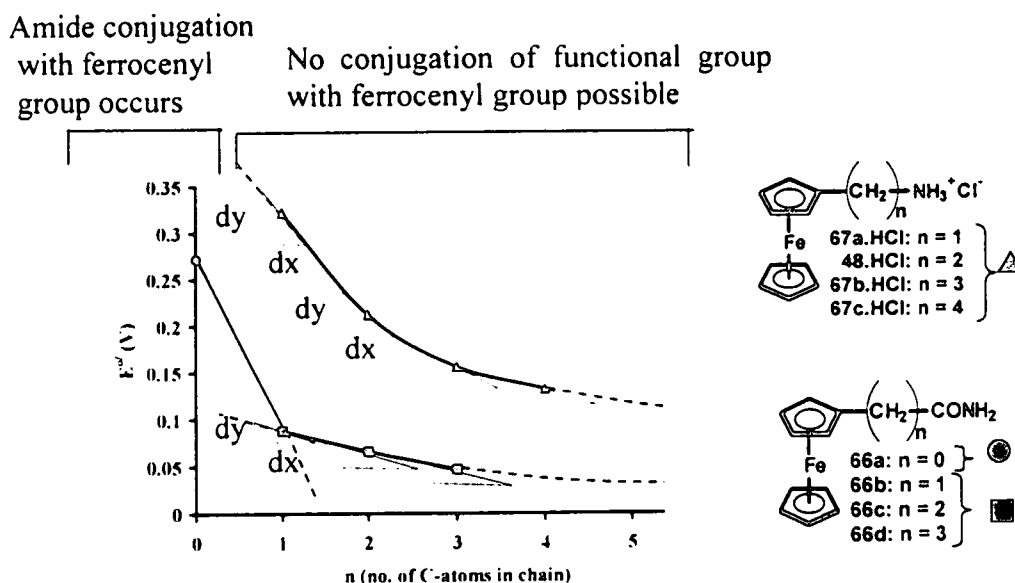


Figure 3.6 Relation between $E^{o'}$ and n . " n " is the number of CH_2 groups that separate the ferrocenyl group from either the NH_3^+ group in compounds of type $\text{Fc}-(\text{CH}_2)_n\text{NH}_3^+$ (48, 67a - c in water, Δ , $E^{o'}$ vs. Ag/AgCl) or from the type CONH_2 group in compounds of the type $\text{Fc}-(\text{CH}_2)_n\text{CONH}_2$ (in acetonitrile, 66a = \bullet , a conjugated system and 66b - d = \blacksquare , non conjugated systems, $E^{o'}$ vs. Ag/Ag $^+$), Fc = ferrocenyl. The slope dy/dx becomes steeper with shorter chain length indicating that with shorter chain lengths the Fc/Fc $^+$ couple is under the influence of stronger electron withdrawing functional groups, here NH_3^+ or CONH_2 . Since dy/dx is larger for NH_3^+ than for the corresponding CONH_2 compounds, it follows that NH_3^+ is a stronger electron-withdrawing group than the CONH_2 group.

The influence of the strongly electron withdrawing NH_3^+ group on the reduction potential of the ferrocenyl/ferricenium couple is most pronounced in 67a where the connecting chain is a single CH_2 group (Note that for this part of the discussion, compound 66a which has NO connecting chain is ignored) as this compound is substantially more difficult to oxidise ($E^{o'}$ =

0.322 V) than the other compounds in this series ($0.132 \text{ V} \leq E^{o'} \leq 0.212 \text{ V}$). As the number of CH_2 groups increases from 1 to 4, the electron-withdrawing influence of the NH_3^+ group diminishes non-linearly to a value of 0.132 V. One would expect that the trend of higher $E^{o'}$ values with shorter connecting chain lengths would be more pronounced in compounds with strong electron-withdrawing substituents compared with what is observed for weak electron-withdrawing substituents. This expectation is confirmed when one compares the drift in $E^{o'}$ values for the amide functionalised ferrocene compounds **66a – d** with that of the NH_3^+ -ferrocenes of this section as shown in Figure 3.6. For example, the slope, dy/dx , at $n = 1$ is much smaller for $\text{Fc-CH}_2\text{-CONH}_2$ than for $\text{Fc-CH}_2\text{-NH}_3^+$ (see Figure 3.9) because the electron-withdrawing capabilities of the R-NH_3^+ group exceeds that of the carbonyl moiety in an amide group by far.

3.3.1.3 Ferrocene-amine electrochemistry in acetonitrile

The ferrocene-amine hydrochlorides of the previous section are, of course, also soluble in organic solvents as the free base. Hence a cyclic voltammetric study of the basic ferrocene-amines **48** and **67a – c** was also undertaken in the organic solvent acetonitrile. Approximately 1 mmol dm^{-3} solutions of the ferrocene-containing amines **48**, **67a–c** containing 0.1 mol dm^{-3} tetrabutylammonium hexafluorophosphate as supporting electrolyte in acetonitrile were used for cyclic voltammetric studies. A three electrode system consisting of a Pt wire as auxiliary electrode, a Pt working electrode and a Ag/Ag^+ non-aqueous reference electrode were used.

Some cyclic voltammogram of **48** and **67a – 67c** is shown in Figure 3.7. The amines **48**, **67b** and **67c** show normal cyclic voltammetric behaviour, but the cyclic voltammograms of ferrocenylmethylamine, **67a**, shows two peaks indicated by couple I and couple II. This

observation will shortly be attempted to be explained, but first attention will be given to compounds 48, 67b and 67c. All electrochemical results are summarised in Table 3.4.

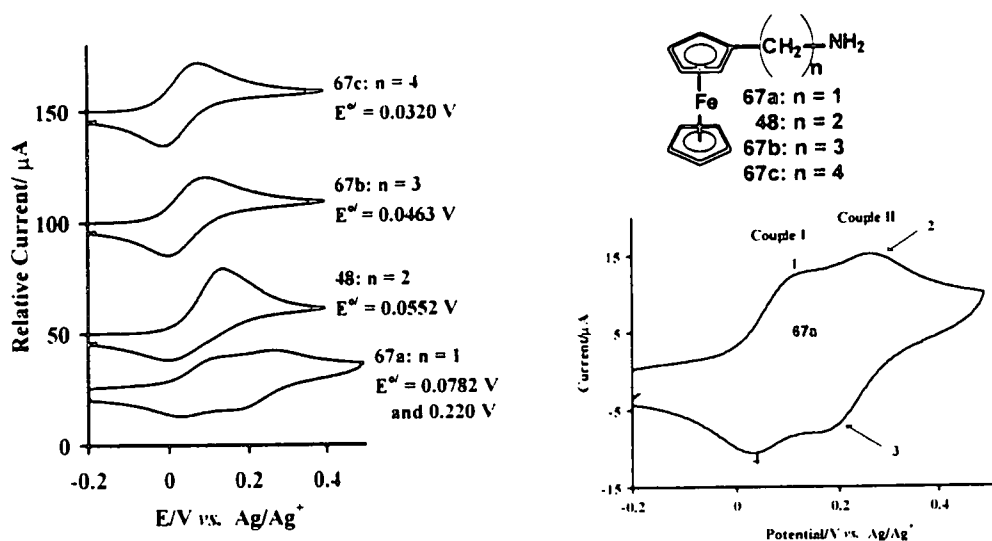


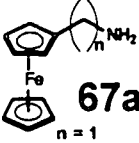
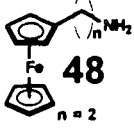



Figure 3.7 Cyclic voltammograms of *ca.* 1 mmol dm⁻³ solutions of the ferrocene-containing amine series (Fc-(CH₂)_n-NH₂) in CH₃CN containing 0.1 mol dm⁻³ tetrabutylammonium hexafluorophosphate at 25°C at a scan rate of 250 mV/s on a Pt working electrode. Insert bottom right: Enlargement of the 200 mV/s scan of 67a highlighting the two observed electrochemical couples for this compound.

Excluding compound 67a the difference in peak anodic, E_{pa}, and peak cathodic, E_{pc}, potentials, ΔE_p, for all ferrocene-containing amines 48, 67a and 67c indicate quasi electrochemical reversibility. For the purpose of this study, when the measured ΔE_p ≤ 80 mV, the electrochemical processes are regarded as electrochemically reversible¹⁰⁵ (in theory ΔE_p = 59 mV). Any ΔE_p value larger than 80 mV is considered as a quasi-reversible electrochemical process.

The current ratio i_{pc}/i_{pa} (where i_{pc} and i_{pa} are the peak cathodic and peak anodic currents) are all well below 1. This implies that the electrochemical oxidation of the iron (II) nucleus of the ferrocenyl groups is not followed exclusively by an electrochemically induced reduction

of the Fe (III) nucleus of the ferricenium group. It follows therefore that oxidation of the ferrocenyl group in these amines is electrochemically irreversible although it may be chemically reversible.

Table 3.4 Electrochemical data for the ferrocene-containing amines 48, 67b and 67c in CH_3CN containing 0.1 mol dm^{-3} tetrabutylammonium hexafluorophosphate as a supporting electrolyte at 25°C .

| Compound | Scan rate mV/s | E_{pa} V | ΔE_p mV | E^0 V | i_{pa} μA | i_{pc}/i_{pa} |
|--|-------------------|---------------|--------------------|------------|---------------------------|-----------------|
| Couple I | | | | | | |
|  67a $n=1$ | 50 | 0.108 | 60 | 0.078 | 4.35 | 0.94 |
| | 100 | 0.109 | 64 | 0.077 | 6.35 | 0.90 |
| | 150 | 0.113 | 71 | 0.077 | 8.00 | 0.88 |
| | 200 | 0.116 | 74 | 0.078 | 9.50 | 0.81 |
| | 250 | 0.118 | 76 | 0.079 | 10.66 | 0.79 |
| | Average | | | | 0.078 | |
| Couple II | | | | | | |
|  48 $n=2$ | 50 | 0.252 | 59 | 0.227 | 3.05* | 0.94 |
| | 100 | 0.251 | 61 | 0.221 | 4.07* | 0.91 |
| | 150 | 0.251 | 66 | 0.218 | 5.09* | 0.95 |
| | 200 | 0.251 | 71 | 0.216 | 6.36* | 1.00 |
| | 250 | 0.251 | 71 | 0.216 | 7.12* | 1.00 |
| | Average | | | | 0.220 | |
|  67b $n=3$ | 50 | 0.093 | 96 | 0.045 | 11.16 | 0.73 |
| | 100 | 0.103 | 104 | 0.051 | 15.76 | 0.71 |
| | 150 | 0.114 | 117 | 0.056 | 20.02 | 0.66 |
| | 200 | 0.125 | 127 | 0.062 | 23.96 | 0.59 |
| | 250 | 0.135 | 141 | 0.065 | 27.70 | 0.52 |
| | Average | | | | 0.055 | |
|  67c $n=4$ | 50 | 0.096 | 91 | 0.050 | 8.99 | 0.94 |
| | 100 | 0.086 | 83 | 0.045 | 12.94 | 0.85 |
| | 150 | 0.092 | 93 | 0.045 | 14.97 | 0.90 |
| | 200 | 0.089 | 94 | 0.042 | 17.11 | 0.93 |
| | 250 | 0.096 | 97 | 0.047 | 19.02 | 0.92 |
| | Average | | | | 0.046 | |
|  67c $n=4$ | 50 | 0.069 | 79 | 0.030 | 9.86 | 0.87 |
| | 100 | 0.071 | 81 | 0.030 | 13.05 | 0.91 |
| | 150 | 0.072 | 84 | 0.031 | 15.66 | 0.90 |
| | 200 | 0.073 | 88 | 0.029 | 17.98 | 0.90 |
| | 250 | 0.091 | 106 | 0.038 | 20.01 | 0.87 |
| | Average | | | | 0.032 | |

* i_{pc} values as i_{pa} was inaccurate.

The spread of formal reduction potentials of the ferrocene-containing amine derivatives **48**, **67b** and **67c** is small. The least positive formal reduction potential value is 0.0386 V for ferrocenylbutylamine, **67c**, whereas the most positive $E^{o'}$ value is 0.055 V (compound **48**) or 0.078 V (couple I for **67a**). This very small spread in $E^{o'}$ values is the result of very poor communication between the ferrocenyl group and the amino group *via* the isolating $(\text{CH}_2)_n$ linking chains. Communication is the result of a field effect through space and not conjugation along double bonds.

Table 3.4 and Figure 3.8 shows or demonstrate the decrease in formal reduction potentials, $E^{o'}$, for the ferrocenyl compounds with an increase in the length of the linear aliphatic segment that links the ferrocenyl fragment with the amine and NH_3^+ functional group.

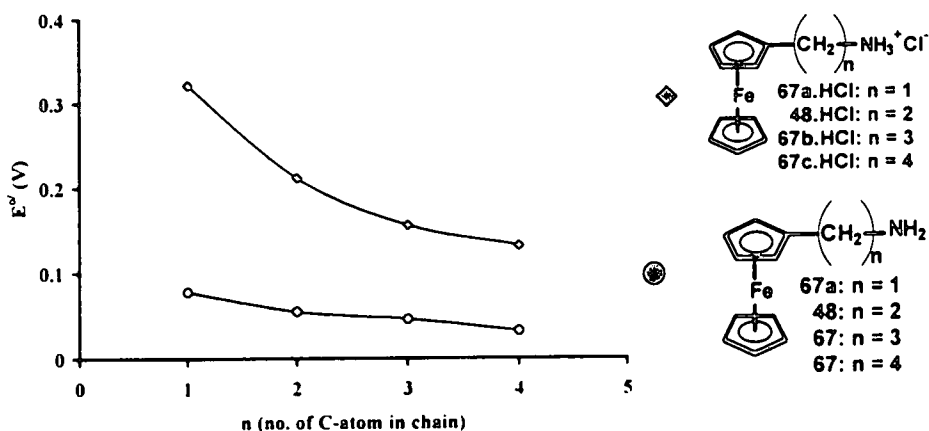
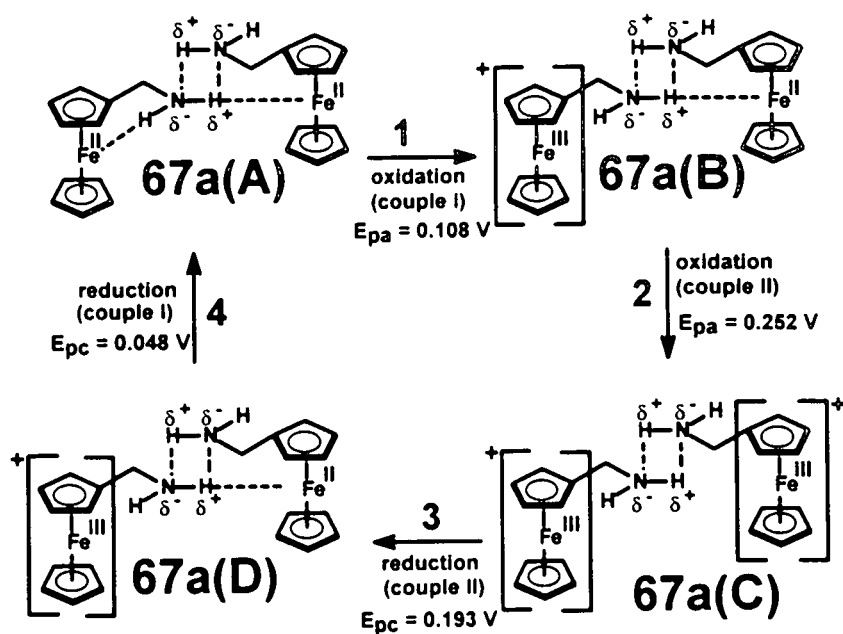


Figure 3.8 Relation between $E^{o'}$ and n . 'n' is the number of CH_2 groups that separates the ferrocenyl group from the NH_2 group of the type $\text{Fc}(\text{CH}_2)_n\text{NH}_2 = (\odot)$ (**48**, **67a - c** in acetonitrile, $E^{o'}$ (V) vs. Ag/Ag^+) and NH_3^+Cl^- of the type $\text{Fc}(\text{CH}_2)_n\text{NH}_3^+\text{Cl}^- = (\diamond)$, in water, $E^{o'}$ (V) vs. Ag/AgCl , Fc = ferrocenyl. For **67a**, couple I was used in this plot.

When we compare the drift in $E^{o'}$ values for NH_3^+ -ferrocene compounds (Table 3.3, page 60) with that of the NH_2 -ferrocene compounds of this section, it is obvious that the NH_3^+

compounds have a larger influence on the $E^{0'}$ values than the $-NH_2$ group. This effect is also shown in Figure 3.8.

Returning to the cyclic voltammogram of ferrocenylmethylamine, **67a**, (Figure 3.7, page 64 insert graph), two ferrocenyl/ferricenium couples were observed. Couple I displayed the expected formal reduction potential of 0.078 V. Couple II showed a $E^{0'}$ value of 0.220 V which indicates that in this couple, the ferrocenyl group is subjected to a much stronger electron withdrawing group than in couple I. An immediate NMR of amine **67a** proved that this compound had not decomposed. Furthermore, amine **67a** does not show 2 couples in water when the amine is converted to the $NH_3^+Cl^-$ salt (see section 3.3.1.2 page 59). This observation indicated that some hydrogen bonding network may result in the observed two couples. It is known that the iron (II) nucleus of ferrocene can interact with H^+ .¹³⁷ Making use of this property, one may conceive a hydrogen bonding network as proposed for structure **67a (A)** in Scheme 3.10.



Scheme 3.10 The possible explanation of the broadening of the peaks of ferrocenylmethylamine, **67a**, during oxidation-reduction processes.

Structure 67a(A) proposes that 67a actually exists as a stable dimer in acetonitrile solutions. If this is the case, then the observed two redox couples of 67a are easy to explain. First, the reader's attention is drawn to the cyclic voltammogram of the β -diketone diferrocenoyl-methane, 53e.⁹³ This is shown in Figure 3.9.

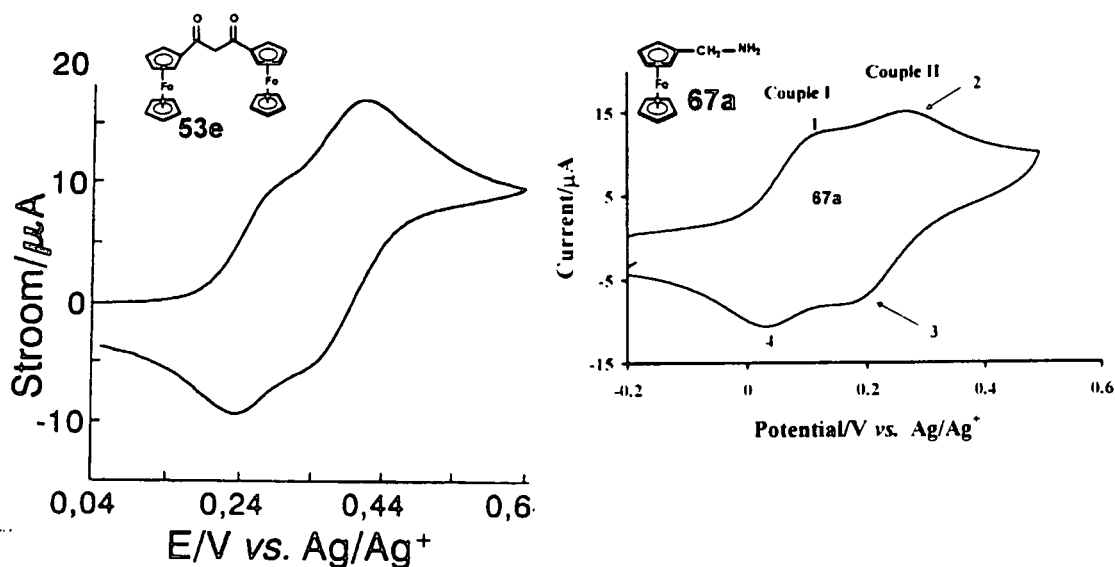
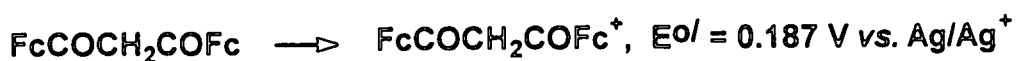


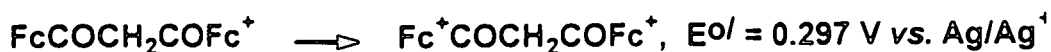
Figure 3.9 Cyclic voltammogram and structure of diferrocenoylmethane 53e (left) and ferrocenylmethylamine 67a (right).

The similarity of these two cyclic voltammograms is obvious. The two peaks that were observed for diferrocenoylmethane was explained by observing that the two ferrocenyl groups are not oxidised simultaneously at the surface of the electrode. First one ferrocenyl group (Fc) is oxidised in the reaction

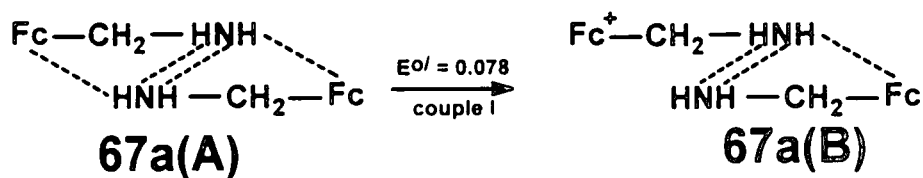


The group electronegativity⁹³ of an Fc^+ group ($\chi_{\text{Fc}^+} = 2.82$) is, however, much more than that of a Fc group ($\chi_{\text{Fc}} = 1.87$). It is in fact almost as electron withdrawing as a CF_3 (for structure, see Scheme 2.6, page 29 compound 53a) group ($\chi_{\text{Fc}} = 3.01$). This meant that the second Fc group that still has to be oxidised in $\text{FcCOCH}_2\text{COFc}^+$ is now, by means of conjugation,

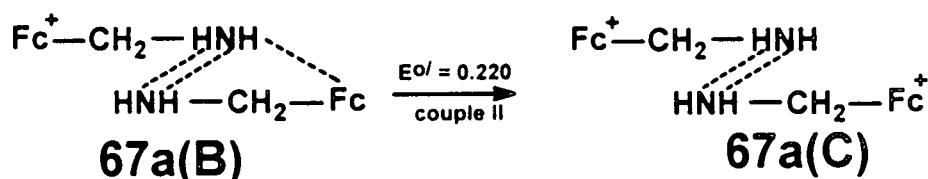
experiencing the rather strong electron withdrawing properties of the Fc^+ group making it much more difficult to oxidise.



It is proposed that a similar process is taking place in **67a** when it is electrochemically oxidised. However, there is no conjugation possible in **67a** as there is in diferrocenylmethane **53e**. Communication here must be restricted to a thorough-space, inductive field effect. Therefore, when the dimer **67a(A)** in Scheme 3.10 is oxidised in couple I, we propose that **67a(B)** with only one Fc^+ group is formed through the reaction



Through hydrogen bonding the remaining unoxidised ferrocenyl group of **67a(B)** (see Scheme 3.10) is now experiencing the strong electron withdrawing properties of an Fc^+ group as was in the case for diferrocenylmethane. The oxidation of **67a(B)** to give the double oxidised ferricenium dimer **67a(C)**, therefore, takes place at a much higher potential than the potential that was necessary to oxidise **67a(A)** to **67a(B)** (see also Scheme 3.10).



In the cathodic cycle, the above two processes are reversed. The overall effect of formation of a stable dimer would therefore be two redox couples in the cyclic voltammogram of **67a**. We have found these two couples at formal reduction potentials of 0.078 V (couple I) and 0.220 V (couple II).

ΔE_p values for both couples were ideal at slow scan rates (60 and 56 mV respectively) but i_{pc}/i_{pa} ratios could not be determined very accurately due to poor resolution of the two redox waves. Peak anodic currents and i_{pc}/i_{pa} ratios documented in Table 3.4 were estimated from superimposing the decay current for peak 2 on peak 1 and the decay current of peak 4 on peak 3. The current ratios are surprisingly close to 1 especially at low scan rates. This indicated that the free electrons of the amino group in 67a(A) to 67a(C) were indeed largely occupied by something, providing further proof for our proposed dimer 67a(A). Peak currents for couple I were not exactly identical bearing in mind the inherent inaccuracy of determining peak current values from the unresolved couples in the cyclic voltammogram of 67a (Figure 3.7, page 64). However, they did not deviate so much from each other that it was inconsistent with our proposed structural dimer 67a(A) – 67a(C). Indications therefore are that couple I and couple II actually had about the same amount of ferrocenyl groups that were redox active (i.e. 50% each for the dimer 67a(A) – 67a(C)).

3.3.2 Cyclic voltammetry of water-soluble polymer-bound ferrocenes

The electrochemistry of the polymers 69 – 72 was investigated in water. The electrode system used for these aqueous cyclic voltammetry measurements consisted of a Pt wire auxiliary electrode, glassy carbon working electrode and a Ag/AgCl reference electrode. The supporting electrolyte was always 1 mol dm⁻³ KCl and the concentration of each polymer was such that the ferrocenyl concentration was *ca.* 1 mmol dm⁻³. The cyclic voltammograms of polymers 69 – 72 are shown in Figure 3.10 and results are summarised in Table 3.5, page 72.

The ΔE_p values of polymers 69, 70 and 71 were found to be very close to the theoretical value of 59 mV at 50 mV/s scan rate (70 mV, 59 mV and 59 mV respectively), whereas for 72, it

was found to be 99 mV (Table 3.5). The reason for this observation is not quite clear but the larger side chain of 72 ($n = 4$) is probably instrumental in it.

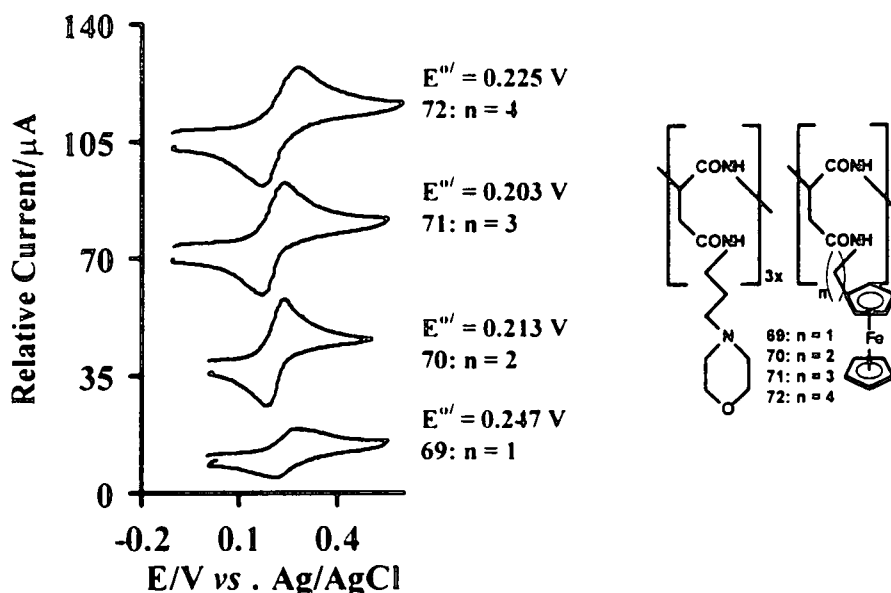
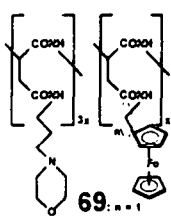
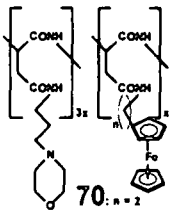
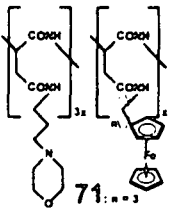
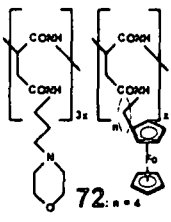


Figure 3.10 Cyclic voltammograms of 1 mmol dm⁻³ solution of polymers 69 – 72 in water containing 1 mol dm⁻³ at 25°C at a scan rate of 100 mV/s on a glassy carbon working electrode.

The influence of the CH₂ spacer was also observed on the current ratios, i_{pc}/i_{pa} . The average i_{pc}/i_{pa} values moved closer to 1 from 0.70 to 0.95 in polymers 69 - 72 respectively) as the length of the (CH₂)_n spacer that separates the amide functional group linking polymer main chain with the ferrocenyl moiety increases. This is probably due to the greater 'nakedness' (more exposedness) of the ferrocenyl group in polymers with longer side chains (e.g. 72, $n = 4$) as compared to polymers with shorter side chains. To explain, shorter ferrocenyl side chain polymers possess a ferrocenyl group locked between aminopropyl morpholine side chains, while this becomes progressively less in the case for polymers with long ferrocenyl side chains. Figure 3.11, page 73 shows how the ferrocenyl group in 69 is actually more easily accessible for the N:-group of the morpholino moiety than in the case for 72.

Table 3.5 Peak anodic potentials, E_{pa} , difference in peak anodic and peak cathodic potentials, $\Delta E_p = (E_{pa} - E_{pc})$, formal reduction potentials, $E^{o'} = (E_{pa} + E_{pc})/2$, peak anodic currents, i_{pa} and peak cathodic/anodic current ratios, i_{pc}/i_{pa} , (i_{pc} = peak cathodic currents) for the polymeric conjugates 69 - 72. [Polymeric conjugates] = 1 mmol dm⁻³, with 1 mol dm⁻³ KCl) as supporting electrolyte.

| Compound | Scan rate mV/s | E_{pa} V | ΔE_p mV | $E^{o'}$ V | i_{pa} μA | i_{pc}/i_{pa} |
|---|-------------------|---------------|--------------------|--------------------------|---------------------|-----------------|
|  69...1 | 50 | 0.282 | 70 | 0.247 | 4.30 | 0.73 |
| | 100 | 0.282 | 69 | 0.248 | 6.14 | 0.76 |
| | 150 | 0.297 | 93 | 0.250 | 8.21 | 0.71 |
| | 200 | 0.281 | 77 | 0.242 | 9.50 | 0.68 |
| | 250 | 0.292 | 89 | 0.247 | 10.50 | 0.63 |
| Average | | | | 0.247 | | 0.70 |
|  70...2 | 50 | 0.235 | 59 | 0.210 | 12.21 | 0.84 |
| | 100 | 0.237 | 58 | 0.213 | 17.18 | 0.82 |
| | 150 | 0.244 | 60 | 0.214 | 20.49 | 0.85 |
| | 200 | 0.245 | 66 | 0.212 | 23.64 | 0.83 |
| | 250 | 0.245 | 67 | 0.213 | 26.39 | 0.84 |
| Average | | | | 0.212 | | 0.83 |
|  71...3 | 50 | 0.234 | 58 | 0.205 | 12.35 | 0.90 |
| | 100 | 0.239 | 71 | 0.203 | 17.29 | 0.88 |
| | 150 | 0.241 | 70 | 0.205 | 20.79 | 0.87 |
| | 200 | 0.247 | 80 | 0.206 | 23.43 | 0.88 |
| | 250 | 0.254 | 95 | 0.207 | 26.30 | 0.86 |
| Average | | | | 0.205 | | 0.88 |
|  72...4 | 50 | 0.266 | 99 | 0.227 ^a | 13.33 | 0.97 |
| | 100 | 0.281 | 113 | 0.225 ^a | 18.08 | 0.97 |
| | 150 | 0.282 | 113 | 0.226 ^a | 21.67 | 0.96 |
| | 200 | 0.281 | 134 | 0.224 ^a | 23.75 | 0.98 |
| | 250 | 0.291 | 137 | 0.222 ^a | 25.67 | 0.94 |
| Average | | | | 0.225^a | | 0.95 |

^a The potential of 0.225 V for 72 is an anomaly. Adding 59/2 mV to the E_{pc} value (not listed) indicates a value of $E^{o'} = 166 + 59/2 = 195$ mV, which may be more realistic.

In paragraph 3.3.1.1 and 3.3.1.2 it was demonstrated that the inter- or intramolecular electron transfer reactions from the free electron pair on N-atom is much more effective than electron transfer from the free electron pair on an O-atom.

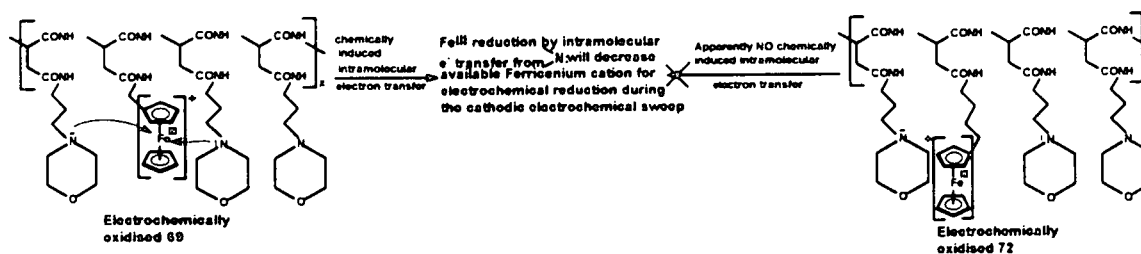


Figure 3.11 Chemically induced intramolecular electron transfer for the oxidised form of polymer 69 is more possible than for the oxidised form of polymer 72.

It is clear from Figure 3.11 that electron transfer from the free electron pair on the N-atom of the morpholino group to a electronically generated ferricenium group is much more feasible for 69 than for 72, simply by means of the easier access of an N:-group to a Fe^{III} centre in 69 than compared to the more difficult access in 72. This being the case, it is obvious that in 69 not all electrochemically generated oxidised 69 will be available for reduction during the cathodic sweep of cyclic voltammetry as some Fe^{III} centers may be chemically reduced by intramolecular electron transfer from a N:-atom from the morpholino group. Apparently the longer ferrocene side chains of 72 prevent this intramolecular electron transfer. This observation clearly explains why the $i_{\text{pc}}/i_{\text{pa}}$ ratio is best for 72 and poorest for 69.

Again the same tendency of decreasing formal reduction potentials with increasing aliphatic side chain length was observed in Table 3.6. Formal reduction potential, E^{of} , values decreased from 0.247 V to 0.203 V (for polymers 69 and 71 respectively). Polymer 72 showed a slightly higher E^{of} value (0.225 V) than polymers 70 and 71 (0.213 V and 0.203 V respectively). The reason for this may be centered therein that the structure of polymer 72 ($n = 4$) is such that the redox active ferrocenyl site cannot get access to electrodes for the same

reason as described in the previous section (see Figure 3.11). From Table 3.5 E_{pa} values in particular appears to be accessively large. The E_{pc} values of *ca.* 166 mV (not listed) are more in line of what is expected for this compound. By adding half the ideal ΔE_p value to the E_{pc} values, a more "expected" $E^{o'}$ value of $166 + 59/2 = 196$ mV vs. Ag/AgCl may be found.

Figure 3. 12 show the relationship of formal reduction potential ($E^{o'}$) against 'n', the number of carbon atoms separating the ferrocenyl moiety from the amide, amine, ammonium hydrochloride and polymer-amide functional groups from ferrocenyl moiety.

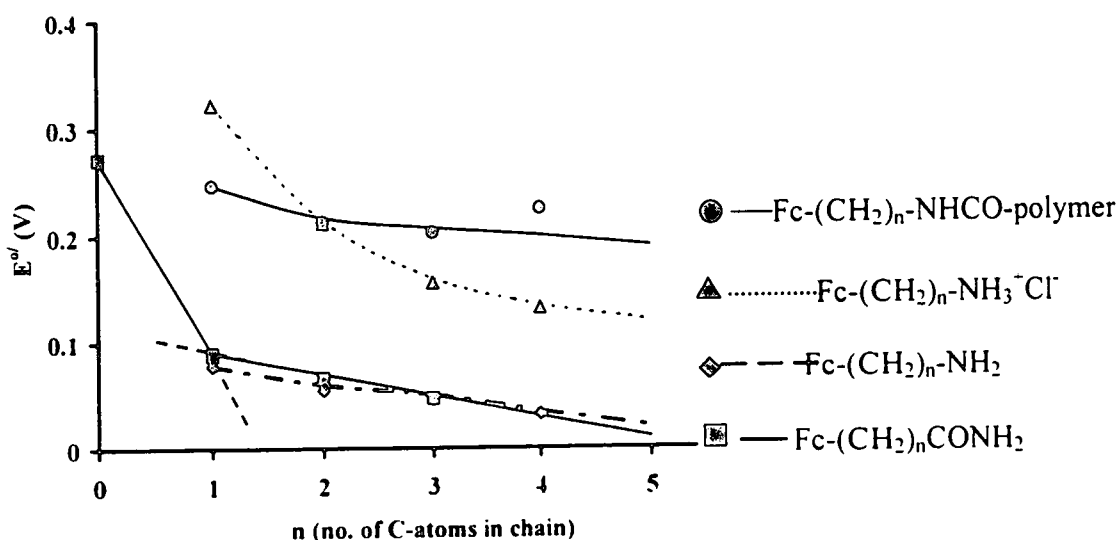


Figure 3. 12 Comparison of $E^{o'}$ vs. n (number of CH_2 groups separating the indicated functional group from the ferrocenyl moiety) for the ferrocene-containing amides 66a - d (◻), amines 48, 67a - c (◇), amine hydrochlorides 48.HCl, 67(a - c).HCl (△) and polymers 69 - 72 (○). n = 0, 1, 2, 3 or 4.

With the exception of polymer 72, the results above show that the ferrocenyl formal reduction potential ($E^{o'}$) decreases with increase in the length of the $(\text{CH}_2)_n$ chain linking ferrocenyl group with functional group. The deviation of 72 from this trend, $\Delta E^{o'} = 20$ mV is not explainable at this stage. The biggest influence is observed where $n = 0$ ($\text{Fc}-(\text{CH}_2)_n\text{-CONH}_2$

series) and this is where conjugation between the ferrocenyl group and the amide group is possible. The trend of change in $\Delta E^{o'}$ with size of 'n' is much smaller when no conjugation is possible ($n > 1$). In the studied families of compounds, it was found that the charged ammonium species, NH_3^+ , has a larger influence on the $E^{o'}$ value with shorter separating chains than the $-\text{NH}_2$, $-\text{NHCO}-$ or $-\text{CONH}_2$ groups. This is attributed to the greater electron-withdrawing properties the $-\text{NH}_3^+$ group has compared to a $-\text{NH}_2$, $-\text{NHCO}-$ or CONH_2 groups.

3.3.3 Conclusion

The electrochemistry performed on all the ferrocene-containing compounds **48**, **66**, **67** and polymers **69** – **71** above showed that the compounds with the least positive formal reduction potentials were in every series that compounds with the largest $(\text{CH}_2)_n$ spacer separating the ferrocenyl group from a functional group.

Based on earlier results obtained in this laboratory, it is expected that these compounds will also be the most active in chemotherapy, and that the polymer derivatives **69** – **72** should also be more active based on actual drug content than the monomeric amide or amine precursors **66**, **48** and **67** respectively. This hypothesis was put to the test with a study of the cytotoxicity of these compounds on two human cancer cell lines and results will be discussed in the next section, paragraph 3.4.

3.4 Cytotoxicity studies

The experimental part of the cytotoxic studies were performed by Mrs Elke Krefl from the Department of Immunology, Institute for pathology at the University of Pretoria. The author thanks her for her efforts.

3.4.1 Introduction

The cytotoxicity of ferrocene-containing amides, **66a** – **66d**, amines, **48**, **67a** - **c** and polymers **69** - **72**, were determined by observing their effects *in vitro* on cultured HeLa and CoLo DM320 cell lines for 1 day and/or 7 days of continuous drug exposure. HeLa is a human cervix epitheloid cancer cell line, while CoLo DM320 is an intrinsically multidrug resistant human colorectal cell line. After incubation at 37°C, cell survival was measured as a percentage of living cells in relation to a control that was not exposed to the drug by means of the colorometric 3-(4,5-dimethylthiazol-2-yl)-diphenyltetrasodium bromide (MTT) assay.¹³⁵

Survival curves indicating percentage cell survival were plotted as a function of drug dose (in µg/ml or mg/ml for the polymers). Figure 3.13 shows a set of these survival curves after 7 days of incubation with the monomeric amides and monomeric amines respectively. IC₅₀ values (drug dose required for 50% cell death) were estimated by extrapolation and are summarised in Table 3.6.

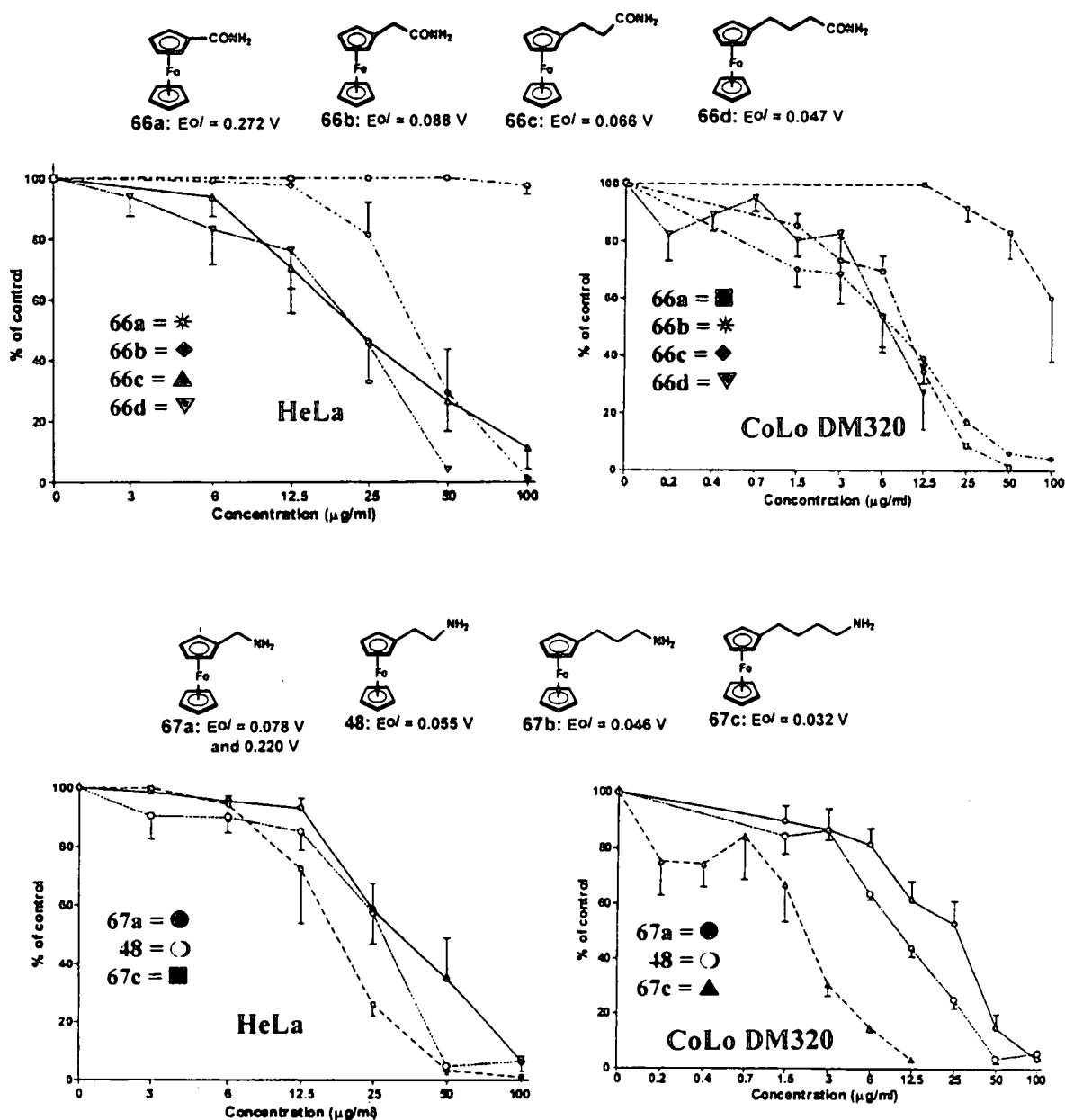


Figure 3.13 Percentage cell survival for HeLa and DM320 cancer cell lines, relative to the control vs. concentration ($\mu\text{g/ml}$) of amides 66a - 66d and amines 48, 67a and 67c (see structures above graphs) after 7 days incubation. Sited potentials are versus a Ag/Ag^+ reference in acetonitrile.

3.4.2 Small molecule ferrocene-amides and -amines

It was found that the amide 66a had no observable effect on HeLa cell line at concentrations up to 100 $\mu\text{g/ml}$ while for CoLo DM320 cell line a slight effect was only observed at

concentrations larger than 25 $\mu\text{g/ml}$ (see Figure 3.13). Results are summarised in Table 3.6 (page 79).

The activity of amides **66a - d** improves on HeLa and CoLo DM320 cancer cell lines with increase in $(\text{CH}_2)_n$ chain length that separates the amide group from the ferrocenyl group. From the IC_{50} values summarised in Table 3.6 amide **66d** is the most effective in killing both HeLa ($\text{IC}_{50} = 23.4 \mu\text{g/ml}$) and CoLo ($\text{IC}_{50} = 6.3 \mu\text{g/ml}$) cell lines in the amide series of compounds. It is strikingly evident that all the amides **66** are about 4 times effective in killing the multi drug resistant CoLo DM320 cell line than the HeLa cell line. This is an unusual observation as most drugs are more active against HeLa than CoLo DM320 cancer cells. It was also evident that compounds with less formal reduction potential, $E^{o'}$ values are more active, while those with more positive $E^{o'}$ values (**66a** has $E^{o'} = 0.272 \text{ V vs. Ag/Ag}^+$) are less active or totally inactive (Table 3.6).

The activity of ferrocene-containing amines **48**, **67a** and **67c** against HeLa and CoLo DM320 cell lines (Figure 3.13), showed a similar trend as the precursor amides in that

Table 3.6 Formal reduction potentials, $E^{o'}$, (vs. Ag/Ag⁺ in acetonitrile) and IC_{50} values of the amides **66** and amines **48** and **67** in *in vitro* cancer cells after 7 days of incubation utilising CoLo DM320 and HeLa cell lines.

| Compound ^a | $E^{o'}$ (V) | IC_{50} ($\mu\text{g}/\text{cm}^3$) ^c | |
|-----------------------|-----------------------------|--|-----------------|
| | | HeLa | CoLo DM320 |
| 66a | 0.272 | >50 | >100 |
| 66b | 0.088 | 39.7 | 10.2 |
| 66c | 0.066 | 21.6 | 6.8 |
| 66d | 0.047 | 23.4 | 6.3 |
| 67a | 0.0782 (0.322) ^b | 28.5 | 29 |
| 48 | 0.0552 (0.212) ^b | 28.0 | 9.5 |
| 67c | 0.0463 (0.156) ^b | -- ^d | -- ^d |
| 67d | 0.0320 (0.132) ^b | 18.2 | 2.0 |

^a For structures see Figure 3.15, page 74.

^b The potentials vs. Ag/AgCl in brackets are for the hydrochloride salts, $\text{Fc}-(\text{CH}_2)_n-\text{NH}_3^+\text{Cl}^-$, obtained (section 3.3.1.2, page 59), in water containing 10 mmol dm^{-3} HCl.

^c Data from three experiments and expressed as the mean drug concentration causing 50% cell death.

^d No measurements could be made as the drug decomposed during the experiment. For the HeLa cells one experiment could be performed with this compound giving an inaccurate estimate of $IC_{50} = 12 - 25 \mu\text{g}/\text{cm}^3$.

compounds with longer $(\text{CH}_2)_n$ spacers separating the ferrocenyl and amine groups from each other are more active in inducing cell death. This tendency is also demonstrated in Table 3.7 with IC_{50} values becoming smaller with longer $(\text{CH}_2)_n$ chains. Like the amides, the free amines were also more effective in destroying CoLo DM320 cells than HeLa cells. Using IC_{50} values in Table 3.6 amine **67c**, the most active amine, was 9 times more active in killing CoLo DM320 than HeLa cells. Like the amides, in Table 3.6 it can be seen that the amines also become more active in inducing cancer cell death with decrease in ferrocenyl formal reduction potential.

Figure 3.14 shows the relation between $E^{0'}$ and IC_{50} as well as "n" (in $(CH_2)_n$) and IC_{50} for both the amines and the amides. From the graphs in Figure 3.16 it is deduced that the amines with longer side chain lengths are better anticancer drugs than the precursor amides.

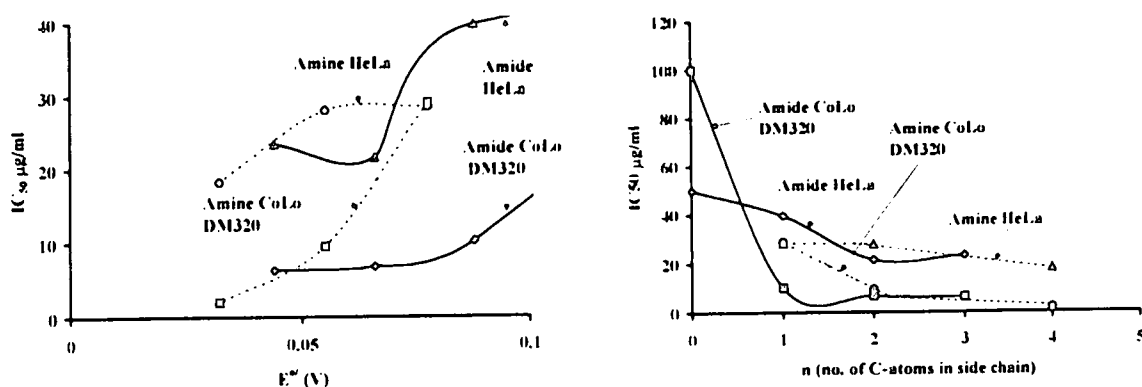


Figure 3.14 Relation between $E^{0'}$ (V) and IC_{50} ($\mu\text{g/ml}$) (left), and between "n" (in $(CH_2)_n$) and IC_{50} ($\mu\text{g/ml}$) (right) for the amides 66 and amines 48, 67a and 67c.

3.4.3 Polymeric conjugates

The activity of polymers 69 – 72 were measured after 1 day and after 7 days of incubation with HeLa and CoLo DM320 cancer cell lines (Figure 3.15). IC_{50} values for the different experiments are summarised in Table 3.7.

The first deduction that can be made from the IC_{50} values listed in Table 3.7 is that IC_{50} values from 1 day exposure experiment are consistently substantially higher than those from the 7 day exposure experiment. This observation is consistent with the possibility that an induction period is required to pass before the polymeric drugs become active. Such an observation will fit in with the explanation that the polymer needs to be at least partially enzymatically degraded (Chapter 2, page 11) before the drug is activated for cancer therapy.

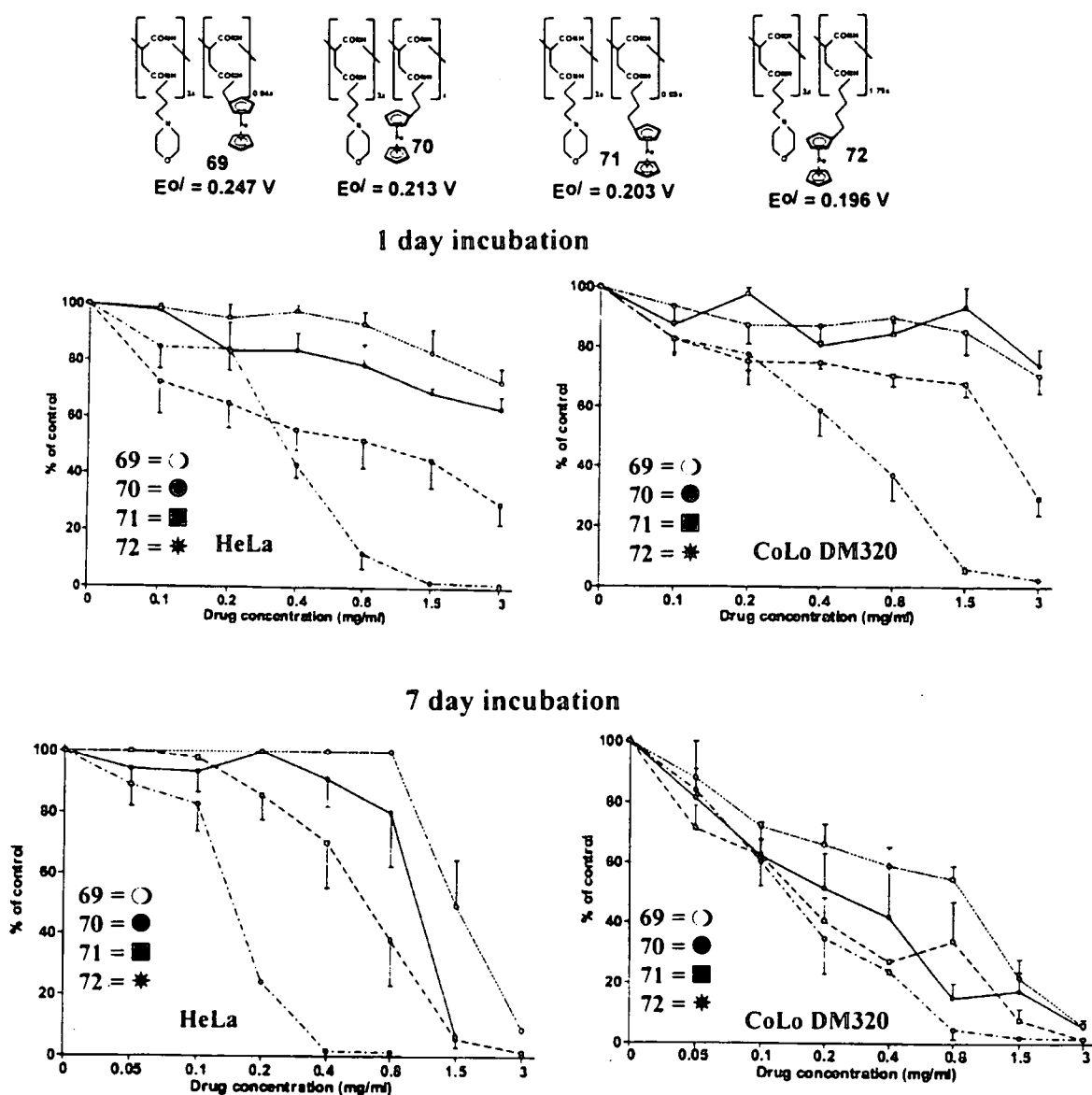


Figure 3. 15 Effects of polymers 69, 70, 71 and 72 on HeLa and CoLo DM320 cancer cell lines after 24 hours and 7 days of incubation. Cited potentials are versus an Ag/AgCl reference electrode in water. Percentage cell survival are expressed as a percentage of living cells in relation to a control that was not exposed to the drug.

The second piece of information that can be extracted from Figure 3.15 (and Table 3.7) is that in all cases, the most effective drug is once again that drug which has the longer spacer between drug moiety (the ferrocenyl group) and the polymer backbone, here polymer 72, which has $IC_{50} = 0.15$ mg/ml (7 day exposure).

Table 3.7 HeLa and CoLo DM320 cell lines cell death after 24 hours and 7 days incubation with polymer-ferrocene drugs, Fc = ferrocenyl.

| Compound | E ^{o'} (V) ^a | IC ₅₀ (mg/ml) ^b | | | | | |
|----------|-------------------------------------|---------------------------------------|---|--------------------------------------|---------------------------------------|---|--------------------------------------|
| | | HeLa | | | CoLo DM320 | | |
| | | 24 h ^c total polymer | 7 days ^c total polymer | 7 days ^d Fc content | 24 h ^c total polymer | 7 days ^c total polymer | 7 days ^d Fc content |
| 69 | 0.247 | >3 | 2.25 | 0.49 | >3 | 1.15 | 0.25 |
| 70 | 0.213 | >3 | 1.15 | 0.24 | >3 | 0.25 | 0.052 |
| 71 | 0.203 | 1.14 | 0.66 | 0.14 | 2.4 | 0.15 | 0.034 |
| 72 | 0.195 | 0.37 | 0.18 | 0.031 | 0.5 | 0.15 | 0.030 |

^a Data from paragraph 3.3.2, page 69.

^b IC₅₀ = dose in mg/cm³ required to induce 50% cell death.

^c Calculated for the total mass of polymer-based drug used.

^d Calculated for the actual drug content (ferrocenyl content) on the polymer administered.

Activity decreases, as the connecting chain between polymer chain and drug becomes shorter. The lowest activity was observed for **69** (IC₅₀ = 2.25 mg/ml and 1.15 mg/ml for 7 days incubation with HeLa and CoLo DM320 cells respectively). Unlike what was found for the non-polymer bound drugs, the polymeric devices **69** – **72** appeared to be more effective in killing the HeLa cells than the CoLo DM320 cells. This is more apparent by looking at the concentration where total cell death is achieved rather than looking at the IC₅₀ values in Table 3.7. Polymer **72** in particular achieved total HeLa cell death at a concentration of 0.4 mg/ml, while a concentration of *ca.* 1 mg/ml was needed for total CoLo DM320 cell death (7 days incubation), see Figure 3.15.

As was found for the free amines and amides of the previous paragraphs, the activity of the polymers also increased with lower formal reduction potentials for the ferrocenyl group.

Figure 3.16, left, demonstrate the graph for HeLa and right for CoLo DM320 cell lines tests.

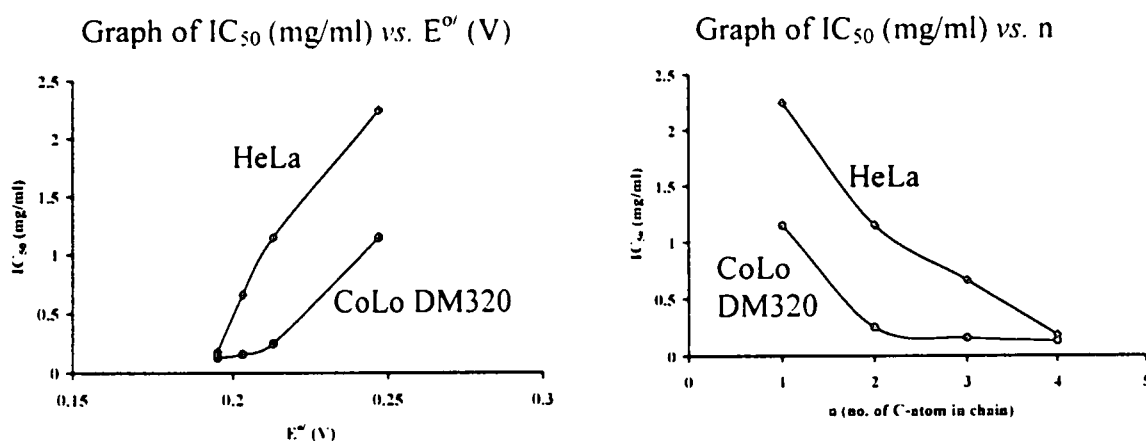


Figure 3. 16 Relation between E^{o'} and IC₅₀ (left) and between "n" (in (CH₂)_n) and IC₅₀ (right) on HeLa and CoLo DM320 cell lines for polymers 66 – 72.

The last thing that remains to be verified is if there was an improvement in the activity of the drug when anchored onto a water-soluble drug carrier as compared with the activity of the free drug. Table 3.7 gives IC₅₀ values both in terms of the total mass of polymer administered, and in terms of actual content of Fc-(CH₂)_n-NH fragment. The best polymeric drug was 72 with IC₅₀ value for HeLa cells in terms of actual drug content 31 μg/ml. The corresponding amine, compound 67c, and amide, compound 66b, had IC₅₀ values for the HeLa cell line of 18.2 and 23.4 μg/ml. This is rather a disappointing result as other results from this laboratory led us to expect an improvement at least of one order of magnitude in drug activity. To try and explain the lack of improvement in drug performance found in this study one need to examine the structural influence of the amides 66a – d and polymers 69 – 72 more closely. Figure 3.17 is a graph of IC₅₀ values against side chain length for 66 and 69 – 72 (utilising actual drug content IC₅₀ values for the polymers, (NOT total drug administered

values). It is evident that side chain length has a much larger influence on the activity of the polymeric

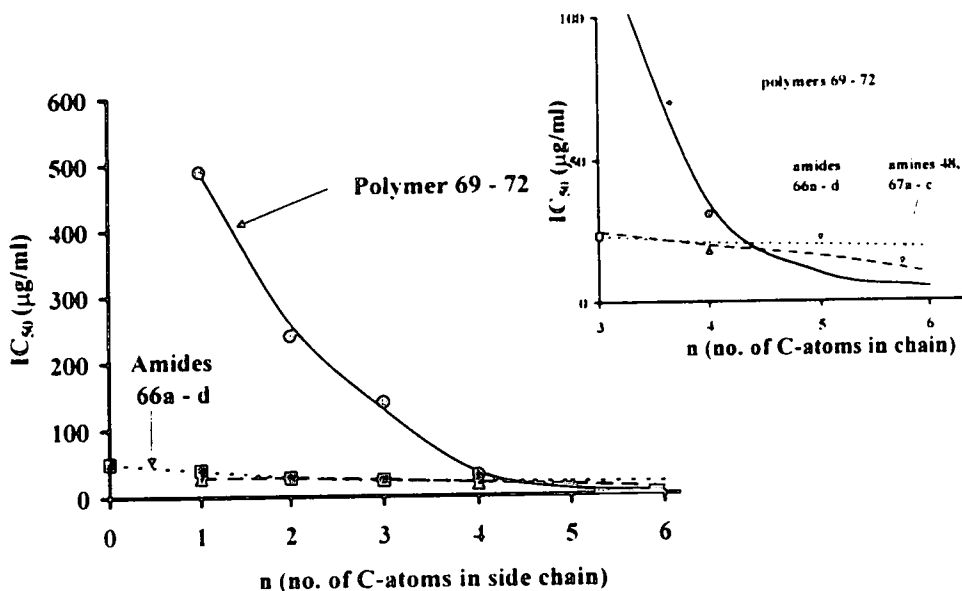


Figure 3.17 Relation between HeLa cell IC_{50} values against side chain length for the amides 66a - d, the amines 48, 67a, 67c and the polymers 69 - 72. Actual drug content IC_{50} values for the polymers and not the total polymer drug values were used in this graph. The insert graph is a blow up of the main graph for better reading.

drug than on the activity of the free, monomeric, drug. Extrapolation of the side chain length connecting either polymer main chain or with the ferrocenyl group raises the possibility that a polymer having a side chain connecting chain length of $(\text{CH}_2)_5$ or larger (that is only 1 or at worst maybe 2 C-atoms longer than was obtained in this study), probably will end up having a more active drug moiety than 72 or its monomeric precursors. The validity of this hypothesis will be tested in future studies (see Figure 3.18 and text thereafter).

For this study, the indications therefore are that there is a certain minimum side chain length that must be exceeded before a polymer-bound drug will end up more active than a free, monomeric, drug. Figure 3.18 predicts that this entry side chain length before

pharmacological benefits may obtained by a polymeric drug carrier may be 5 or 6 atoms between polymer and drug moiety. This deduced criterion was tested on a series of polymers that this laboratory reported on earlier in 2001.⁹ It was found that polymer **29** (Figure 3.18) were almost 10 times more effective than the free drug **49** in cytotoxic tests. Polymer **29** has 6 atoms separating the ferrocenyl group from the polymer main chain. Polymer **72** has only 4.

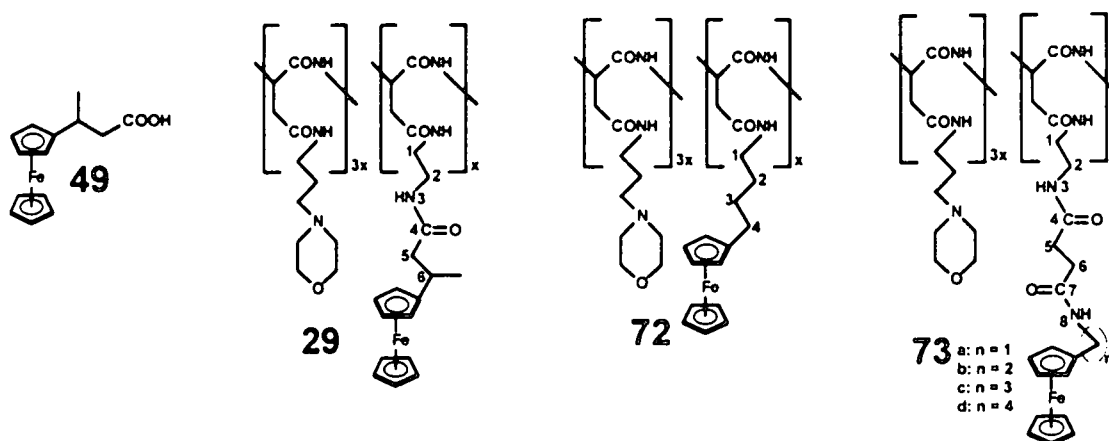


Figure 3. 18 Examples of polymers.

It appears thus the predictions from the graphs in Figure 3.15 that 5 – 6 spacer atoms are required before polymeric drug carriers will enhance cytotoxic activity of a ferrocene-containing drug, may be true. With this background research is currently underway to synthesise polymers **73** having 9 – 12 spacer atoms between ferrocenyl group and polymer main chain to test this hypothesis.

CHAPTER 4

EXPERIMENTAL

4.1 Materials

Solid reagents (Merck, or Aldrich) were used without further purification. Liquid reactants and solvents were distilled prior to use, water was double distilled. Dry, air-free acetonitrile was obtained by refluxing under nitrogen over calcium hydride before distilling onto alumina for storage. Dry, air-free diethyl ether and tetrahydrofuran (THF) were obtained by refluxing under nitrogen over sodium wire for 2 and 3 hours respectively.

4.2 Techniques and apparatus

4.2.1 Infrared (IR) Spectroscopy

IR-spectroscopy was conducted on a Hitachi 270-50 spectrometer with data processor. Solids samples were recorded in KBr pellets, while all the liquid samples were recorded as thin films between two NaCl discs.

4.2.2 Nuclear Magnetic Resonance (NMR) Spectroscopy

Proton ^1H NMR spectra at 298 K were recorded on a Bruker AM-300 FT-instrument with deuterated solvents as internal standards, while chemical shifts are presented as δ -values referenced to SiMe_4 at 0.00 parts per million (ppm).

4.2.3 Determination of the melting points (m.p.)

Melting points were determined with a Reichert Thermopan microscope, with a Koffler hot-stage and are uncorrected. This instrument can only detect melting points lower than 200°C.

4.2.4 Dialyses and freeze drying of polymers

Dialyses were performed against running tap water in 12000 molecular mass cut-off cellulose membrane tubing followed by freeze drying on an EZ-DRY 550Q instrument at -43°C and 63mTorr.

4.2.5 Column chromatography

Merck silica gel 60 (particle size 0.040-0.063 mm) was used for column chromatography and aluminium sheets coated with silica gel 60 F₂₅₄ were used for thin layer chromatography.

4.2.6 Cyclic voltammetry

Measurements on *ca.* 2 mmol dm⁻³ solutions of amides and 1 mmol dm⁻³ amines in acetonitrile with 0.1 mol dm⁻³ tetrabutylammonium hexafluorophosphate (Fluka, electrochemical grade) as supporting electrolyte were conducted under a blanket of purified argon at 25.0°C utilising a BAS model CV-27 voltammograph interfaced with personal computer. A three-electrode cell, which utilised a Pt auxiliary electrode, a Pt working electrode with surface area 0.03142 cm², and a Ag/Ag⁺ (0.0100 mol dm⁻³, AgNO₃) reference electrode mounted on a Luggin capillary¹⁰⁵ was employed. Aqueous electrochemistry of all amine hydrochloride and polymers were performed in water containing 1 mol dm⁻³ KCl as well as 10 mmol dm⁻³ HCl as supporting electrolyte, substrates concentrations were 1 mmol dm⁻³. The working electrode in the aqueous medium was a glassy carbon electrode of surface area 0.0707 cm².

For cleaning, electrodes were polished with 3µm Diapat diamond paste, rinsed with ethanol, acetonitrile followed by water and dried before each experiment. All measurements were referenced against Ag/AgCl electrode. Scan rates were between 50 and 250 mV/s. Data, uncorrected for junction potentials, were collected with an Adalab-PC™ and Adapt™ data acquisition kit (Interactive Microwave, Inc.) with locally developed software, and analysed with Hyperplot (JHM International, Inc.). The temperature was kept constant to within 0.5°C.

4.2.7 Cytotoxicity tests

The author acknowledges Mrs. Elke Kreft from the Department of Immunology, Institute for Pathology at the University of Pretoria for performing these experiments.

Sample preparations: Polymers, 69 – 72, were dissolved in water giving stock concentration of 50 mg/ml. Amides and amines (66a – 66d and 67a, 48, 67c, 67d respectively), were dissolved in DMSO to give stock concentration of 10 mg/cm³ and diluted in the appropriate growth medium supplemented with fetal calf serum (FCS) to give final DMSO concentrations not exceeding 0.5% and drug concentrations of 1-3000 µg/cm³ prior to cell experiments.

Cell cultures: A human colorectal cell line, CoLo DM320 (ATCC CCL-220), was grown as a suspended culture in RPMI 1640. The human cervix epitheloid cancer cell line, HeLa (ATCC CCL-2), were grown as a monolayer culture in MEM. Growth media was at 37°C under 5% CO₂ and fortified with 10% FCS, and 1% penicillin and streptomycin. Appropriate solvent control systems were included. Cells were seeded at 2000 cells/well for 24 h incubation experiments and 400 cells/well for 7 days incubation experiments in 96 well microtiter plates in a final volume of 200 µl of growth medium in the presence or absence of different concentrations of experimental drugs. Wells without cells and with cells but without drugs were included as controls. After incubation at 37°C for 1 day or 7 days cell survival was measured by means of the colometric 3-(4,5-dimethylthiazol-2-yl)-diphenyltetrasodium bromide (MMT) assay.¹³⁵

4.3 Synthesis and functionalisation of the ferrocene

4.3.1 2-Chlorobenzoylferrocene⁹⁷ (60) [Scheme 3.1, page 42]

A clean dry 1L three-necked round-bottom flask was immersed in an ice bath, and flushed with nitrogen gas. Ferrocene, **37a**, (18.603 g, 100 mmol), 2-chlorobenzoylchloride (17.5 g, 12.7 mmol), and dichloromethane (200 cm³) were added while stirring. When the solution was chilled thoroughly, solid anhydrous aluminium chloride (14.021 g, 100 mmol) was added in small portions at a rate so that the temperature of the reaction mixture does not exceed 5°C (about 20 min). The appearance of a deep blue colour indicated that the reaction was taking place. Stirring was continued for 30 min in the ice bath and then for 16 hours at room temperature. The reaction mixture was then cooled in ice, ice water (200 cm³) was cautiously added, and the resulting heterogeneous mixture stirred vigorously for 30 min before the separated aqueous layer was extracted with dichloromethane (3 x 200 cm³). The dichloromethane extracts were combined with the original organic layer before it was first washed with an equal volume of water, then twice with 10% aqueous NaOH (100 cm³), and dried over MgSO₄. Removal of the solvent under reduced pressure yielded dark red solid 2-chlorobenzoylferrocene, **60**, (21.89 g, 67.4%); m.p. 80 – 82 °C. δ_{H} (CDCl₃, spectrum 1): 8.06-8.21 (4 H, m, C₆H₄), 4.78-4.60 (4H, m, C₅H₄), 4.30 (5H, s, C₅H₅)

4.3.2 Ferrocenoic acid⁹⁷ (47a) [Scheme 3.1, page 42]

In a clean, dry round-bottom flask, 1,2-dimethoxyethane (180 cm³), potassium tert-butoxide (33.1 g, 294.9 mmol), and water (1.6 cm³) were mixed while stirring, producing a slurry. To this slurry was added 2-chlorobenzoylferrocene, **60**, (21.89 g, 67.4 mmol) to give a red coloured mixture which was refluxed for 1 hour. As the reaction proceeded, the colour changed to tan. The reaction mixture was cooled to room temperature and transferred into

water (1 L) containing small amounts of ice and extracted with diethyl ether (3 x 200 cm³). The combined ether extracts were back extracted with 10 % aqueous NaOH, followed by acidification with concentrated HCl. The precipitate was collected by vacuum filtration and air dried to give an air stable yellow powder of ferrocenoic acid, **47a**, (18.75 g, 86 %); m.p. 198 - 210°C. (decomp.). δ_{H} (CDCl₃): 4.84 (2H, t, C₅H₄), 4.45 (2H, t, C₅H₄), 4.25 (5H, s, C₅H₅). IR (KBr)/cm⁻¹: 1617 (C=O).

4.3.3 N,N-dimethylaminomethylferrocene methiodide^{85,86} (**61**) [Scheme 3.1, page 42]

To a solution of N,N-dimethylaminomethylferrocene, **45**, (20.10 g, 81.92 mmol) in methanol (54 cm³), methyl iodide (11.63 g, 5 cm³, 81.92 mmol) was slowly added and the reaction mixture was heated in an oil bath at 100°C for 30 min. After cooling to room temperature, diethyl ether (74 cm³) was also added. The crude methiodide, **61**, separated as oil that quickly crystallizes. The solid was filtered, washed with ether, and air dried overnight at room temperature to give N,N-dimethylaminomethylferrocene methiodide **61** (25.00 g, 79%); m.p. 175-185°C. δ_{H} (CDCl₃, spectrum 2): 4.29 (2H, t, C₅H₄), 4.20 (2H, t, C₅H₄), 4.18 (2H, s, C₅H₄CH₂), 4.05 (5H, s, C₅H₅), 2.71 (9H, m, (CH₃)₃).

4.3.4 Ferrocenylacetonitrile⁸⁶ (**62**) [Scheme 3.1, page 42]

A solution of N,N-dimethylaminomethylferrocene methiodide, **61**, (21.16 g, 54.8 mmol) and potassium cyanide (21.52 g, 330.49 mmol) in water (210 cm³) was refluxed for 2.5 hours. The dark brown reaction mixture with fine precipitate at the bottom was then cooled to room temperature before the liquid was decanted slowly and as carefully as possible. The decanted aqueous solution was first extracted with ether (3 x 200 cm³), and then with toluene (2 x 200 cm³). The remaining aqueous layer was left overnight in the fumehood to form crystals,

which were extracted with dichloromethane, washed with water, dried with Na_2SO_4 , and evaporated to dryness. The fine solid that remained after decantation was dissolved in toluene. All the ethereal and toluene fractions were combined and washed well with water, dried with Na_2SO_4 , and evaporated to dryness under reduced pressure. The combined solid residues obtained, was then recrystallised from boiling hexane to give yellow crystals of ferrocenylacetonitrile, **62**, (9.45 g, 76 %); m.p. 78-80 °C. δ_{H} (CDCl_3 , spectrum 3): 4.20-4.24 (9H, m, C_{10}H_9), 3.44 (2H, s, CH_2). IR (KBr)/ cm^{-1} : 2248 ($\text{C}\equiv\text{N}$).

4.3.5 Ferrocenylacetic acid^{86,98} (**47b**) [Scheme 3.1, page 42]

A suspension of ferrocenylacetonitrile, **62**, (3.43 g, 16.015 mmol) in ethanol (34 cm^3) was added to a solution of potassium hydroxide (8.5 g, 151.49 mmol) in water (85 cm^3) and refluxed for 5 hours. After the evolution of ammonia had ceased, ethanol was concentrated *in vacuo* to bring the volume to about 20 cm^3 . The residual aqueous suspension was dissolved in water (80 cm^3), extracted twice with equal volumes of diethyl ether and then filtered. Acidification of the alkaline aqueous solution with 85% phosphoric acid to pH 1-2 afforded golden crystals. The product was collected by filtration as a yellowish solid and air-dried to yield ferrocenylacetic acid, **47b**, (2.743 g, 80%); m.p. 150-155°C. δ_{H} (CDCl_3 , spectrum 4): 4.20-4.05 (9H, m, C_{10}H_9), 3.71 (2H, s, CH_2). IR (KBr)/ cm^{-1} : 1710 ($\text{C}=\text{O}$).

4.3.6 Ferrocenecarboxaldehyde⁸⁷ (**46**) [Scheme 3.1, page 42]

A solution of N-methylformanilide (2.16 g, 160 mmol) and phosphorus oxychloride (15.3 g, 100 mmol), was stirred vigorously, while ferrocene, **37a**, (11.16 g, 60 mmol) was added in small portions over a period of 10-15 min. The purple viscous mixture was stirred for 1 hour at room temperature and then at 65 - 70°C for 2 hours under nitrogen atmosphere. Hereafter

the reaction mixture was cooled to 0°C before a solution of sodium acetate (50 g, 609,5 mmol in 400 cm³ water) was added. Stirring continued overnight before the mixture was extracted with diethyl ether (3 x 400 cm³). The ether extracts were combined and washed with equal volumes of 1 mol dm⁻³ HCl, water, saturated sodium bicarbonate solution and finally with water (all saturated with sodium chloride). The ether phase was dried over MgSO₄ and evaporated to a volume of about 50 cm³. The product was purified by column chromatography on silica gel with ether-hexane (1:1) as eluent. Removal of the solvent under reduced pressure yielded reddish-brown crystals of ferrocenecarboxaldehyde, **46**, (9.76 g, 76%); m.p 120–122°C. δ_{H} (CDCl₃): 9.95 (1H, s, C₁₀H₉CHO), 4.80 (2H, s, CH), 4.62 (2H, s, CH), 4.30 (5H, s, C₅H₅). IR (KBr)/cm⁻¹: 1638 (C=O).

4.3.7 3-Ferrocenylacrylic acid⁹⁹ (**63**) [Scheme 3.1, page 42]

Ferrocenecarboxaldehyde, **46**, (5.00 g, 23 mmol), malonic acid (5.00 g, 48 mmol) and piperidine (100 drops; 1 cm³) were dissolved in pyridine (120 cm³) and heated in an oil bath at 110°C for 2 hours in nitrogen atmosphere. The cooled solution was diluted with water, extracted with chloroform (3 x 200 cm³) and the combined chloroform extracts were washed with 2 mol dm⁻³ HCl and water, and then extracted with 2 mol dm⁻³ NaOH. Acidification of the aqueous layer with 2 mol dm⁻³ HCl precipitated the brick red product 3-ferrocenylacrylic acid, **63**, after filtration, (5.31 g, 73%); m. p. 190–192°C. δ_{H} (CDCl₃): 7.70 (1H, d, CH=CHCOOH), 6.07 (1H, d, CH=CHCOOH), 4.55 (2H, s, 2,5-H), 4.45 (2H, s, 3,4-H) 4.20 (5H, s, C₅H₅). IR (KBr)/cm⁻¹: 3412 (s) (O-H), 1665 (s) (C=O), 1611 (CH=CH).

4.3.8 3-Ferrocenylpropanoic acid⁹⁹ (47c) [Scheme 3.1, page 42]

3-Ferrocenylacrylic acid, **63**, (2.45 g, 9.6 mmol) was suspended in absolute ethanol (100 cm³) and palladium activated charcoal was added while stirring. Hydrogen gas was bubbled through the stirred heterogeneous mixture for 7 hours, before the reaction mixture was filtered through a small amount of silica gel. Equal volumes of water and ice were added to the yellow ethanolic mixture before the solution was extracted with diethyl ether (2 x 150 cm³). The combined ether extract was thoroughly washed with enough water to remove the excess ethanol. The solution was dried over MgSO₄ and evaporated under reduced pressure to give 3-ferrocenylpropanoic acid **47c** (2.00 g, 81%); m. p. 115–117°C. δ_{H} (CDCl₃, spectrum 5): 4.14 (5H, s, C₅H₅), 4.09 (4H, s, C₅H₄), 2.71 (2H, t, CH₂COOH), 2.61 (2H, t, C₅H₄CH₂). IR (KBr)/cm⁻¹: 1710 (C=O).

4.3.9 3-Ferrocenoylpropanoic acid^{100,101} (64) [Scheme 3.1, page 42]

In a 500 cm³ two-necked flask, a solution of succinic anhydride (2.7 g, 27 mmol) in dichloromethane (100 cm³) was added to a mixture of ferrocene (10.02 g, 53.7 mmol) and aluminium chloride (7.2 g, 54 mmol) in methylene chloride (200 cm³) in a nitrogen atmosphere. The deep purple mixture was refluxed for 2 hours, and poured into water (200 cm³) containing water. The aqueous phase was thoroughly washed with dichloromethane, and the combined organic phases were washed well with water. The organic phase was then extracted with 2 mol dm⁻³ NaOH, followed by acidification with 2 mol dm⁻³ HCl to pH 1, giving a tan precipitate after filtration. 3-ferrocenoylpropanoic acid, **64**, (4.85 g, 31.5%); m.p. 169 – 171°C. δ_{H} (CDCl₃, spectrum 6): 4.85 (2H, t, C₅H₄), 4.55 (2H, t, C₅H₄), 4.25 (5H, s, C₅H₅), 3.10 (2H, t, C₅H₄-CO-CH₂), 2.75 (2H, t, -CH₂COOH). IR (KBr)/cm⁻¹: 1716 (s) (C=O, keto), 1658 (C=O, acid).

4.3.10 4-Ferrocenylbutanoic acid^{100,101} (47d) [Scheme 3.1, page 42]

First zinc amalgam was prepared by washing 20 g of zinc dust briefly with 2 mol dm⁻³ HCl after which 27 cm³ water, 2 g mercuric chloride and 1.1 cm³ concentrated HCl were added. The mixture was left for 10 min after which all liquids were decanted from the gray solid residue. After the formed amalgam had been washed with small amounts of water, ethanol, 2 mol dm⁻³ HCl and again with water, it was quickly dried at 60 - 65°C under reduced pressure.

4-Ferrocenylbutanoic, 47d, acid was prepared by Clemmensen reduction of 3-ferrocenoylpropanoic acid, 64, (5.04 g, 17.62 mmol) in a (1:1:5 ratio) refluxing mixture of concentrated HCl, glacial acetic acid and water (280 cm³) in the presence of zinc amalgam (4 g) under nitrogen for 42 hours. Fresh concentrated HCl (2 cm³ aliquots) was added to the mixture at 12 hours intervals. Isolation of the product was achieved by diluting the ice cooled reaction mixture with ice water (150 cm³) and extraction with diethyl ether. The ether extracts were combined and washed thoroughly with water, and extracted with 0.5 mol dm⁻³ NaOH. Acidification of the basic aqueous phase with ice-cooled 1 mol dm⁻³ HCl precipitated 4-ferrocenylbutanoic acid, 47d, after filtration, (3.4 g, 67%); m.p. 107–109°C. δ_{H} (CDCl₃, spectrum 7): 4.12 (4H, m, C₅H₅), 4.09 (5H, s, C₅H₄), 2.41 (4H, m, C₅H₄CH₂CH₂CH₂COOH), 1.90 (2H, m, C₅H₄CH₂CH₂). IR (KBr)/cm⁻¹: 1704 (C=O).

4.3.11 Ferrocenecarboxaldoxime¹³² (68) [Scheme 3.3, page 48]

To a solution of ferrocenecarboxaldehyde, 46, (0.58 g, 2.710 mmol) in ethanol was added a solution of hydroxylamine hydrochloride [(1.21 g, 17.67 mmol) in water (5 cm³)] and sodium hydroxide [(0.516 g, 12.90 mmol) in water (5 cm³)]. After 2 hours of refluxing, the reaction mixture was extracted with chloroform, and the organic layer washed with water, dried over

Na_2SO_4 and the solvent removed under reduced pressure. The red solid was recrystallised from hexane to give ferrocenecarboxaldoxime, **68**, (0.28 g, 48 %), m.p. 116°C (dec.). δ_{H} (CDCl_3 , spectrum 8): 7.96 (1H, s, =C(H)), 4.51 (2H, m, C_5H_4), 4.35 (2H, m, C_5H_4), 4.21 (5H, s, C_5H_5).

4.3.12 Ferrocenylcarboxamide¹²⁶ (**66a**) [Scheme 3.2, page 45]

All ferrocene-containing amides were obtained by reacting aqueous ammonia with a ferrocene-containing acid chloride. Owing to the instability of the acid chlorides they were not isolated and stored, but immediately reacted *in situ* with aqueous ammonia. The acid chlorides were obtained by reacting the corresponding carboxylic acids with oxalyl chloride, thionyl chloride or phosphorus trichloride.

4.3.12.1 Oxalyl chloride method¹¹⁸

To a solution of ferrocenoic acid, (**47a**), (1.0014 g, 4.39 mmol) in dry dichloromethane (20 cm^3) was added oxalyl chloride (2.3 cm^3 , 11.6 mmol) and a drop of pyridine. The mixture was stirred for 12 hours at room temperature and then at 45°C for 8 hours. The red solution of the ferrocenoyl chloride could not be isolated in high yield or stored because of its instability. Hence the reaction mixture was immediately used for the synthesis of ferrocenylcarboxamide, **66a**. Aqueous ammonia 25%, (20 cm^3) was added through the top of the condenser on the dichloromethane layer and stirring continued for 2 hours at room temperature. The organic phase was separated from the aqueous phase and stored. The aqueous phase was extracted with dichloromethane ($2 \times 100\text{ cm}^3$), and all the combined organic phases washed well with equal volumes of water, and 10% NaOH solution. Finally the organic solvent was dried over MgSO_4 followed by removal of the organic solvent under

reduced pressure to give a fine reddish powder of ferrocenylcarboxamide, **68**, (0.412 g, 41%); m.p. 165°C. δ_{H} (CDCl_3 , spectrum 9): 4.70 (2H, t, C_5H_4), 4.40 (2H, t, C_5H_4), 4.21 (5H, s, C_5H_5). IR (KBr)/ cm^{-1} : 3424 (NH_2), 1638 ($\text{C}=\text{O}$), 1540 (NH, amide II).

4.3.12.2 *Thionyl chloride method*^{110,111}

Ferrocenoic acid, **47a**, (2.00 g, 8.26 mmol) was dissolved in thionyl chloride (50 cm^3 , 82 g, 689 mmol) and refluxed for four days. The excess thionyl chloride was removed by distillation at 150-155°C, for identification purposes a small sample of the acid chloride was dissolved in petroleum ether (b.p. 60-80°C) and the IR spectrum was recorded. The residue was dissolved in dichloromethane (50 cm^3) and immediately treated with saturated aqueous ammonia (50 cm^3) and stirred for 30 min at room temperature. The organic phase was separated from the aqueous phase and stored. The aqueous phase was extracted with dichloromethane (2 x 100 cm^3), and the combined organic phases washed well with equal volumes of water, and 10% NaOH solution and finally dried over MgSO_4 followed by removal of the organic solvent under reduced pressure to give a reddish solid ferrocenylcarboxamide, **66a**, (0.232 g, 11%); m.p. 165°C.

4.3.12.3 *Phosphorus trichloride method*¹²⁴

To a solution of ferrocenoic acid, **47a**, (2.00 g, 8.656 mmol) in toluene (12 cm^3), phosphorus trichloride (2.6 cm^3 , 4.09 g, 29.78 mmol) was added and refluxed at 86°C for 2 hours. The excess PCl_3 and solvent was removed under reduced pressure and to the crude residue was added toluene (10 cm^3) followed by the addition under vigorous stirring of an excess of aqueous ammonia (20 cm^3). Stirring continued at room temperature for 30 min before the

reaction mixture was extracted with diethyl ether, dried over MgSO_4 and solvent removed under reduced pressure to give a yellow solid **66a** (0.77 g, 38%), m.p. 165°C .

4.3.13 Ferrocenylacetamide^{118,121,126} (**66b**) [Scheme 3.2, page 45]

The thionyl chloride method was not appropriate for this synthesis as the ferrocenyl group is oxidized during the course of the reaction.

4.3.13.1 *Oxalyl chloride method*¹¹⁸

To a solution of ferrocenylacetic acid, **47b**, (0.5024 g, 2.06 mmol) in dry dichloromethane (10 cm^3), oxalyl chloride (1 cm^3 , 11.6 mmol) and a drop of pyridine were added. The reaction mixture was stirred for 15 hours at room temperature, and then refluxed for 2 hours. During refluxing, the colour of the reaction mixture changed from deep red to blue. Aqueous ammonia 25%, (30 cm^3) was added through the top of the condenser on the dichloromethane layer, and dichloromethane (10 cm^3) was also added to increase the volume of the solvent. Stirring continued for 2 hours at room temperature. The organic phase was separated from the aqueous phase and extracted with dichloromethane (3 x 50 cm^3). The combined organic phases were washed well with equal volumes of water, and 2% NaOH solution and finally dried over MgSO_4 and evaporated under reduced pressure to give a yellow solid ferrocenylacetamide, **66b**, (0.12 g, 24 %); m.p. $163\text{--}165^\circ\text{C}$. δ_{H} (CDCl_3 , spectrum 10): 4.20 (9H, m, C_{10}H_9), 3.35 (2H, s, CH_2), 1.52 (2H, s, NH_2). IR (KBr)/ cm^{-1} : 3424 (NH amide I), 1638 (C=O) and 1404 (NH amide II).

4.3.13.2 *Phosphorus trichloride method*¹²¹

To a solution of ferrocenylacetic acid, **47b**, (2.00 g, 8.26 mmol) in toluene (12 cm^3), phosphorus trichloride (2.6 cm^3 , 4.09 g, 29.78 mmol) was added and refluxed at 86°C for 2

hours. The excess PCl_3 and solvent were removed under reduced pressure. To the crude residue was added toluene (15 cm^3) followed by the addition under vigorous stirring an excess of aqueous ammonia (30 cm^3). Stirring continued at room temperature for 30 min before the reaction mixture was extracted with diethyl ether, dried over MgSO_4 and solvent removed under reduced pressure to give ferrocenylacetamide, **66b**, (0.924 g, 46%), m.p. 163–165°C.

4.3.14 3-Ferrocenylpropionamide^{121,126} (**66c**) [Scheme 3.2, page 45]

Neither the oxalyl chloride nor thionyl chloride method was successful in this synthesis.

To a solution of ferrocenylpropanoic acid, (**47c**), (1.00 g, 3.876 mmol) in benzene (5.9 cm^3), was added phosphorus trichloride (1.27 cm^3 , 2.00 g, 14.56 mmol). The solution was refluxed at 85°C for 2 hours. The excess PCl_3 and solvent was removed under reduced pressure and to the residue was added toluene (15 cm^3) followed by the addition under vigorous stirring an excess aqueous ammonia (30 cm^3). Stirring continued at room temperature for 30 min before the reaction mixture was extracted with diethyl ether, dried with MgSO_4 and solvent removed under reduced pressure to give a yellow solid 3-ferrocenylpropionamide, **66c**, (0.62 g, 62%); m.p. 96–99°C. δ_{H} (CDCl_3 , spectrum 11): 4.15 (9H, m, C_{10}H_9), 2.71 (2H, t, CH_2), 2.41 (2H, t, CH_2CONH_2). IR (KBr)/ cm^{-1} : 3424 (HN_2), 1638 (C=O), 1540 (NH, amide II).

4.3.15 4-Ferrocenylbutanamide^{121,126} (**66d**) [Scheme 3.2, page 45]

To a solution of 4-ferrocenylbutanoic acid, **47d**, (1.25 g, 4.576 mmol) in toluene (7.35 cm^3), was added PCl_3 (0.41 cm^3 , 0.64 g, 4.66 mmol). The solution was refluxed at 86°C for 2 hours. The excess PCl_3 and solvent was removed under reduced pressure and to the residue was added benzene (15 cm^3) followed by the addition under vigorous stirring an excess aqueous ammonia (30 cm^3). Stirring continued at room temperature for 40 min before the reaction

mixture was extracted with diethyl ether, dried over MgSO_4 and solvent removed under reduced pressure to give 4-ferrocenylbutyramide, **66d**, (0.91 g, 73%); m. p. 82–84°C. δ_{H} (CDCl_3): 4.20 (5H, s, C_5H_5), 4.08 (4H, s, C_5H_4), 2.40 (2H, t, $\text{C}_5\text{H}_4\text{CH}_2$), 2.25 (2H, t, CH_2), 1.85 (2H, t, CH_2CONH_2). IR (KBr)/ cm^{-1} : 3424 (NH_2), 1638 (C=O), 1540 (NH, amide II).

4.3.16 Ferrocenylmethylamine¹³³ (**67a**)

4.3.16.1 Reduction of amide method¹³³ [Scheme 3.2, page 45]

To a solution of ferrocenylcarboxamide, **66a**, (0.6 g, 2.619 mmol) in dry tetrahydrofuran (30 cm^3), was added powdered lithium aluminium hydride (0.216 g, 5.691 mmol). The reaction mixture was refluxed at 69°C for 24 hours, after which the excess LiAlH_4 was destroyed by the addition of water (50 cm^3). The THF-water mixture was extracted with chloroform and the organic layer washed well with water, dried over Na_2SO_4 and the solvent removed under reduced pressure. The product was purified by column chromatography on silica using methanol/aqueous ammonium solution (95:5 v/v) as eluent to give after solvent removal ferrocenylmethylamine, **67a**, (0.31 g 55%) as a dark brown oil. δ_{H} (CDCl_3 , spectrum 12): 4.15 (9H, m, C_9H_{10}), 3.54 (2H, s, CH_2), 1.25 (2H, b. NH_2). IR (NaCl disk)/ cm^{-1} : 3360 (NH_2), 1584 (NH, amine II).

4.3.16.2 Ferrocenecarbaldehyde oxime method^{132,133} [Scheme 3.3, page 48]

Ferrocenecarbaldehyde oxime, **68**, (0.25 g, 1.152 mmol) was dissolved in dry THF (8.9 cm^3) and an excess of lithium aluminium hydride (0.19 g, 5.007 mmol) was added portion-wise with care. After 6 hours of refluxing under nitrogen atmosphere, benzene (8.9 cm^3) and ethyl acetate (1.6 cm^3) were added with caution, followed by few a drops of 5 mol dm^{-3} NaOH until precipitation of the inorganics was complete. Filtration of the mixture yielded a yellow

filtrate and a gummy solid residue. The filtrate residue was washed with copious amounts of benzene:methanol (80:20 v/v) solution. The filtrate was then evaporated to dryness and inorganic impurities removed by dissolving the residue in dichloromethane followed by filtration and evaporation of the organic solvent under reduced pressure. The product was purified by column chromatography on silica using methanol/ aqueous ammonium (95:5 v/v) solution as eluent to give after solvent removal ferrocenylmethanamine, **67a**, (0.14 g, 56%).

4.3.17 2-Ferrocenylethylamine^{85,86,133} (**48**)

4.3.17.1 *By the reduction of ferrocenylacetonitrile^{85,86} (**62**) [Scheme 3.4, page 49]*

Into a 500 cm³ round bottomed flask, a suspension of lithium aluminium hydride (2.04 g, 54 mmol) in diethyl ether (100 cm³) was stirred under reflux at 34°C for 1 hour. To the reaction mixture a solution of 2-ferrocenylacetonitrile, **62**, (3.027 g, 13.4 mmol) in ether (20 cm³) was added slowly. After 2 hours of refluxing, the reaction mixture was cooled in ice, and water (20 cm³), 20% NaOH (15 cm³) and water (90 cm³) were added consecutively. The ethereal layer was slowly decanted from the solid followed by the addition to 2 mol dm⁻³ NaOH, and extracted with more ether and washed with equal volume of water, dried (Na₂SO₄) and the solvent removed under reduced pressure to give a dark brown oil residue. The residual oil was distilled at 0.5 mm to give (2.41 g, 81%) of 2-ferrocenylethylamine; b.p. 120 – 135°C. δ_{H} (CDCl₃, spectrum 13): 4.12 (5H, t, C₅H₅), 4.07 (2H, s, C₅H₄), 4.02 (2H, s, C₅H₄), 2.79 (2H, t, C₅H₄CH₂), 2.47 (2H, s, CH₂NH₂).

4.3.17.2 *By the reduction of 2-ferrocenylacetamide¹³³ (**66b**) [Scheme 3.2, page 45]*

To a solution of 2-ferrocenylacetamide, **66b**, (0.4 g, 1.646 mmol) in dry tetrahydrofuran (40 cm³) powdered lithium aluminium hydride (0.25 g, 6.5869 mmol) was added. The reaction

mixture was refluxed at 69°C for 24 h, after which the excess LiAlH₄ was destroyed by the addition of water (30 cm³). The THF-water layer was extracted with chloroform and washed well with water, dried over Na₂SO₄ and the solvent removed under reduced pressure. The product was purified by column chromatography on silica using methanol/aqueous ammonium solution (95:5v/v) as eluent to give after solvent removal 2-ferrocenylethylamine, **48**, (0.23g, 58 %) as a dark brown oil.

4.3.18 3-Ferrocenylpropylamine¹³³ (**67b**) [Scheme 3.2, page 45]

Powdered lithium aluminium hydride (0.29 g, 7.652 mmol) was added to a solution of 3-ferrocenylpropionamide, **66c**, (0.8 g, 0.3889 mmol) in dry THF (40 cm³). The reaction mixture was refluxed at 69°C for 24 hours, after which the excess LiAlH₄ was destroyed by addition of water (60 cm³). The THF-water mixture was extracted with chloroform (3 x 50 cm³) and the organic solvent was washed thoroughly with water, dried (Na₂SO₄) and removed under reduced pressure to give 62% yield of a dark brown, oily product. The product was purified by column chromatography on silica using methanol/aqueous ammonium solution (95:5 v/v) as eluent to give after solvent removal (0.24 g, 30 %) of 3-ferrocenylpropylamine, **67b**. δ_{H} (CDCl₃, spectrum 14): 4.17 (5H, s, C₅H₅), 4.01 (4H, s, C₅H₄), 2.80 (2H, t, C₅H₄CH₂), 2.40 (2H, s, C₅H₄CH₂CH₂), 1.70 (2H, s, C₅H₄CH₂CH₂CH₂NH₂).

4.3.19 4-Ferrocenylbutylamine¹³³ (**67c**) [Scheme 3.2, page 45]

To a solution of 4-ferrocenylbutyramide, **66d**, (0.75 g, 2.746 mmol) in dry THF (38 cm³), was added powdered lithium aluminium hydride (0.27 g, 7.114 mmol). The reaction mixture was refluxed at 69°C for 24 hours, after which the excess LiAlH₄ was destroyed by the addition of water (75 cm³). The THF-water mixture was extracted with chloroform (3 x 50 cm³) and the

organic solvent washed thoroughly with water, dried (Na_2SO_4) and removed under reduced pressure. Dark brown, oily residue oil was purified by column chromatography on silica using methanol/aqueous ammonium solution (95:5 v/v) as eluent to give after solvent removal (0.38 g, 51%) of 4-ferrocenylbutylamine, **67c**. δ_{H} (CDCl_3 , spectrum 15): 4.05 (5H, s, C_5H_5), 4.00 (4H, s, C_5H_4), 2.69 (2H, t, $\text{C}_5\text{H}_4\text{CH}_2$), 2.31 (2H, t, $\text{C}_5\text{H}_4\text{CH}_2\text{CH}_2$). 1.45 (4H, s, $\text{C}_5\text{H}_4\text{CH}_2\text{CH}_2\text{CH}_2\text{CH}_2\text{NH}_2$).

4.4 Synthesis of the polymeric carriers and the anchoring of the ferrocene

4.4.1 Poly-DL-succinimide⁴² (2) (Scheme 3.5, page 50)

Finely powdered DL-aspartic acid, **1**, (5.00 g, 37.57 mmol) and 85% orthophosphoric acid (5.00 g, 51.02 mmol) were thoroughly mixed in a 250 cm³ round bottomed flask. The flask (connected to a rotary evaporator fitted with a vacuum pump and manometer) was carefully submerged at atmospheric pressure into an oil bath preheated to 200°C with slow rotation. Care must be taken that the reaction mixture does not froth out of the flask. After 5 min of rotation, the oil bath temperature was lowered slightly and maintained at 170–190°C for 2.5 hours, while the pressure was reduced to below 2 torr. After the reaction mixture was cooled to ca. 50°C, DMF (30 cm³) was poured onto the warm reaction mixture, and was rotated slowly on the rotary evaporator overnight to afford a homogeneous, light brown solution. This solution was poured, with vigorous stirring, into a beaker containing water (500 cm³), and the resulting polymer was filtered and thoroughly washed with water (5 x 250 cm³). The solid was ground under liquid nitrogen and dried at 56°C under reduced pressure over P_2O_5 in an Aberhalden drying tube, using boiling acetone as a heat source to give a white solid (3.44 g, 95%) of poly-DL-succinimide **2**. δ_{H} (DMSO, spectrum 16): 5.28 (1H, s, CH), 3.13 (2H, s, CH_2), 2.70 (2H, s, CH_2). IR (KBr)/cm⁻¹ 1710 (C=O), 1413 (C-N).

4.4.2 Polymer⁴² (69) [Scheme 3.6, page 52]

Remark: The syntheses of polymers 69, 70, 71 and 72 are performed in exactly the same manner. Only the synthesis of polymer 69 will be given as a representative example. Yields and characterization data is presented for all the compounds after the representative synthesis procedure. Abbreviation: Asp = aspartyl group of the main chain of the poly(aspartamide) polymers.

To a stirring solution of poly-DL-succinimide, 2, (0.128 g, 1.320 mmol repeating units) in anhydrous DMF (1.8 cm³) was slowly added a solution of ferrocenylmethylamine, 67a, (0.0709 g, 0.330 mmol) in anhydrous DMF (0.5 cm³) at 0°C. The reaction mixture was stirred for a further 1 hour at 0°C and then overnight at room temperature. Hereafter the stirred solution was again cooled to 0°C before N-(3-aminopropyl)-morpholine (0.152 g, 0.99 mmol) in DMF (0.5 cm³) was slowly added. Stirring continued for a further 1 hour at 0°C and then at room temperature for 5 hours. This reaction mixture was dialyzed for 24 hours in 12 000 molecular mass cut-off membrane tubing against running tap water, followed by freeze drying, to give the final product as a yellowish spongy solid polymer, 69, (0.24 g, 18%). δ_{H} (D₂O, spectrum 17): 1.48 (6H, s, β -CH₂), 2.15 (6H, s, γ -CH₂), 2.31 (12H, s, δ -CH₂), 2.58 (10H, s, 4 asp-CH₂ + α' -CH₂), 2.99 (6H, s, α -CH₂), 3.50 (12H, s, ϵ -CH₂), 3.91-4.05 (9H, s, C₁₀H₉), 4.28-4.44 (4H, s, asp-CH). IR (KBr)/cm⁻¹: 1661 (NH, amide I), 1550 (NH, amide II).

Polymer 70 was obtained in (0.15g, 18%). δ_{H} (D₂O, spectrum 18): 1.50 (6H, s, β -CH₂), 2.00-2.49 (20H, m, δ -CH₂ + γ -CH₂ + β' -CH₂), 2.63 (8H, s, 4 asp-CH₂), 3.04 (8H, s, α -CH₂ + α' -CH₂), 3.52 (12H, s, ϵ -CH₂), 3.97 (9H, s, C₁₀H₉), 4.26-4.44 (4H, s, asp-CH). IR (KBr)/cm⁻¹: 1661 (NH, amide I), 1550 (NH, amide II).

Polymer 71 was isolated in (0.27 g, 18%). δ_{H1} (D_2O , spectrum 19): 1.56 (6H, s, β - CH_2), 2.20 (6H, s, γ - CH_2 + β' - CH_2), 2.45 (14H, s, δ - CH_2 + γ' - CH_2), 2.70 (8H, s, 4 asp- CH_2), 3.06 (8H, s, α - CH_2 + α' - CH_2), 3.50 (12H, s, ϵ - CH_2), 4.00 (9H, s, $C_{10}H_9$), 4.35-4.56 (4H, s, asp-CH). IR (KBr)/ cm^{-1} : 1661 (NH, amide I), 1550 (NH, amide II).

Polymer 72 was isolated in (0.35 g, 17%). δ_{H1} (D_2O , spectrum 20): 1.14-1.16 (10H, m, β - CH_2 + β' - CH_2 + λ - CH_2)_{1.75}, 1.82-3.21 (36H, m, 4 asp- CH_2 + δ - CH_2 + γ - CH_2 + α - CH_2 + α' - CH_2 + γ' - CH_2)_{1.75}, 3.50 (12H, s, $CH_{2\epsilon}$), 3.89 (9H, s, $C_{10}H_9$)_{1.75}, 4.12-4.44 (4H, s, asp-CH)_{1.75}. IR (KBr)/ cm^{-1} : 1661 (NH, amide I), 1550 (NH, amide II).

CHAPTER 5

SUMMARY, CONCLUSIONS AND FUTURE

PERSPECTIVES

The goals of this study can be summarised as the synthesis and electrochemical characterisation of ferrocene-containing water-soluble polymers with anti cancer activity. To achieve this, the author had to perform a number of tasks.

A Synthesis

- 1 A series of ferrocene-containing carboxylic acids of the type $\text{Fc}-(\text{CH}_2)_n\text{-COOH}$ with $0 \leq n \leq 3$ and Fc = ferrocenyl were synthesised.
- 2 A general method of converting those acids to the acid chlorides $\text{Fc}-(\text{CH}_2)_n\text{-COCl}$ utilising PCl_3 as chlorinating reagent was developed.
- 3 The acid chlorides were then converted to the amides $\text{Fc}-(\text{CH}_2)_n\text{-CONH}_2$ following reaction with aqueous ammonia under *Schotten Baumann* conditions.
- 4 A further general synthetic procedure was developed to reduce the obtained amides to the corresponding amines, $\text{Fc}-(\text{CH}_2)_n\text{-NH}_2$, $1 \leq n \leq 4$, *via* LiAlH_4 . Some of the obtained amines were also prepared *via* alternative routes. These were spectroscopically identical with the compounds obtained from the LiAlH_4 path.
- 5 A general technique was then developed to anchor all the obtained amines onto a water-soluble poly(aspartic acid) derivative.
- 6 In total 24 compounds were synthesised, 12 of which were new. Appropriate compounds were characterised utilising *inter alia* techniques such as elemental analysis, melting point determination, IR spectroscopy and ^1H NMR spectroscopy.

B Electrochemistry

- 1 A cyclic voltammetric study of all the amides and amines in acetonitrile showed that the formal reduction potential, E° , is dependent on the length of the $(\text{CH}_2)_n$ chain that links the ferrocenyl group with the amine or amide functional groups. Longer $(\text{CH}_2)_n$ chains

- lowered the formal reduction potential of the Fc/Fc⁺ couple. For the amides, $E^{o'}$ was found to lie between 0.047 V and 0.272 V (CH₂) vs. Ag/Ag⁺, while for the amines it is $0.032 \text{ V} \leq E^{o'} \leq 0.078 \text{ V}$.
- 2 Aqueous electrochemistry was also conducted on the amines after converting them to the hydrochloride salt. Again, the formal reduction potential (vs. Ag/AgCl) was found to be dependent on the length of the (CH₂)_n chain. Shorter chains led to higher reduction potentials and values were found to be $0.132 \text{ V} \leq E^{o'} \leq 0.320 \text{ V}$.
 - 3 Aqueous electrochemistry of all ferrocene-containing polymers again showed shorter side chains that link the ferrocenyl group to the polymer main chain resulted in higher formal reduction potentials.
 - 4 Almost all the compounds were found to exhibit electrochemical reversibility at slow scan rates, but cathodic reduction of electrochemically generated ferricenium cations were not always qualitative to give i_{pc}/i_{pa} ratio of 1. It was found that wherever there were free electron pairs on the compounds that were investigated, especially free electron pairs on an -NH-group, intra or intermolecular electron transfer occurred to chemically reduce the electrochemically generated ferricenium species, with resulting decrease in i_{pc}/i_{pa} ratios.

C Cytotoxic studies

- 1 The ferrocene-containing amides, amines and polymers that were synthesised in this study were then subjected to cytotoxic tests utilising HeLa, a human cervix epitheloid cancer cell line, and CoLoDM320, an intrinsically multidrug resistant human colorectal cell line.

- 2 It was found that compounds with the lowest Fc/Fc^+ reduction potential and with the longest $(CH_2)_n$ chain separating the ferrocenyl group from another functional group are the most active in killing cancer cells.
- 3 A further result from this study is that anchoring of an antineoplastic drug onto a polymeric drug carrier does not automatically imply enhanced pharmacological activity. There appears to be a threshold in chain length that links drug moiety with polymeric main chain that must be crossed before the potential advantage of drug carriers becomes experimentally observable. At this stage of our knowledge it appears that a $(CH_2)_5$ or $(CH_2)_6$ linking group is the threshold before the benefits of a polymeric drug carrier can actually be observed in drug activity of a polymer-bound drug compared with the activity of the free drug.

In this study the author has developed techniques to anchor amine-containing ferrocenes on a water-soluble polymeric drug carrier and, from cytotoxic studies, demonstrated the antiproliferative activity some ferrocenyl derivatives possess. However, many questions still remain to be answered. These would include how different drugs will behave on the same and different polymeric drug carriers. To answer these questions research is currently being conducted in this laboratory to determine the pharmacological activity of platinum group metals, particularly rhodium and iridium complexes, other metallocenes such as cobaltocene or ruthenocene and phthalocyanine derivatives when polymer-bound or as the free drug. Alternative drug carriers are also under investigation, the most notable of which are derivatives of polyepichlorohydrins and polyphosphazenes.

REFERENCES

- 1 S. E. Sharman and S. J. Lippard, *Chem. Rev.*, 1153, **87** (1987).
- 2 H. J. Wallace and D. J. Higby in *Platinum coordination complexes in cancer therapy*; eds. T. A. Connors and J. J. Roberts, Springer-Verlag, Heidelberg, 1974, p. 128, 167.
- 3 G. Caldwell, E. W. Neuse and C. E. J. van Rensburg, *J. Inorg. Organomet. Polym.*, 217, **7** (1999).
- 4 G. R. Gale, L. M. Atkins, S. J. Meischen, A. B. Smith and E. Walker, *Cancer Treat. Rep.*, 445, **61** (1977).
- 5 W. M. Sharman, C. M. Allen and J. E. Van Lier, *Drug Discovery Today*, 507, **44** (1999).
- 6 R. Duncan and J. Kopecek, *Adv. Polymer Sci.*, 51, **57** (1984).
- 7 E. W. Neuse and C. W. N. Mbonzana in *Inorganic and Metal-containing Polymeric Materials*; eds. J. E. Sheats, C. E. Carraher, C. U. Pittman, M. Zeldin and B. Currell, New York, Plenum Press, 1990, pp 139-150.
- 8 J. C. Swarts and C. E. J. van Rensburg, *Provisional Patent 20007167*.
- 9 J. C. Swarts, D. M. Swarts, E. W. Neuse, C. La Madeleine and J. E. Van Lier, *Anticancer Res.*, in Press, 2001.
- 10 S. G. Bown, *J. Photochem. Photobiol. B: Biol.*, 12, **6** (1990).
- 11 M. K. Wolpert-DeFillipes, *Cancer Treat. Rep.*, 1453, **63** (1979).
- 12 J. Drobnik and P. Horacek, *Chem. -Biol. Interactions I*, 223, **7** (1973).
- 13 W. R. Leopold, E. C. Miller and J. A. Miller, *Cancer Res.*, 913, **39** (1979).
- 14 P. Köpf-Maier and H. Köpf, *Struct. Bonding*, 103, **70** (1988).
- 15 M. J. Poznansky and R. L. Juliano, *Pharm. Rev.*, 277, **36(4)** (1984).
- 16 N. Freudenberg, K. H. Riese and M. A. freudenberg, *The Vascular Endothelial System*, Gustav Fisher, Stuttgart, 1983.
- 17 A. Martinez-Herandez in *Microcirculation*; eds. R. Effros, H. Schmid-Shonben and J. Ditzel, Academic Press, New York, 1981, pp 125-146.
- 18 E. Ruoslahti, M. E. Piersbacher, C. Hayman and E. Engvall, *Trends Biochem. Sci.*, 188, **7** (1983).
- 19 C. Meuret, *Hematol. Bluttransfus.*, 11, **27** (1981).
- 20 B. M. Altura and T. M. Saba, *Pathophysiology of the Reticuloendothelial System*, Raven Press, New York, 1981.

- 21 D. S. Nelson, *Clin. Exp. Immunol.*, 225, **45** (1981).
- 22 E. Unanue, *Adv. Immunol.*, 1, **31** (1981).
- 23 D. O. Adams, *Fed. Proc.*, 2193, **41** (1982).
- 24 R. M. Steinman, I. S. Mellman, W. A. Muller and Z. A. Cohn, *J. Cell Biol.*, 1, **96** (1983).
- 25 E. M. De Robertis, *Cell*, 1021, **32** (1983).
- 26 G. Schatz and R. A. Butow, *Cell*, 1021, **32** (1983).
- 27 J. T. Sparrow and A. M. Gotto, *Ann. N. Y. Acad. Sci.*, 187, **348** (1980).
- 28 A. J. Barrett and M. F. Heath in *Lysosomal Enzymes in Lysosome, a Laboratory Handbook*; ed. J. T. Dingle, Elsevier, Amsterdam, 1977, p. 19.
- 29 Y. J. Schneider, P. Tulkens, C. de Duve and A. Trouet, *J. Cell Biol.*, 466, **82** (1979).
- 30 A. E. Taylor and D. N. Granger, *Fed. Proc.*, 2440, **42** (1983).
- 31 E. Wisse and M. A. De Leeuw in *Microsphere and Drug Therapy Pharmaceutical Immunology and Medical Aspects*; eds. S. S. Davis, L. Illum, J. G. McVie and E. Tomlinson, Elsevier, Amsterdam, 1984, pp 1-23.
- 32 K. Nishida, K. Mihara, T. Takino, S. Nakani, Y. Takakura, M. Hashida and H. Sezaki, *Pharm. Res.*, 437-444, **8** (1991).
- 33 M. L. de Machado, E. W. Neuse, A. G. Perlwitz and S. Schmitt, *Poly. Adv. Technol.*, 275, **1** (1990).
- 34 H. Sezaki, Y. Takakura and M. Hashida, *Adv. Drug Del. Rev.*, 247, **3** (1989).
- 35 J. Kopecek, *Makromol. Chem.*, 2169, **178** (1977).
- 36 J. Kopecek in *Biodegradation of Polymers for Biomedical Use: IUPAC Macromolecules*; eds. H. Benoit and P. Rempp, Pergamon Press, Oxford, 1982, p. 305.
- 37 P. Rejmanová, B. Obereigner and J. Kopecek, *Makromol. Chem.*, 1899, **182** (1981).
- 38 Sprinkle, *J. Biomed. Mat. Res.*, 953, **10** (1976).
- 39 R. Duncan, M. K. Pratten, H. C. Cable, H. Ringsdorf and J. B. Lloyd, *J. Biochem.*, 49, **196** (1981).
- 40 J. F. Fauvarque and J. Malinge, *Synthesis of biodegradable hydrosoluble polymers in Proceeding of the International Symposium on Polymers in Medicine*, Porto Cervo, Sardinia, 1982, pp 41.

- 41 D. Braswell, G. Nelson, T. St Prerre, R. Reams and E. A. Lewis, *Synthesis of biodegradable hydrosoluble polymers in Proceeding of the International Symposium on Polymers in Medicine*, Porto Cervo, Sardinia, 1982, pp 41.
- 42 P. Neri and G. Antoni, *Macromol. Synth.*, 25, 8 (1982).
- 43 G. Giammona, B. Carlisi, G. Cavallaro, I. Donato, F. Pinio and V. Turco Liveri, *Int. J. Pharm.*, 239-242, 64 (1990).
- 44 F. Castelli, G. Giammona, A. Raudino and G. Puglisi, *Int. J. Pharm.*, 43-52, 70 (1991).
- 45 F. Rypáček, W. R. Banks and D. Noskova, *J. Med. Chem.*, 1850, 37 (1994).
- 46 J. C. Swarts and M. D. Maree, unpublished results.
- 47 E. S. Schallenberg and M. Calvin, *J. Am. Chem. Soc.*, 2779, 77 (1955).
- 48 J. C. Swarts, G. J. Lamprecht and E. W. Neuse, *J. Inorg. Organomet. Polym.*, 143, 4 (1994).
- 49 U. Chiba, E. W. Neuse, J. C. Swarts and G. J. Lamprecht, *Angew. Makromol. Chem.*, 137, 214 (1994).
- 50 P. Molz, H. Ringsdorf, G. Abel and P. J. Cox, *Int. J. Biol. Micromol.*, 245, 2 (1980).
- 51 V. Hofmann, H. Ringsdorf and G. Maucevic, *Makromol. Chem.*, 1929, 176 (1975).
- 52 R. Duncan, D. Starling, F. Rypacek, J. Drobnik and J. B. Lloyd, *Biochim. Biophys. Acta*, 248, 717 (1982).
- 53 E. W. Neuse and A. G. Perlwitz in *Polyamides as Drug Carriers: Water-Soluble Polymers*; eds. S. W. Shalaby, C. L. McCormick and G. B. Butler, *American Chemical Society*, Washington DC, 1991, ch. 25, pp 395-404.
- 54 E. W. Neuse, A. G. Perlwitz and A. P. Barbosa, *J. Appl. Polym. Sci.*, 57, 54 (1994)
- 55 P. J. Graham, R. V. Lindsey, G. W. Parshall, M. L. Peterson and G. M. Whitman, *J. Am. Chem. Soc.*, 3416, 79 (1957).
- 56 A. Ratajczak, B. Czech and L. Drobek, *Synth. React. Inorg. Met.-Org. Chem.*, 557, 12 (1982).
- 57 J.C. Swarts, unpublished results.
- 58 M. Rosenblum and R. B. Woodward, *J. Am. Chem. Soc.*, 5443, 80 (1958).
- 59 E. W. Neuse, B. B. Patel and C. W. N. Mbonzana, *J. Inorg. Organomet. Polym.*, 147, 1 (1991).

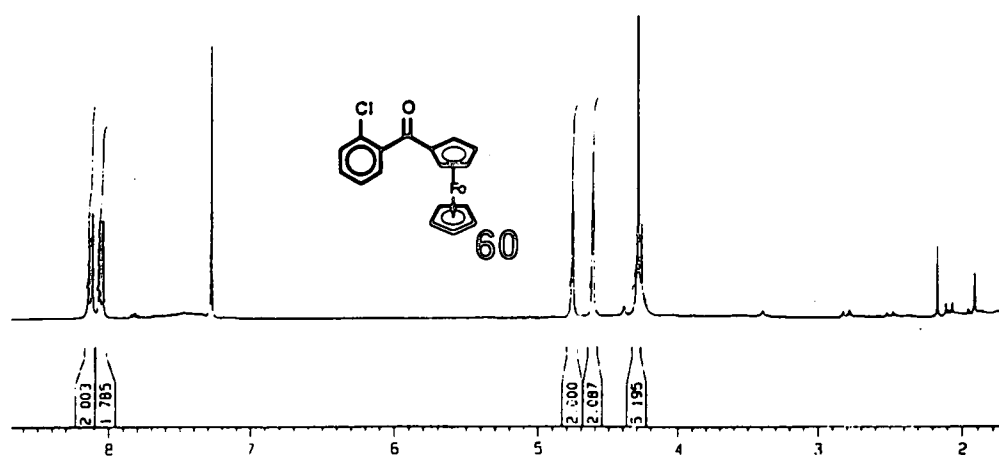
- 60 C. W. N. Mbonzana, E. W. Neuse and A. G. Perlwitz, *Appl. Organomet. Chem.*, 279, 7 (1993).
- 61 E. W. Neuse, G. Caldwell and A. G. Perlwitz, *J. Inorg. Organomet. Polym.*, 195, 5 (1995).
- 62 G. Caldwell, E. W. Neuse and A. G. Perlwitz, *J. Inorg. Organomet. Polym.*, 111, 7 (1997).
- 63 E. W. Neuse and G. Caldwell, *J. Inorg. Organomet. Polym.*, 163, 7 (1997).
- 64 E. W. Neuse, *Polym. Adv. Technol.*, 786, 9 (1998).
- 65 G. Caldwell, E. W. Neuse and C. E. J. van Rensburg, *J. Inorg. Organomet. Polym.*, 189, 13 (1999).
- 66 B. Schechter, G. Caldwell, M. G. Meirim and E. W. Neuse, *Appl. Organomet. Chem.*, 701, 14 (2000).
- 67 B. Schechter, R. Pauzner, R. Arnon and M. Wilchek, *Cancer Biochem. Biophys.*, 289, 8 (1986).
- 68 B. Schechter, M. Wilchek and R. Arnon, *Int. J. Cancer*, 409, 39 (1987).
- 69 B. Schechter, A. Neumann, M. Wilchek and R. Arnon, *J. Contr. Release*, 75, 10 (1989).
- 70 R. Epton, M. E. Hobson and G. Marr, *J. Organomet. Chem.*, 231, 149 (1978).
- 71 B. Carlson, L. L. Miller, P. Neta and J. Grodkowski, *J. Am. Chem. Soc.*, 7233, 106, (1984).
- 72 J. R. Pladziewicz and M. S. Brenner, *Inorg. Chem.*, 3629, 26 (1987).
- 73 V. A. Nefedov and L. K. Tarygina, *Russ. J. Org. Chem. (Eng. Transl.)*, 1960, 12 (1976).
- 74 S. Sahami and M. J. Weaver, *J. Solution Chem.*, 199, 10 (1981).
- 75 M. Rosenblum, *Chemistry of the Iron Group Metallocenes*, Part I, Wiley-Interscience, New York, 1965, pp 201-208.
- 76 E. W. Neuse and H. Rosenberg in *Reviews in Macromolecular Chemistry*; eds. K. F. O'Driscoll and M. Shen, Marcel Dekker, New York, 1970, vol. 5.
- 77 D. E. Bublitz and K. L. Rinehart Jr., *Organic Reactions*, 1, 17 (1969).
- 78 G. Wilkinson, *Comprehensive Organometallic Chemistry*, Pergamon Press, Oxford, 1988, vol. 4, ch. 31 and vol. 8, ch. 59.

- 79 D. W. Mago, P. D. Shaw and M. D. Rausch, *Chem. Ind. (London)*, 1388, (1957).
- 80 R. W. Fish and M. Rosenblum, *J. Org. Chem.*, 1253, 30 (1965).
- 81 M. D. Rausch, *Inorg. Chem.*, 414, 1 (1962).
- 82 D. Seyferth, H. P. Hoffman, R. Burton and J. F. Helling, *Inorg. Chem.*, 227, 1 (1962).
- 83 M. D. Rausch, M. Vogel and H. Rosenberg, *J. Org. Chem.*, 900, 22 (1957).
- 84 J. K. Lindsay and C. R. Hauser, *J. Org. Chem.*, 355, 22 (1957).
- 85 D. Lednicer and C. R. Hauser, *Org. Synth.*, 31, 40 (1961).
- 86 D. Lednicer, J. K. Lindsay and C. R. Hauser, *J. Org. Chem.*, 653, 23 (1958).
- 87 D. E. Bublitz and K. L. Rinehart Jr., *Org. Reactions*, 76, 17 (1969).
- 88 M. Rosenblum, A. K. Banerjee, N. Danieli, R. W. Fisch and V. Schlatter, *J. Am. Chem. Soc.*, 316, 85 (1963).
- 89 K. Schögl, *Mh. Chem.*, 601, 88 (1957).
- 90 K. Schögl and H. Egger, *Mh. Chem.*, 376, 94 (1963).
- 91 A. Benkeser, Y. Nagai and J. Hooz, *J. Am. Chem. Soc.*, 1450, 86 (1964).
- 92 G. R. Buell, W. E. McEwen and J. Kleinberg, *J. Am. Chem. Soc.*, 40, 84 (1962).
- 93 W. C. du Plessis, J. J. C. Erasmus, G. J. Lamprecht, J. Conradie, T. S. Cameron, M. A. S. Aquino and J. C. Swarts, *Can. J. Chem.*, 378, 77 (1999).
- 94 R. A. Benkeser, D. Goggin and G. Schroll, *J. Am. Chem. Soc.*, 4025, 76 (1954).
- 95 D. Seyferth and J. F. Helling, *Chem. Ind. (London)*, 1568, (1961).
- 96 A. N. Nesmeyanov, V. A. Sazonova and V. N. Drozd, *Izv. Akad. Nauk USSR, Otd. Khim. Nauk*, 45, (1962).
- 97 P. C. Reeves, *Org. Synth.*, 28, 56 (1977).
- 98 D. E. Bublitz and K. L. Rinehart, *Org. Reactions*, 21, (1968).
- 99 G. D. Broadhead, J. M. Osgerby and P. L. Pauson, *J. Chem. Soc.*, 650, (1958).
- 100 N. F. Blom, E. W. Neuse and H. G. Thomas, *Transition Met. Chem.*, 301, 12 (1987).
- 101 K. L. Rinehart Jr., R. J. Curby Jr. and P. E. Sokol, *J. Am. Chem. Soc.*, 3420, 79 (1957); V. Weinmayr, *J. Am. Chem. Soc.*, 3029, 77 (1955).

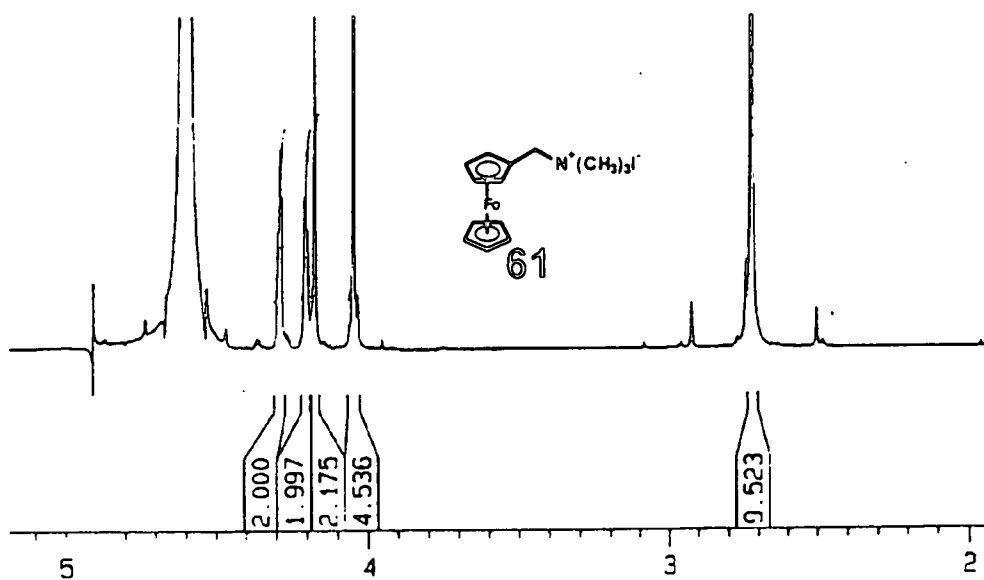
- 102 P. Da Re and E. Sianesi, *Experientia*, 648, **21(11)** (1965).
- 103 R. F. Hudson and G. E. Moss, *J. Chem. Soc.*, 5157, (1962).
- 104 P. Köpf-Maier, H. Köpf and E. W. Neuse, *J. Cancer Res. Clin. Oncol.*, 336, **108** (1984)
- 105 D. H Evans, K. M. O'Connell, R. A. Peterson and M. J. Kelly, *J. Chem. Edu.*, 291, **60** (1983); P. T. Kissinger and W. R. Heineman, *J. Chem. Edu.*, 702, **60** (1983); J. J. van Benschoten, J. Y. Lewis and W. R. Heineman, *J. Chem. Edu.*, 772, **60** (1983); D. T. Sawyer and J. L. Roberts Jr., *Experimental Electrochemistry for Chemists*, Wiley, New York, 1974, pp 118.
- 106 T. Ogata, K. Oikawa, T. Fujisawa, S. Motoyama, T. Izumi, A. Kasahara and N. Tanaka, *Bull. Chem. Soc. Jpn.*, 3723, **54** (1981).
- 107 E. W. Neuse and F. Kanzawa, *Appl. Organomet. Chem.*, 19, **4** (1990).
- 108 D. Osella, M. Ferrali, P. Zanello, F. Laschi, M. Fontani, C. Nervi and G. Cavigliolo, *Inorg. Chim. Acta*, 42, **306** (2000).
- 109 J. March, *Advance Organic Chemistry* 4th ed., Wiley Interscience, New York, 1992, p. 437.
- 110 E. L. Martin and L. F. Fieser, *Org. Synth.*, 569, **2**.
- 111 B. S. Furniss, A. J. Hannaford, P. W. G. Smith and A. R. Tatchell, *Vogel's Textbook of Practical Organic Chemistry* (5th ed.), Wiley, New York, 1994, p 692.
- 112 P. Carre and P. Mauclere, *Compt. Rend.*, 1422, **192** (1934).
- 113 J. P. E. Human and J. A. Mills, *Nature*, 877, **158** (1946).
- 114 L. F. Fieser and M. A. Peters, *J. Am. Chem. Soc.*, 4373, **54** (1932).
- 115 J. A. Cade and W. Gerrard, *Nature*, 29, **172** (1953).
- 116 H. H. Bosshard, R. Mory, M. Schmid and H. Zollinger, *Hel. Chim. Acta*, 1653, **42** (1959).
- 117 M. A. Beg and H. N. Singh, *Z. Physik. Chemie*, 129, **237** (1968).
- 118 F. W. Knobloch and W. H. Rauscher, *J. Polym. Sci.*, 656, **54** (1961).
- 119 A. Wissner and C. V. Grudzinskas, *J. Org. Chem.*, 3972, **43** (1978).
- 120 P. J. Beeby, *Tetrahedron Lett.*, 3379, **34** (1977).
- 121 C. F. H. Allen and W. E. Barker, *Org. Synth. Coll. Vol. 2*, 156, (1943).

- 122 F. J. Villani and M. S. King, *Org. Synth. Coll. Vol. 1*, 394, (1941).
- 123 A. Mooradian, C. J. Cavallito, A. J. Bergman, E. J. Lawson and C. M. Suter, *J. Am. Chem. Soc.*, 3372, 71 (1949).
- 124 C. G. Young, A. Epp, B. M. Craig and H. R. Sallans, *J. Am. Oil. Chemist Soc.*, 107, 34 (1957).
- 125 A. L. J. Beckwith in *Synthesis of Amides: The Chemistry of Amides Part One*; ed. J. Zabicky, Interscience Publ., New York, 1970, pp 75-185.
- 126 J. March, *Advanced Organic Chemistry (3rd ed.)*, Wiley-Interscience, New York, p. 370.
- 127 O. H. Wheeler and O. Rosado in *Chemistry of Imidic compounds: The Chemistry of Amides Part One*; ed. J. Zabicky, Interscience Publ., New York, 1970, pp 335-381.
- 128 J. March, *Advanced Organic Chemistry (3rd ed.)*, Wiley-Interscience, New York, p. 371.
- 129 A. L. J. Beckwith in *Synthesis of Amides: The Chemistry of Amides Part One*; ed. J. Zabicky, Interscience Publ., New York, 1970, pp 105-109.
- 130 A. L. J. Beckwith in *Synthesis of Amides: The Chemistry of Amides Part One*; ed. J. Zabicky, Interscience Publ., New York, 1970, pp 96-105.
- 131 B. C. Challis and J. A. Challis in *Reactions of the Carboxamide Group; The Chemistry of Amides Part Two*; ed. J. Zabicky, Interscience, New York, 1970, pp 795-801.
- 132 W. Bell and C. Glidwell, *J. Organomet. Chem.*, 229, 405 (1991).
- 133 P. D. Beer and D. K. Smith, *J. Chem. Soc., Dalton Trans.*, 417, (1998).
- 134 J. March, *Advanced Organic Chemistry (3th ed.)*, Wiley-Interscience, New York, p. 1099.
- 135 B. K. Keppler, M. Henn, U. M. Juhl, M. R. Berger, R. Niebl and F. E. Wagner, *Progress in Clinical Biochemistry and Medicine*, 41 - 69, 10 (1989).

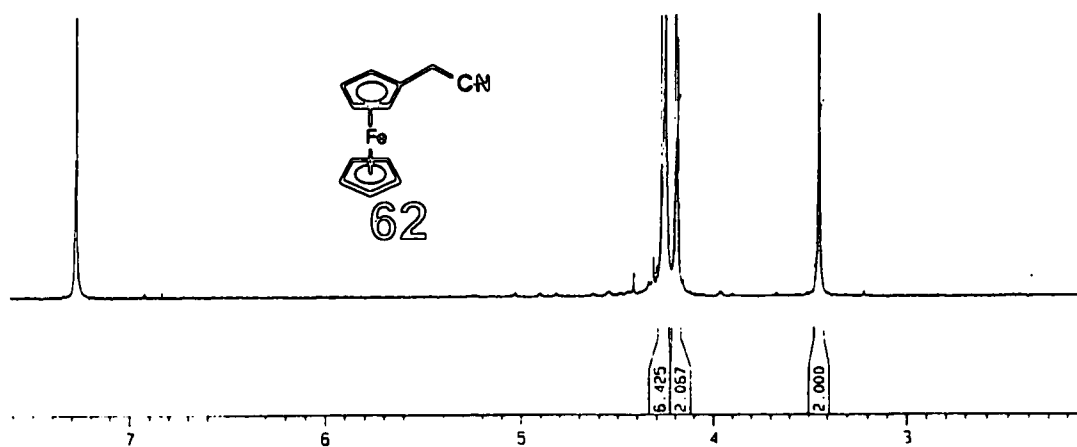
NUCLEAR MAGNETIC RESONANCE



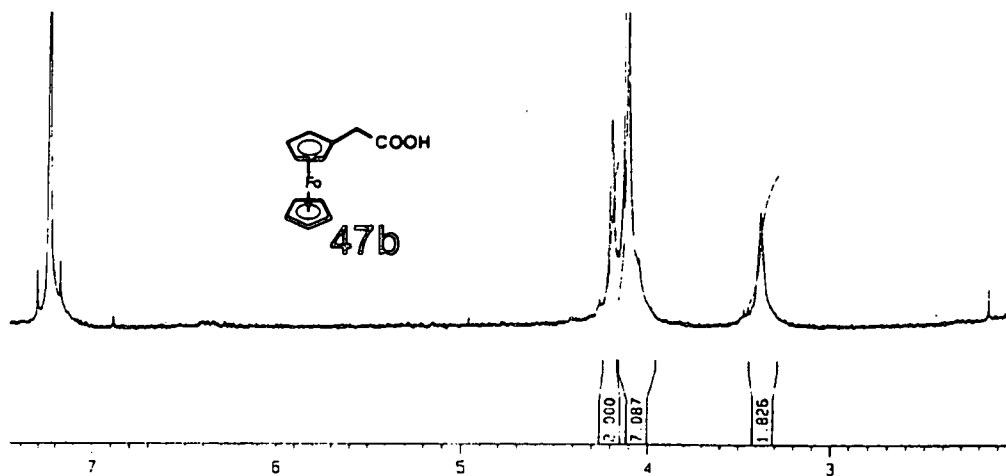
Spectrum 1 2-Chlorobenzoylferrocene (60) in CDCl_3 .



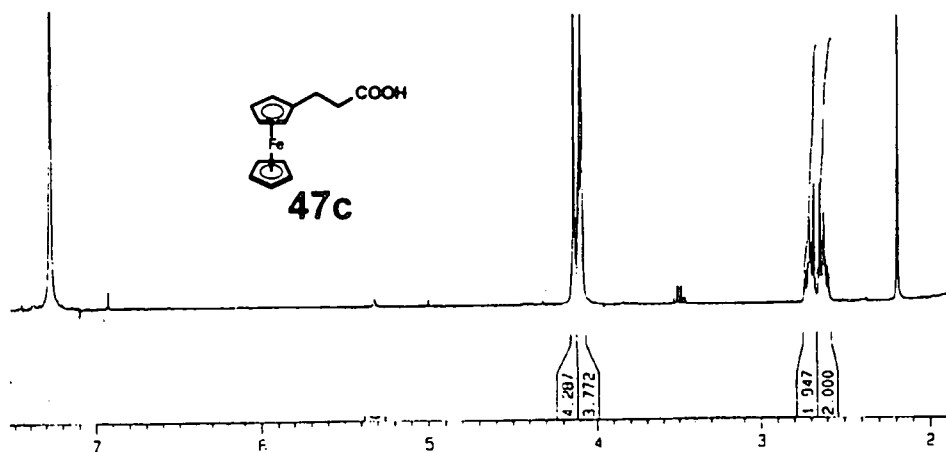
Spectrum 2 N,N-dimethylaminomethylferrocene methiodide (61) in D_2O .



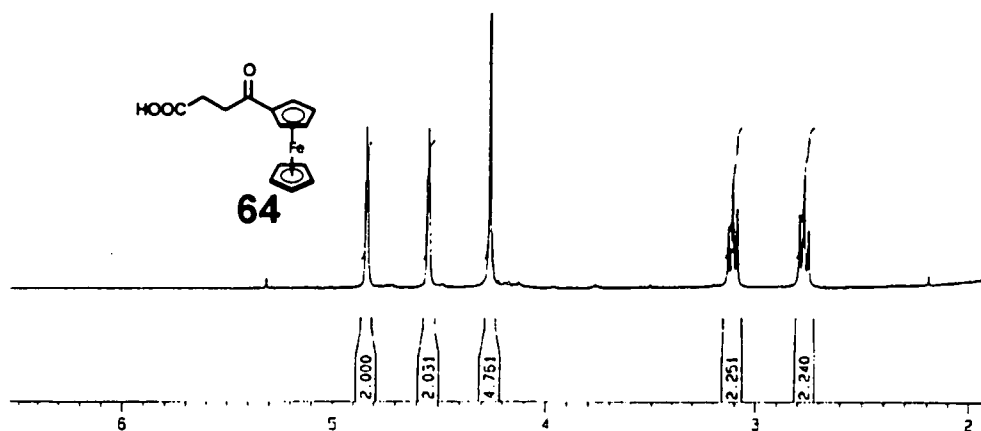
Spectrum 3 Ferrocenylacetonitrile (62) in CDCl_3 .



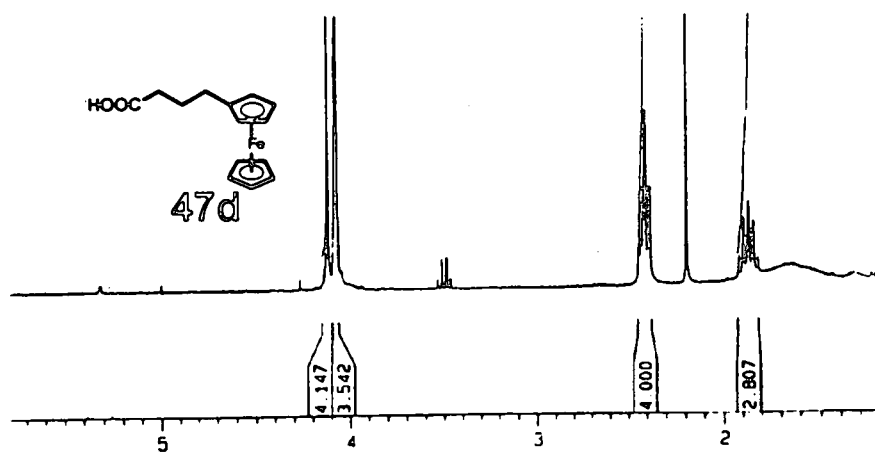
Spectrum 4 Ferrocenylacetic acid (47b) in CDCl_3 .



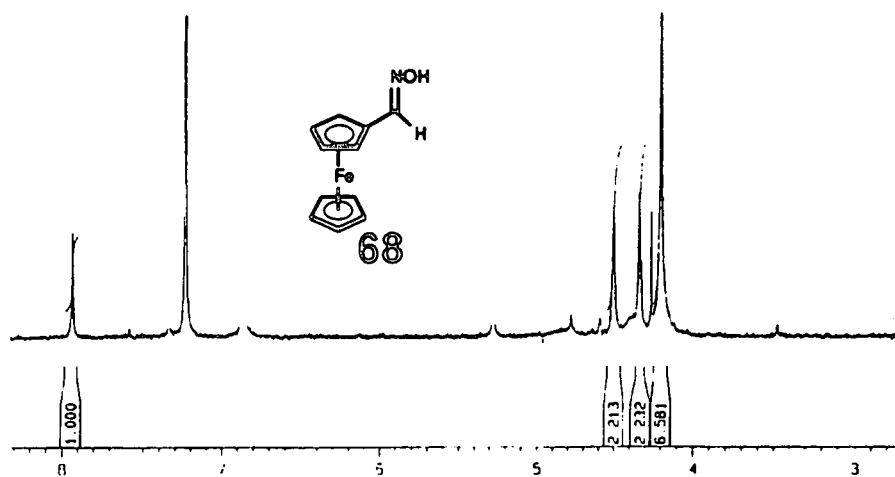
Spectrum 5 3-Ferrocenylpropanoic acid (47c) in CDCl_3 .



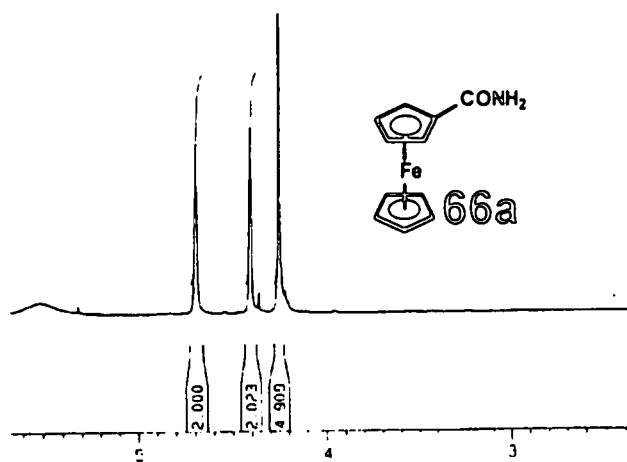
Spectrum 6 3-ferrocenylpropanoic acid (64) in CDCl_3 .



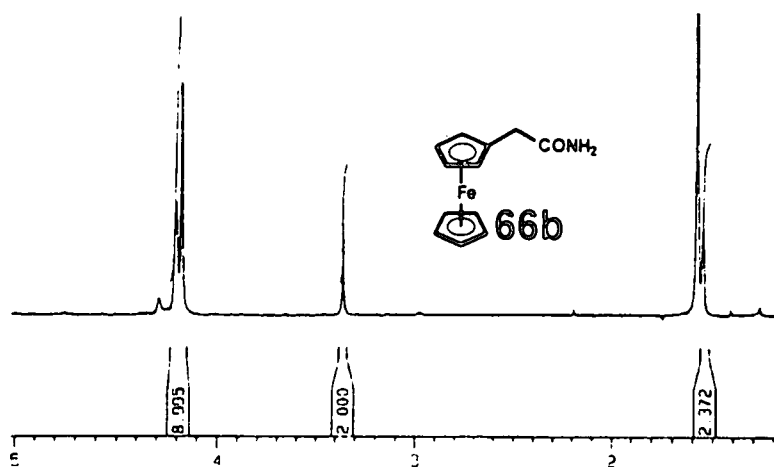
Spectrum 7 4-Ferrocenylbutanoic acid (47d) in CDCl₃.



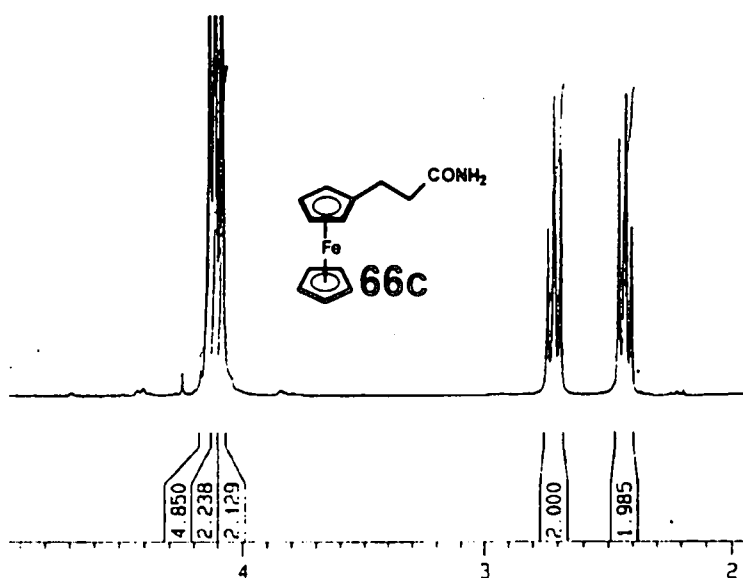
Spectrum 8 Ferrocenecarboxaldoxime (68) in CDCl₃.



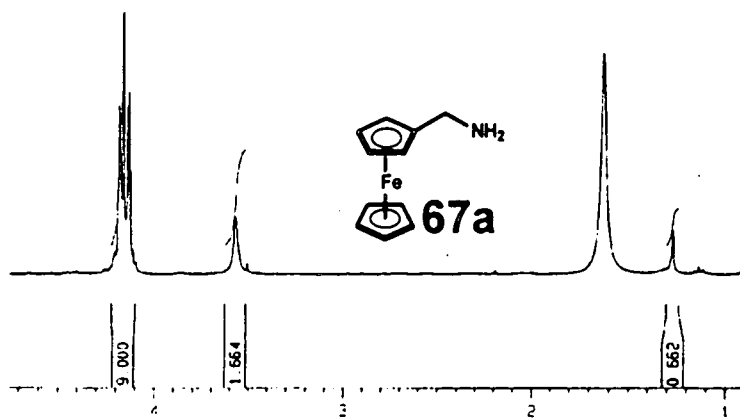
Spectrum 9 Ferrocenylcarboxamide (66a) in CDCl₃.



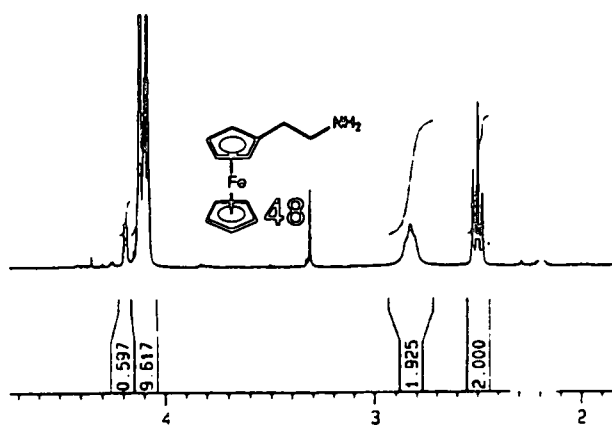
Spectrum 10 Ferrocenylacetamide (66b) in CDCl_3 .



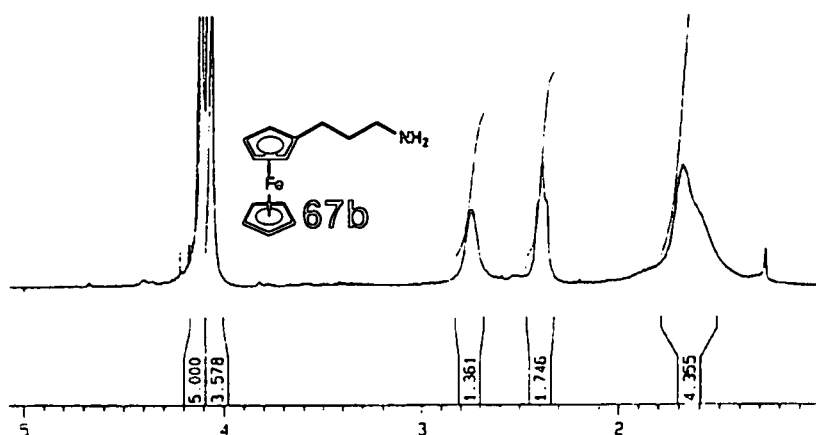
Spectrum 11 3-Ferrocenylpropionamide (66c) in CDCl_3 .



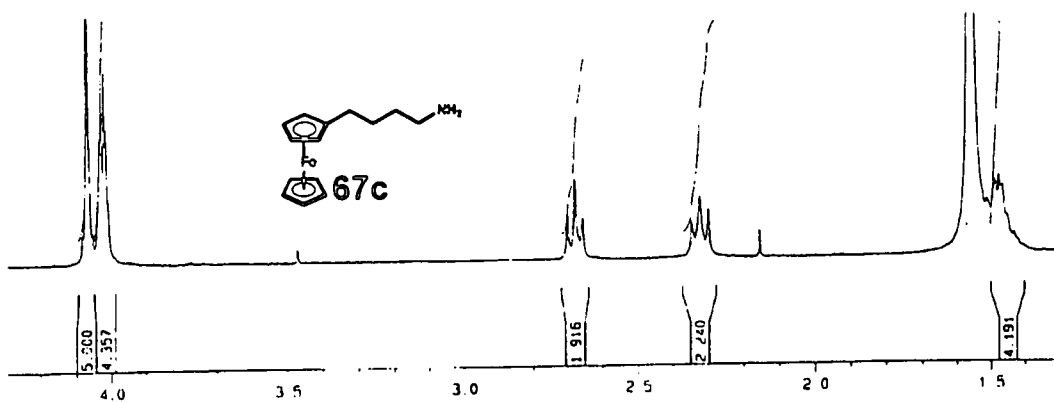
Spectrum 12 Ferrocenylmethylamine (67a) in CDCl_3 .



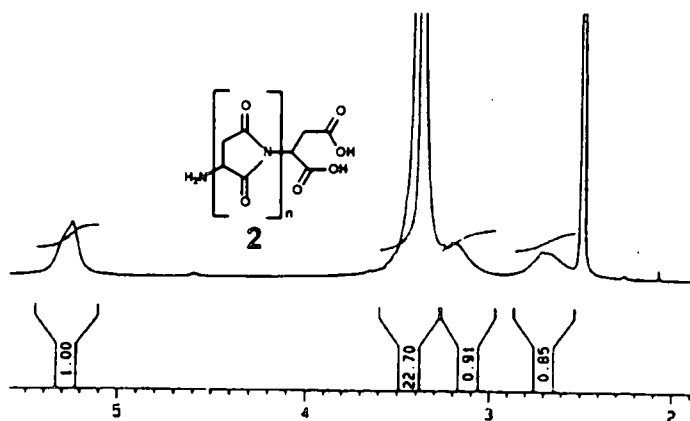
Spectrum 13 2-Ferrocenylethylamine (48) in CDCl_3 .



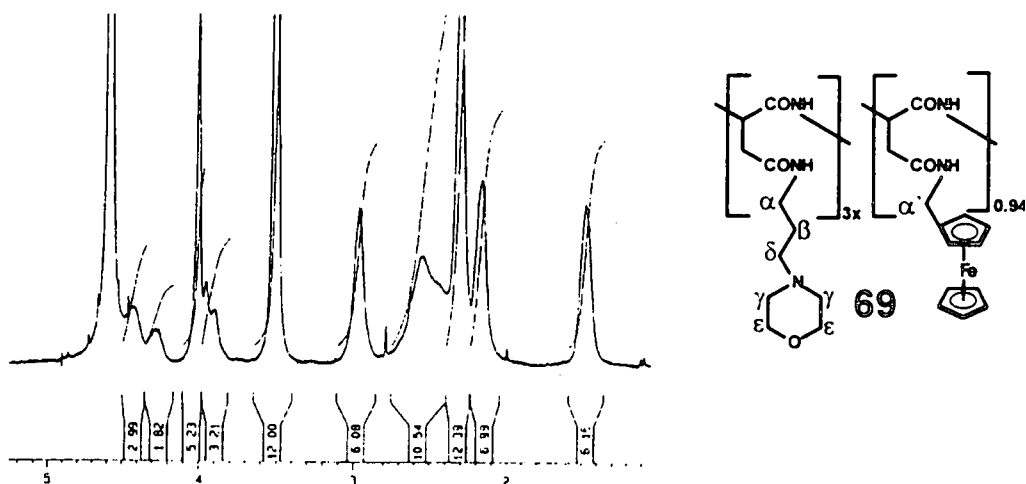
Spectrum 14 3-Ferrocenylpropylamine (67b) in CDCl_3 .



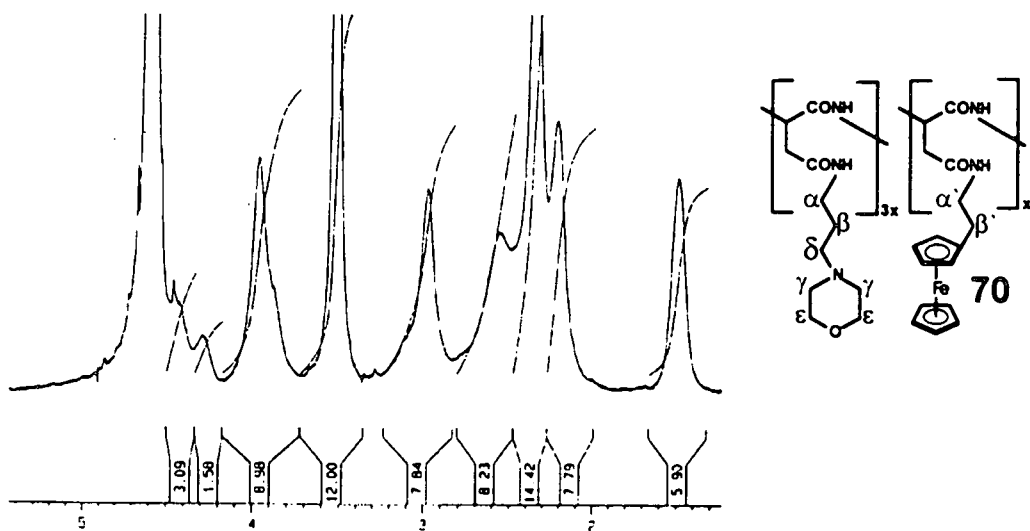
Spectrum 15 4-ferrocenylbutylamine (67c) in CDCl_3 .



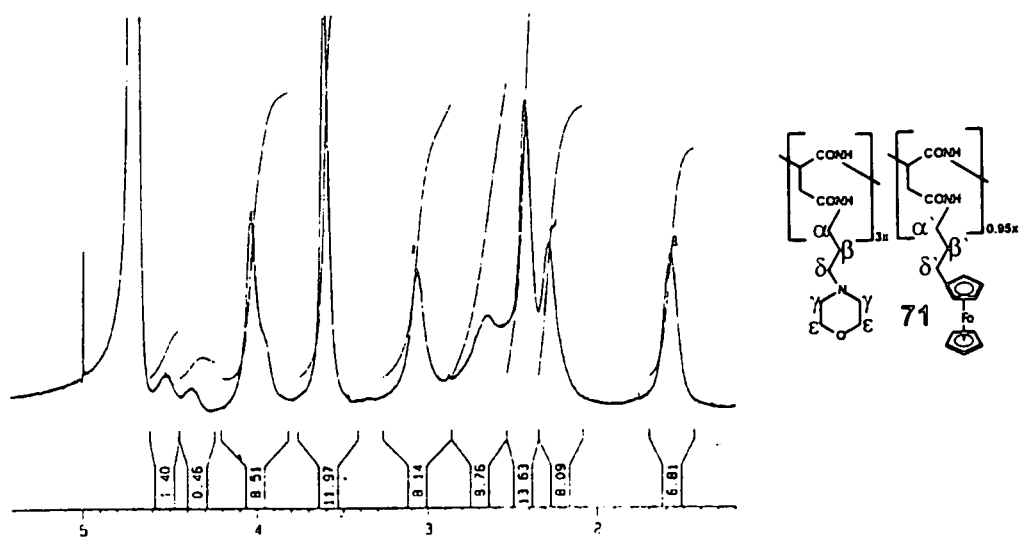
Spectrum 16 Poly-DL-succinimide (2) in DMSO-d₆.



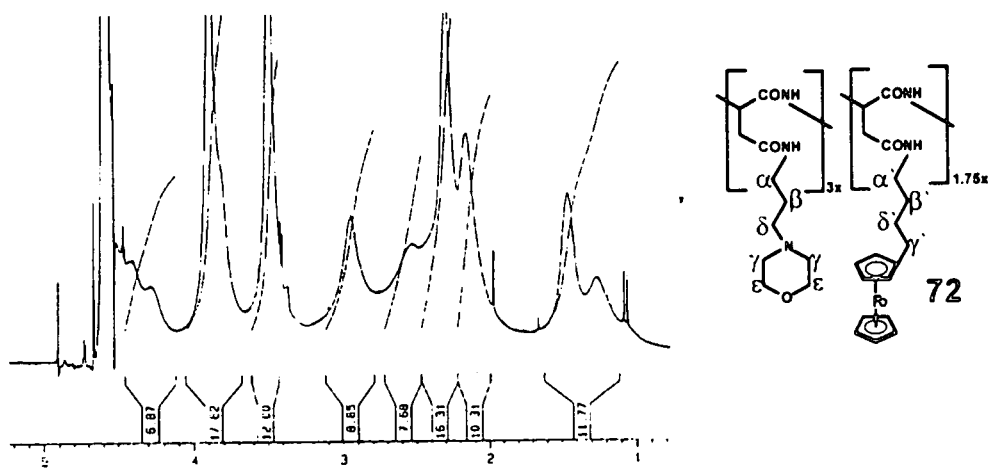
Spectrum 17 Polymer (69) in D₂O.



Spectrum 18 Polymer (70) in D₂O.



Spectrum 19 Polymer 71 in D_2O .



Spectrum 20 Polymer (72) in D_2O .

I declare that the dissertation hereby submitted by me for the Magister Scientiae degree at the University of the Free State is my own independent work and has not previously been submitted by me at another university/faculty I further cede copyright of the dissertation in favour of the University of the Free State.

Patrick Thabo Ndaba Nonjola

Signed 03 January 2002

U.O.F.S. BIBLIOTEK